



UNIFORMED SERVICES UNIVERSITY OF THE HEALTH SCIENCES
F. EDWARD HÉBERT SCHOOL OF MEDICINE
4301 JONES BRIDGE ROAD
BETHESDA, MARYLAND 20814-4799



September 6, 2005

**BIOMEDICAL
GRADUATE PROGRAMS**

Ph.D. Degrees

Interdisciplinary
-Emerging Infectious Diseases
-Molecular & Cell Biology
-Neuroscience

Departmental
-Clinical Psychology
-Environmental Health Sciences
-Medical Psychology
-Medical Zoology
-Pathology

Doctor of Public Health (Dr.P.H.)

Physician Scientist (MD/Ph.D.)

Master of Science Degrees

-Molecular & Cell Biology
-Public Health

Masters Degrees

-Comparative Medicine
-Military Medical History
-Public Health
-Tropical Medicine & Hygiene

Graduate Education Office

Dr. Eleanor Metcalf, Acting Associate Dean
Janet Anastasi, Program Coordinator
Heather DeLloyd, Educational Assistant

Web Site

www.usuhs.mil/geo/gradpgm_index.html

E-mail Address

graduateprogram@usuhs.mil

Phone Numbers


Commercial: 301-295-9474
Toll Free: 800-772-1747
DSN: 295-9474
FAX: 301-295-6772

APPROVAL SHEET

Title of Dissertation: "The Modulation of Polymorphonuclear Neutrophil Function by Cytotoxic Necrotizing Factor Type-1 Uropathogenic *Escherichia coli*"

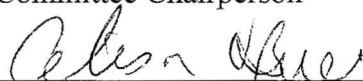
Name of Candidate: Jon Davis
Doctor of Philosophy Degree
19 September 2005

Dissertation and Abstract Approved:


Ann Jerse, Ph.D.

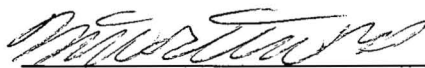
Department of Microbiology & Immunology
Committee Chairperson

9-19-05
Date

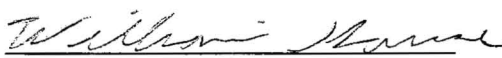

Alison O'Brien, Ph.D.

Department of Microbiology & Immunology
Committee Member


9-20-05
Date


Martin Ottolini, Col, MC, USAF
Department of Pediatrics
Committee Member

9-19-05
Date


William Gause, Ph.D.
UMDNJ
Committee Member

9-21-05
Date

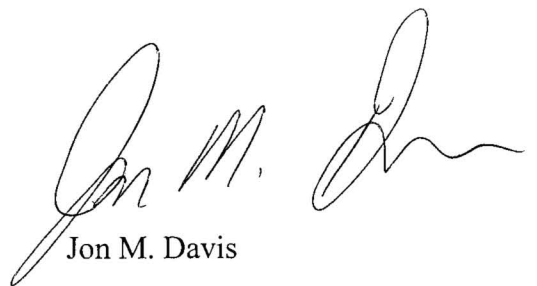

Ajay Verma, M.D., Ph.D.
Department of Neurology
Committee Member

9-19-2005
Date

The author hereby certifies that the use of any copyrighted material in the thesis manuscript entitled:

“The Modulation of Polymorphonuclear Neutrophil Function by Cytotoxic Necrotizing Factor Type 1 - Expressing Uropathogenic *Escherichia coli*.”

beyond brief excerpts is with the permission of the copyright owner, and will save and hold harmless the Uniformed Services University of the Health Sciences from any damage which may arise from such copyright violations.

A handwritten signature in black ink, appearing to read 'Jon M. Davis', with a stylized flourish at the end.

Jon M. Davis

Department of Microbiology and Immunology

Uniformed Services University of the Health Sciences

Abstract

Title of Dissertation:

The Modulation of Polymorphonuclear Neutrophil Function by Cytotoxic Necrotizing
Factor Type 1 - Expressing Uropathogenic *Escherichia coli*

Jon M. Davis, Doctor of Philosophy, 2005

Thesis Directed by:

Alison D. O'Brien, Ph.D.

Professor, Department of Microbiology and Immunology

Uropathogenic *Escherichia coli* (UPEC) cause more than 85% of all urinary tract infections (UTI). These infections primarily affect women, and over half of all women will experience at least one UTI in their lifetime. Animal models of UTI pathogenesis have provided some insight into the role of various UPEC virulence factors. In these animal studies, the toxin Cytotoxic Necrotizing Factor type 1 (CNF1) has been shown to have a significant role in the pathogenesis of UTI. One of the most striking features of CNF1-expressing UPEC infection in the in vivo models was magnitude of the acute

inflammatory response. Compared to a *cnf1* isogenic mutant, CNF1-expressing UPEC elicited an acute inflammatory response characterized by an extensive infiltration of polymorphonuclear leukocytes (PMN) into tissue infected with CNF1-expressing UPEC. In spite of the enhanced acute inflammatory response, the CNF1-expressing UPEC had a significant survival advantage compared to the *cnf1* isogenic mutant. CNF1 is an AB toxin that deamidates the catalytically-active glutamine residue in the Rho family of small GTPases. The Rho family GTPases are intracellular signaling molecules responsible for the control of many cellular function in eukaryotic cells such as PMNs. In PMNs, Rho GTPases control the processes of phagocytosis and chemotaxis in addition to the generation of reactive oxygen species (ROS). These observations formed the foundation of the hypothesis that CNF1-expressing UPEC modulate PMN function. This hypothesis was tested *in vitro* with elicited mouse PMNs and showed that CNF1-expressing UPEC modulate the antimicrobial response of PMNs through several mechanisms. First, CNF1-expressing UPEC alter the capacity of PMNs to remodel their plasma membrane and cluster CD11b in response to serum-opsonized UPEC which leads to a diminished PMN phagocytic capacity. Second, CNF1 expressed by UPEC results in an increase in the amount of Rac2 in PMNs. Third, PMNs co-incubated with CNF1-expressing UPEC generate an enhanced intracellular ROS. Finally, CNF1-expressing UPEC release CNF1 via outer membrane vesicles that interact with the PMN membrane. These results support the hypothesis that CNF1 is a UPEC virulence factor and lead to a new molecular model of UPEC interaction with the host innate immune system.

**The Modulation of Polymorphonuclear Neutrophil Function
by Cytotoxic Necrotizing Factor Type 1 – Expressing
Uropathogenic *Escherichia coli***

By

Jon Michael Davis

Dissertation submitted to the Faculty of the Department of Microbiology and
Immunology Graduate Program of the Uniformed Services University of the Health
Sciences

F. Edward Hèbert School of Medicine

in partial fulfillment of the
requirements for the degree of
Doctor of Philosophy 2005

Acknowledgements

This work would not have been possible without the support and assistance of many different people and organizations. In no particular order, I would like to thank:

The United States Army Long Term Health Education and Training Scholarship for providing me a few years to pursue this education

My thesis advisor, you made this experience possible by opening your laboratory and by your teaching

My thesis committee for their guidance and feedback

The friends I made here, whether studying or not

Ronald Rosenberg, Colonel, U.S. Army (Ret.) for the opportunity to experience medical research in the laboratory and in the field

My lab mates, especially Sharon who could always be counted on for some reality, some laughs, great friendship and a cup of coffee

My wife, Brenda, who patiently tolerated the ups and downs of school and believed in me

Table of Contents

Introduction.....	1
Preface.....	2
Urinary Tract Infections.....	3
Definitions and Public Health Impact.....	3
Pathogenesis - <i>Synopsis</i>	4
Pathogenesis - Fimbriae of UPEC	7
Toxins	9
Urinary Tract Defenses	11
Cytotoxic Necrotizing Factor Type 1	13
Discovery of CNF1 and Phenotypic Effects on Tissue Culture Cells	13
Cell Binding and Enzymatic Activities of CNF1	16
Export of CNF1.....	21
Epidemiology of UPEC that Produce CNF1 and Potential Role of CNF1 in	
Pathogenesis of UTIs	22
CNF1 and Rho Family GTPases.....	24
Polymorphonuclear neutrophils and Rho GTPases	34
Rho GTPases and Neutrophil Response – <i>Chemotaxis</i>	38
Rho GTPases and Neutrophil Response – <i>Phagocytosis</i>	40
Rho GTPases and Neutrophil Response - <i>NADPH Oxidase Activation</i>	42
Hypothesis and Specific Aims	50

Cytotoxic Necrotizing Factor Type 1 Production by Uropathogenic <i>Escherichia coli</i>	
Modulates Polymorphonuclear Leukocyte Function	51
Abstract.....	52
Introduction.....	53
Materials and Methods.....	56
Results.....	64
CNF1 enhances UPEC replication in the presence of murine PMNs	64
PMN phagocytic capacity and CD11b clustering is altered in the presence of CNF1- expressing UPEC.	72
CNF1-expressing UPEC modify the PMN respiratory burst.....	77
CNF1-expressing UPEC stimulate expression of enhanced levels of activated Rac2 in PMNs.	83
Cytotoxic Necrotizing Factor Type 1 (CNF1) Delivered by Outer Membrane Vesicles of Uropathogenic <i>Escherichia coli</i> Attenuates Polymorphonuclear Neutrophil Antimicrobial Activity and Chemotaxis.....	86
Abstract.....	87
Introduction.....	88
Materials and Methods.....	90
Results.....	98
CNF1 in culture supernatants alters PMN antimicrobial response.	98
Outer membrane vesicles from CP9 are complexed with CNF1.....	102
Vesicles are observed by electron microscopy.	107
Multinucleation of HEp-2 cells by OMVs.....	112

OMVs interact with mouse PMNs.....	112
CNF1-bearing OMVs alter PMN chemotaxis.....	115
Discussion and Future Directions	123
Overview of Results in the Context of the Dissertation Objective and Specific Aims	124
CNF1 modulates the PMN antimicrobial response	125
CNF1 induced changes in PMN phagocytosis.....	126
Alteration of CD11b clustering.....	128
CNF1 enhanced ROS generation.....	129
Membrane vesicles target CNF1 to PMNs	131
CNF1 is complexed with outer membrane vesicles.....	132
OMVs interact with and alter antimicrobial responses of PMNs	134
Conclusions and model	137
Future Directions	140
References.....	142

Table of Figures

Figure 1. Model of UPEC Adherence to the Bladder and Kidney and Host Response to Bacteria.	5
Figure 2. Enzymatic activity of CNF1.	18
Figure 3. Structural changes in Rho family proteins when bound to GTP.	26
Figure 4. Rho GTPase cycles control cellular function.	28
Figure 5. Photomicrograph of a polymorphonuclear neutrophil.	35
Figure 6. Electron transfer reactions and generation of oxygen radical.	44
Figure 7. Influence of untreated- and cytochalasin D-treated PMNs on net replication of CNF1-positive and negative UPEC.	66
Figure 8. Western blot analysis of CNF1 in sonically-disrupted lysates of bacteria and PMNs after co-incubation.	68
Figure 9. Influence of cytochalasin D on PMN antimicrobial capacity.	70
Figure 10. Clustering of CD11b in mouse PMNs in contact with UPEC.	75
Figure 11. Fold change of CD11b fluorescence intensity.	78
Figure 12. PMN spreading in response to UPEC.	80
Figure 13. Rac2 activation in PMNs co-incubated with UPEC.	84
Figure 14. Analysis of supernatants from CNF1-positive and negative-CP9 isogenic strains.	99
Figure 15. Influence of PMNs treated with CP9 or CP9 <i>cnf1</i> culture supernatant on the net replication of CNF1-positive and negative CP9.	103
Figure 16. Immunoblot analysis of supernatant pellet.	105
Figure 17. Detection of O4 antigen in pelleted fraction.	108

Figure 18. Electron micrograph of and activity associated with membrane vesicles prepared from CP9.....	110
Figure 19. Activity of outer membrane vesicles derived from CP9.	113
Figure 20. Fluorescently-labelled outer membrane vesicles interact with PMNs.	116
Figure 21. OMVs from CNF1-expressing CP9 reduce PMN antimicrobial capacity. ..	118
Figure 22. PMN chemotaxis is inhibited in the presence of CNF1-containing OMVs.	121
Figure 23. Proposed model for CNF1 modulation of PMN function.	138

Table of Tables

Table 1. Toxins associated with UPEC.....	10
Table 2. Comparison of CNF1 and CNF2.	15
Table 3. Phagocytic capacity and activity of PMNs exposed to UPECa.....	73
Table 4. Respiratory burst of PMNs exposed to UPEC.....	82
Table 5. Biochemical characterization of OMVs derived from UPEC strain CP9 and its isogenic CNF1-negative mutanta.....	101

Chapter 1

Introduction

Preface

Extraintestinal *Escherichia coli* that are designated uropathogenic *E. coli* (UPEC) represent an *E. coli* pathotype that has successfully exploited the normally sterile urinary tract. These organisms are responsible for two of the most frequent human bacterial infections: urinary tract infections (UTI) and acute bacterial prostatitis. UPEC possess a variety of virulence factors that enable them to colonize the host and survive the host innate immune response. Some of the most well-characterized UPEC virulence factors are adhesins that facilitate host contact while others such as toxins modulate host cellular responses. Despite years of research, the pathogenesis of UPEC-mediated infections remains unclear, and the role of only a few virulence factors is firmly established. This work focuses on the UPEC toxin Cytotoxic Necrotizing Factor type 1 (CNF1) and the role of this virulence factor in the modulation of the host innate immune response. The following sections highlight some aspects of UTI epidemiology and pathogenesis and provide details on the history and biological and enzymatic activities of CNF1. In addition, the relationship between CNF1 production and UPEC virulence is summarized, and the potential role of CNF1 in the pathogenesis of UTI and acute bacterial prostatitis is discussed. Next, the nature of the innate host response to UTIs is outlined. The last sections of the Introduction describe the importance of the Rho family GTPases that are the targets of CNF1 activity in the coordination of the antimicrobial responses of

polymorphonuclear neutrophils. The introduction concludes with the presentation of the central hypothesis and specific aims of this dissertation.

Urinary Tract Infections

Definitions and public health impact

The urinary tract is comprised of the kidneys, the ureters, the bladder, and the urethra. Urinary tract infections represent a spectrum of disease that can affect the bladder (cystitis), or the kidneys and their collecting systems (pyelonephritis), or both. Infections caused by UPEC place a substantial burden on the medical system in terms of physician office visits and economic costs. In 1997, the last year complete data are available, over 6 million cases of cystitis were recorded (Russo and Johnson 2003). The out-patient treatment costs for these cystitis cases exceed US\$1 billion (Russo and Johnson 2003). Both men and women suffer UPEC-mediated UTIs; however, women are disproportionately affected and account for over half of all infections (Foxman 2002). Available evidence suggests that women are 14 times more likely than men to experience a UTI and 33% of women will experience a UTI before reaching 24 years old (Foxman 2002). In spite of the large number of UTIs, the majority of infections remain confined to the bladder where the host immune response frequently controls the infection, and UTIs often resolve without significant medical complications. More invasive infections can result in significant morbidity. Uropathogens that escape the host defenses in the bladder can ascend to the upper urinary tract and enter the kidneys and can cause pyelonephritis.

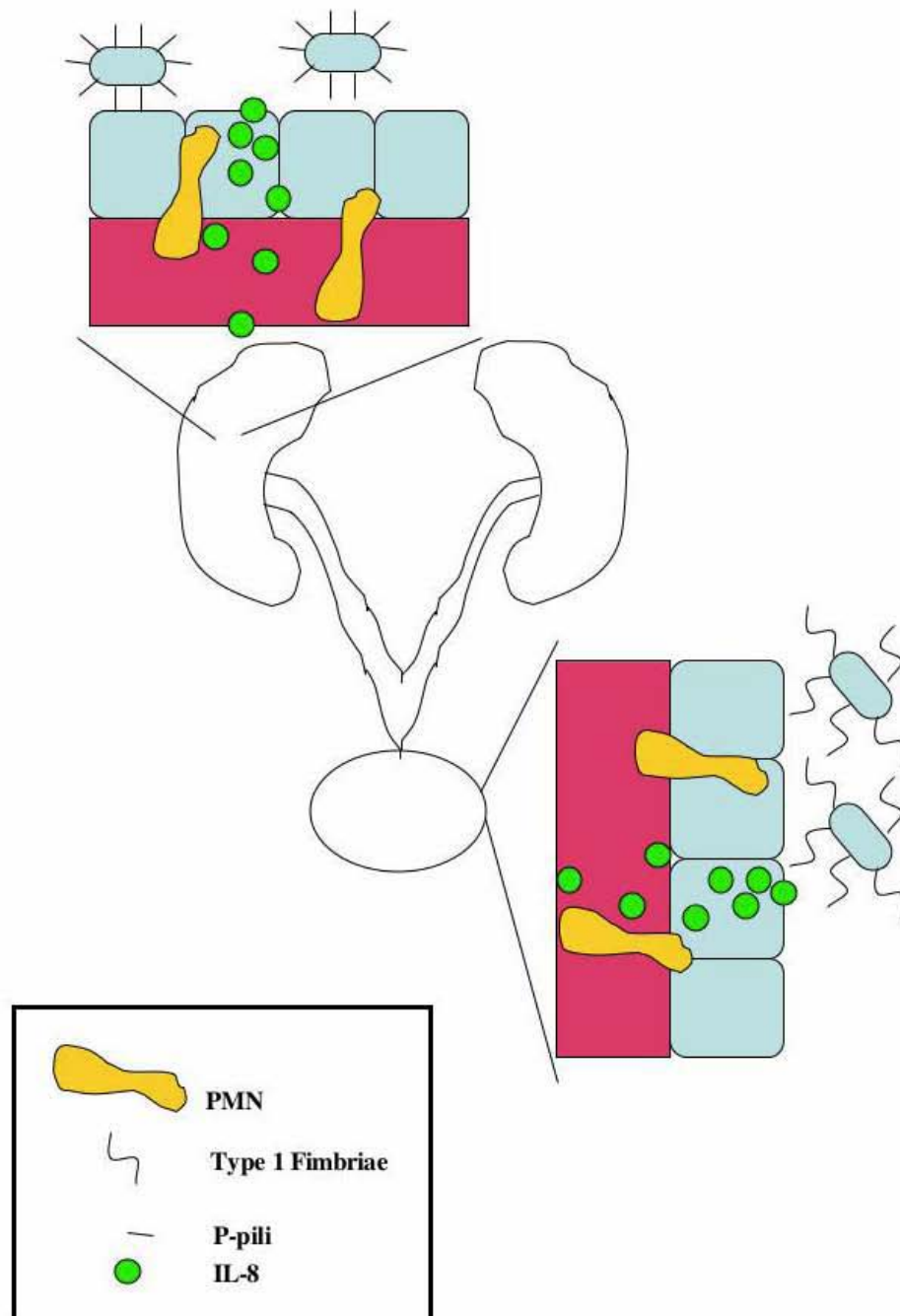
This condition can affect one or both kidneys and, in some cases, can lead to renal scarring. An estimated 250,000 cases of pyelonephritis occurred in 1997 and resulted in treatment costs of at least \$175 million (Russo and Johnson 2003). Infections that progress to pyelonephritis can also lead to urosepsis when UPEC penetrate the one-cell-thick-barrier of the proximal tubules and enter the bloodstream (Kaper, Nataro et al. 2004).

Pathogenesis - *Synopsis*

The pathogenesis of UPEC-mediated UTI is not completely understood; however, it likely involves the coordinated expression of multiple virulence factors by the uropathogen. The critical role of UPEC adhesive factors, such as type 1- and P-fimbriae in the maintenance of UPEC within the urinary tract is well established. Less well defined in the pathogenesis of UTIs is the function of toxins, such as α -hemolysin and CNF1. The following sections discuss these factors as well as the nature of the host response to UTIs. Figure 1 is an illustration based on some current models of UTI pathogenesis and depicts UPEC adherence and the subsequent cytokine response by the host.

Figure 1. Model of UPEC Adherence to the Bladder and Kidney and Host Response to Bacteria.

UPEC initially adhere to bladder epithelial cells of the uroepithelium by means of type 1 fimbriae. This attachment occurs through the interaction of FimH at the tip of type 1 fimbriae with mannose residues on the surface of host cells. UPEC that are so attached to cells are better able to remain in place and are less likely to be washed from the bladder surface by the bulk flow of urine. Epithelial cells respond to the presence of UPEC by secreting a variety of inflammatory mediators, such as IL-8. These secretions result in the attraction of polymorphonuclear neutrophils (PMNs) from the circulation to the site of inflammation where PMNs can phagocytose and inactivate UPEC. Many infections are limited to cystitis wherein UPEC remain confined to the bladder; those UPEC that shut off expression of type 1 fimbriae and begin production of P-pili can leave the bladder and ascend to the kidney. P-pili expression permits UPEC to adhere to kidney epithelial cells and can result in pyelonephritis. Adapted from (Mulvey, Schilling et al. 2000).



Pathogenesis - fimbriae of UPEC

Adherence of UPEC to the uroepithelium is frequently viewed as the first step in the development of a UTI, and this adherence is often facilitated by organelles such as type 1 fimbriae (Lim, Gunther et al. 1998). The importance of adhesion via type 1 fimbriae in UTI pathogenesis has been demonstrated many times (Connell, Agace et al. 1996; Gunther, Lockatell et al. 2001), and recently confirmed by Bahrani-Mougeot and colleagues who used signature-tagged mutagenesis to identify UPEC virulence factors (Bahrani-Mougeot, Buckles et al. 2002). Type 1 fimbriae are hairlike projections composed of multiple structural subunits that extend from the surface of *E. coli* (Connell, Agace et al. 1996). The fimbrial stalk is composed of the major structural sub-unit FimA, and the adhesive tip, FimH that recognizes mannose residues on host glycoproteins. The expression of the entire *fim* operon is subject to phase variation allowing UPEC to control when type 1 fimbriae are expressed (Connell, Agace et al. 1996; Gunther, Lockatell et al. 2001). The role of type 1 fimbriae in UTI has been explored *in vitro* and with animal models *in vivo*. Indeed, type 1 fimbriae are one of the few UPEC virulence factors for which experimental evidence has been generated that fulfills molecular Koch's postulates (Connell, Agace et al. 1996). Animal models have further clarified the importance of type 1 fimbrial adherence in UPEC pathogenesis. For example, *in vivo* studies in ascending UTI animal models demonstrated that expression of type 1 fimbriae correlated with increased bacterial density (CFU/gram) of tissue when expression of type 1 fimbriae

occurred in the bladder but not when type 1 fimbriae were expressed in the kidney (Gunther, Lockatell et al. 2001). Gunther and colleagues further demonstrated that UPEC associated with pyelonephritis shut-off expression of type 1 fimbriae earlier than UPEC associated with cystitis. This observation suggested to Gunther and colleagues that continuous expression of type 1 fimbriae could restrict bacteria to the bladder while the capacity to turn off expression of type 1 fimbriae would enable UPEC to escape the bladder and reach the upper urinary tract (Gunther, Lockatell et al. 2001).

The idea that UPEC associated with the more invasive disease can turn off the expression of type 1 fimbriae is consistent with earlier observations from Xia and colleagues (Xia, Gally et al. 2000). These investigators studied the potential regulatory cross talk between Type 1 fimbriae and P-pili. P-pili are a second type of adhesin almost always expressed by UPEC that are associated with pyelonephritis (Xia, Gally et al. 2000). P-pili recognize and bind to the α -D-galactopyranosyl-(1-4)- β -D-galactopyranoside structure present on glycolipids expressed on erythrocytes and cells in the kidney (Mulvey, Schilling et al. 2000). The expression of P-pili is controlled by the *pap* operon transcriptional regulator PapB; expression of P-pili is enhanced at low levels of PapB expression while P-pili expression is repressed when PapB levels are elevated. In addition to transcriptional control of P-pili, PapB has also been demonstrated to exert control over the expression of type 1 fimbriae (Xia, Gally et al. 2000). PapB was shown to increase the expression of FimE, a recombinase in the *fim* operon that allows the promoter for the FimA major sub-unit to be turned off by inversion. Simultaneously, PapB inhibits the activity of the second fimbrial operon recombinase, FimB, that controls

both on-to-off and off-to-on switching of the FimA promoter. This strategy allows UPEC to coordinate the expression of two major adhesins that facilitate urinary tract colonization. The presence of this type of regulatory mechanism allows for the mutually exclusive expression of adhesins and provides an explanation for the observation that UPEC that possess multiple operons for different adhesins express only one major type at any given time (Nowicki, Rhen et al. 1984).

Toxins

Following successful colonization, UPEC must acquire nutrients, alter host cellular responses, and survive contact with the host defenses. The expression of various toxins by UPEC may represent a strategy whereby the organisms can persist in the face of these obstacles (Table 1). Among the best-characterized toxins expressed by UPEC is α -hemolysin, a secreted toxin. In addition, many strains of UPEC produce CNF1. In fact, these two toxins are frequently co-expressed in many UPEC, and both have a demonstrated role in UPEC pathogenesis (Yamamoto, Nakata et al. 1996; Rippere-Lampe, Lang et al. 2001; Rippere-Lampe, O'Brien et al. 2001). Although the precise role of α -hemolysin in the pathogenesis of UPEC-mediated UTIs is not entirely clear this toxin appears to have different effects on host cells under different concentrations. At high concentrations of α -hemolysin, the toxin can create pores in target cells that result in cell lysis. Such destruction of host cells has been

Table 1. Toxins associated with UPEC.

Toxin	Activity	Cellular target	Frequency in UTI	UTI Syndrome association
CNF1	Deamidase	Rho GTPases	60%	Pyelonephritis
α -hemolysin	Pore formation	Membranes	51%	Pyelonephritis/cystitis
Secreted autotransporter toxin (Sat)	Protease	Various proteins	55%	Pyelonephritis
Protein involved in intestinal colonization of uropathogenic <i>Escherichia coli</i> (PicU)	Protease	Various proteins	22%	Pyelonephritis

proposed a means to liberate nutrients for the expanding UPEC population. The lytic activity of α -hemolysin may also protect UPEC from the antimicrobial response of polymorphonuclear neutrophils (PMNs) that are key cells in the host innate immune response during a UTI. Some recent investigations support an additional role of α -hemolysin in UTI pathogenesis (Uhlen, Laestadius et al. 2000). The results of these investigations have suggested that the concentration of α -hemolysin needed for the lytic activity of the toxin may not be attainable *in vivo* due to the frequent voiding of urine during a UTI (Uhlen, Laestadius et al. 2000; Laestadius, Richter-Dahlfors et al. 2002). These investigators demonstrated that sub-lytic doses of α -hemolysin induced Ca^{2+} oscillations in primary renal epithelial cells (Laestadius, Richter-Dahlfors et al. 2002). The capacity to alter host cell signals at least *in vitro* is a property also shared by CNF1 as discussed in detail in sections that follow.

Urinary tract defenses

The bladder and upper urinary tract is normally sterile as a consequence of several mechanisms that help shield these sites from infection with bacteria. First, the bulk flow of urine provides a constant washing of the urinary tract (Cattell 1996). Second, locally produced secretory IgA (sIgA) in the bladder may interfere with colonization by UPEC (Uehling, Johnson et al. 1999). Third, epithelial cells that line the urinary tract provide a physical barrier between the deeper tissue of the urinary tract and the environment.

When these cells are shed, they help remove uropathogens that have attached to the epithelial cell surface (Schilling, Mulvey et al. 2001). The process responsible for the loss of epithelial cells is thought to involve apoptosis, a form of cell death in which endogenous enzymes degrade host cell DNA and proteins (Mulvey, Lopez-Boado et al. 1998). While type 1 fimbriae have a demonstrated role in the exfoliation of bladder cells by apoptosis, it is likely that other bacterial factors may be involved. For example, lipopolysaccharide (LPS) can induce apoptosis in a variety of cell types; however, the role of LPS in the exfoliation of bladder cells *in vivo* is questionable because mice non-responsive to LPS still exfoliate bladder cells in response to UPEC (Mulvey, Schilling et al. 2000). Although exfoliation of bladder epithelial cells is generally considered a means of defense by the host (Cattell 1996; Uehling, Johnson et al. 1999), such loss of surface cells could simultaneously expose deeper tissue layers of the bladder to the uropathogen and further contribute to the pathology of a UTI.

The fourth general mechanism by which the urinary tract acts to reduce the load of bacteria is for the epithelial cells to secrete inflammatory mediators when pathogens are present (Uehling, Johnson et al. 1999; Schilling, Mulvey et al. 2001). In response to these inflammatory signals, polymorphonuclear neutrophils (PMN) are recruited to the site of infection where they can phagocytose and inactivate pathogens (Uehling, Johnson et al. 1999). The host response to UTIs is rapid and occurs within hours after UPEC make contact with the epithelial surface. Mouse models of UTI have shown that the initial influx of PMNs occurs within 2 hours following challenge with UPEC (Haraoka, Hang et al. 1999). The recruitment of PMNs during a UTI is critical to the clearance of

UPEC from the urinary tract (Haraoka, Hang et al. 1999). PMNs are the most potent antimicrobial cells in the host, and they have the capacity to generate particularly toxic metabolic products that can rapidly inactivate pathogens. The presence of PMNs in patient urine (called pyuria) is frequently observed during a UTI; whether such PMNs are functional remains controversial. The PMNs must be recruited from the circulation into the tissue via chemokines such as IL-6 and IL-8 (MIP2 α in mice) that are secreted by epithelial cells.

Cytotoxic Necrotizing Factor Type 1

Discovery of CNF1 and phenotypic effects on tissue culture cells

In 1983 Caprioli described the existence of a factor, distinct from the known heat stable, heat labile and Shiga toxins expressed by *E. coli*, that was present in the stools of children hospitalized with diarrhea (Caprioli, Falbo et al. 1983). In cell culture assays, the factor caused enlargement and multinucleation of cells when sonic extracts of bacteria were tested, and prolonged incubation of cells with these extracts resulted in cell death (Caprioli, Falbo et al. 1983). Intradermal injection of the factor into rabbits caused an indurated ulcer with a necrotic center and death of the animals within 48 hours; animals that died showed a diffuse pattern of hemorrhage at autopsy with no specific target organ identified (Caprioli, Falbo et al. 1983). All bacteria examined in the Caprioli study that were positive for the new factor were also hemolytic; however, the effects of this factor

could be separated from the hemolytic activity by chromatography (Caprioli, Falbo et al. 1983). All toxic activity was lost when samples of the factor were heated, a finding that suggested that the substance responsible for the effects observed in cells and animals was a protein (Caprioli, Falbo et al. 1983). Based on the cytotoxic and necrotizing activity of the factor, Caprioli and co-workers designated this putative protein CNF for Cytotoxic Necrotizing Factor (Caprioli, Falbo et al. 1983). Later studies identified a second toxin with similar phenotypic effects encoded on the Vir-plasmid of diarrheogenic *E. coli* recovered from calves (De Rycke, Guillot et al. 1987). Some of the features of these two toxins are listed in Table 2. The purification of both CNF and the newly identified factor led to studies that revealed that the two toxins were serologically related and that both produced similar phenotypes in cell culture. Therefore, CNF was renamed CNF1 and the Vir-plasmid associated toxin was designated CNF2 (De Rycke, Gonzalez et al. 1990). Both CNF1 and CNF2 induce similar phenotypic changes in intoxicated cells, such as cellular enlargement and extensive actin rearrangements. In animal models, CNF1 and CNF2 induce dermonecrosis in rabbit, mice, and guinea pigs. There are also several differences between the toxins. In cell culture, CNF1 evokes extensive multinucleation in some intoxicated cells (Figure 2) while CNF2 induces a lesser degree of multinucleation (Horiguchi 2001). An additional effect of CNF1 intoxication is the induction of apoptosis in a cell line derived from bladder epithelial cells; this effect has not been reported in other cell lines and may represent a unique response of uroepithelial cells to CNF1 intoxication (Mills, Meysick et al. 2000).

Table 2. Comparison of CNF1 and CNF2.

	CNF1	CNF2
Location	Chromosome	Plasmid
Weight (kDa)	115	115
Stress fiber formation	Yes	Yes
Multinucleation	Yes, extensive	Yes, limited
Fluid accumulation in rabbits	No	Yes
Mouse footpad necrosis	Yes	Yes
Predominately from	Human	Ruminant

In animal models, CNF1 produces moderate necrosis in both rabbit skin test and mouse footpads while CNF2 induces intense necrosis in the rabbit skin test but not the mouse footpad. Both toxins have been isolated from diarrhea specimens; however, only CNF2 has been shown to induce fluid accumulation in the rabbit ileal loop test (Caprioli, Falbo et al. 1983; De Rycke, Gonzalez et al. 1990). Despite the decades that have elapsed since the identification of CNF1 and CNF2, the precise role of these toxins in pathogenesis still remains unclear. Some animal studies have suggested that CNF1 may have a more significant role in extraintestinal infections such as UTI (Rippere-Lampe, O'Brien et al. 2001) and acute bacterial prostatitis (Rippere-Lampe, Lang et al. 2001) rather than intestinal disease (Elliott, Srinivas et al. 1998), while CNF2 appeared principally involved in ruminant diseases (Van Bost, Roels et al. 2001). More details on the potential role of CNF1 in the pathogenesis of UTIs are presented below.

Cell binding and enzymatic activities of CNF1

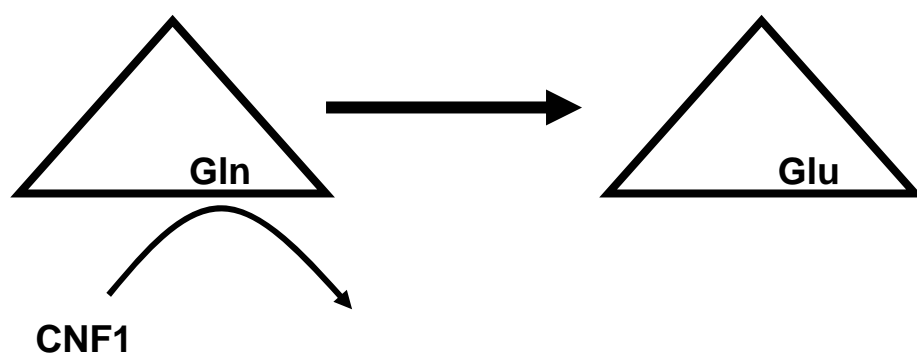
CNF1 and CNF2 are produced as single chain AB toxins with apparent molecular weights of 115 kDa. The single polypeptide chain consists of the binding or B domain located at the N-terminus, a hypothesized transmembrane domain, and the enzymatic or A domain at the C-terminus (Horiguchi 2001). Chung and colleagues identified the cellular receptor for CNF1 when they screened a cDNA library from human brain

microvascular endothelial cells (HBMEC) in a yeast two-hybrid system. They used the N-terminal domain of CNF1 as bait and identified the 37 kDa laminin receptor precursor protein (37LRP) as a CNF1 receptor (Chung, Hong et al. 2003). Additional data that support the role of 37LRP as a receptor came from the reduced invasion of HBMEC by CNF1-expressing *E. coli* when excess purified 37LRP was present; however the failure to completely block invasion suggested that an additional cellular receptor may also be present (Chung, Hong et al. 2003). The 37LRP is expressed in both the cytoplasm and on the plasma membrane of eukaryotic cells. In the cytoplasm, 37LRP is a ribosome-associated protein of unknown function; when expressed on the surface 37LRP has been shown to interact with laminin in the extracellular matrix (Montuori and Sobel 1996; Kim, Chung et al. 2005). The 37LRP is also the precursor to the mature 67 kDa laminin receptor (67LR) and, when post-translationally modified by acetylation, 37LRP forms dimers of approximately 67 kDa that are expressed on the surface of cells (Kim, Chung et al. 2005). The primary function of the 67LR is the stabilization of laminin binding to cell surface integrins (Menard, Tagliabue et al. 1998). The 67 kDa laminin receptor was later identified by Kim as an additional receptor for CNF1 (Kim, Chung et al. 2005). In addition to demonstrating by far Western blotting and co-immunoprecipitation that 67LR could interact with CNF1, Kim and colleagues also showed that 67LR can interact with CNF1. (Kim, Chung et al. 2005).

The enzymatic activity of CNF1 is better characterized than the target-cell-binding function of the toxin. The A domain of this A:B toxin contains deamidase activity that directly modifies the Rho family of small GTP binding proteins (Figure 2). The evidence

Figure 2. Enzymatic activity of CNF1.

The Rho family GTPases are rendered constitutively active by the deamidation of the enzymatically active glutamine residue by CNF1. When bound to GTP, the Rho family GTPases are in an active conformation, and when bound to GDP they are in an inactive conformation. The deamidation of Gln 63 in RhoA and Gln 61 in Rac and Cdc42 prevents the GTPase from hydrolyzing GTP into GDP and thus renders the Rho GTPase constitutively active.



for the involvement of Rho family proteins in CNF1 intoxication came from the phenotype of CNF1 intoxicated cells. In these cells, F-actin accumulates and abundant actin stress fiber formation is observed. The polymerization state of actin is controlled in part by the activation status of Rho family proteins, an observation that suggests that Rho family proteins may be targets of CNF1 (Fiorentini, Arancia et al. 1988). Work by Schmidt showed that CNF1 alters the GTPases activity of RhoA (Schmidt, Sehr et al. 1997). In that same study, the investigators evaluated CNF1-treated RhoA by mass spectrometry and showed that the toxin-exposed RhoA gained a mass of 1 dalton compared to untreated RhoA. Further analysis revealed that Gln⁶³ in RhoA was deamidated to Glu by CNF1. The CNF1 deamidation of RhoA at Gln⁶³ explained both the change in RhoA activity and the shift in molecular weight because Gln⁶³ is required for GTP hydrolysis and deamidation of glutamine increases its molecular weight 1 dalton. When a mutant construct of RhoA that incorporated the CNF1-catalyzed change was microinjected into cells, abundant stress fiber formation occurred; however, no multinucleation was observed. That the complete intoxicated phenotype was not reproduced by microinjection of modified RhoA suggested to the authors of the report (Schmidt, Sehr et al. 1997) that additional targets of CNF1 existed. Accordingly, Lerm et. al (Lerm, Selzer et al. 1999) identified Cdc42 and Rac1 as additional substrates for CNF1 catalyzed deamidation. The specific residue deamidated in Cdc42 and Rac1 were found to be Gln⁶¹, an amino acid that is functionally equivalent to Gln⁶³ in RhoA.

Export of CNF1

A substantial body of work has focused on the biological activity of CNF1 and, to a lesser extent, the role of this molecule in pathogenesis. Still unclear is the mechanism of CNF1 release from the bacteria. CNF1 does not contain a recognized signal sequence, and no studies have directly examined the release of CNF1 from UPEC. However, some investigators have suggested that CNF1 may be present on the outer membrane of the *E. coli* (Chung, Hong et al. 2003; Landraud, Gibert et al. 2003). Indeed, Landraud and colleagues hypothesized that CNF1 may be an outer membrane protein based on data from their study on the regulation of CNF1 expression (Landraud, Gibert et al. 2003). In the course of their investigation, Landraud and colleagues discovered that the transcriptional activator RfaH had a significant role in *cnf1* transcription (Landraud, Gibert et al. 2003). This led them to suggest that CNF1 may be destined for the outer membrane of *E. coli* because RfaH is known to control the expression of many outer membrane proteins in *E. coli* (Landraud, Gibert et al. 2003). Gram negative bacteria are known to release fragments of their outer membrane as membrane vesicles during growth (Beveridge 1999). In fact, Kesty and colleagues recently demonstrated that biologically active heat labile toxin (LT), a toxin that also has no recognized secretion pathway, can be delivered to eukaryotic cells via outer membrane vesicles (Kesty, Mason et al. 2004). The proposal that CNF1 is a part of the outer membrane is significant because it implies that CNF1 may be released with fragments of the outer membrane.

Epidemiology of UPEC that produce CNF1 and potential role of CNF1 in pathogenesis of UTIs

Several lines of evidence implicate CNF1 in the pathogenesis of UTIs caused by UPEC. First, several epidemiological studies link CNF1 expression by *E. coli* to the development of more severe and invasive UTIs. For example, Goullet and colleagues demonstrated that the production of CNF1 was also strongly associated with the more virulent B₂ lineage of pathogenic *E. coli* (Goullet, Picard et al. 1994) that includes *E. coli* serogroups O4 and O6 (Goullet, Picard et al. 1994). Further support for the concept that CNF1-expressing *E. coli* are more virulent comes from Blanco and colleagues (Blanco, Blanco et al. 1994). During an investigation of blood cultures obtained from urosepsis and non-urosepsis patients, these investigators discovered that the majority of serogroup O4 and O6 urosepsis isolates carried *cnf1*, a finding that suggests that *E. coli* carrying *cnf1* may be more likely to cause severe disease than *E. coli* that don't carry *cnf1* (Blanco, Blanco et al. 1994). Additional epidemiological analysis by Foxman again demonstrated a significant association between *cnf1* and the development of UTI in women (Foxman, Zhang et al. 1995). Finally, Yamamoto found that more than 60% of UPEC from symptomatic UTI carried *cnf1* (Yamamoto, Tsukamoto et al. 1995).

A second line of evidence in support of the role of CNF1 in the pathogenesis of UPEC-incurred illness comes from a mouse model of ascending UTI (Rippere-Lampe, O'Brien et al. 2001). In this mouse UTI model, a wild-type CNF1 expressing UPEC, a *cnf1* isogenic mutant derived from it and a complemented clone of the mutant were

compared for capacity to evoke disease in single-strain intraurethral challenge experiments. These researchers found that CNF1 expression by the wild-type and complemented mutant when compared to the mutant, resulted in net replication in the bladder and urine of the mice three days after inoculation and an enhanced inflammatory response in the bladder (Rippere-Lampe, O'Brien et al. 2001). Moreover, the wild-type and complemented mutant also elicited an enhanced inflammatory response characterized by the presence of many PMNs compared to the isogenic mutant in the mouse bladder (Rippere-Lampe, O'Brien et al. 2001). In that same study, mice were challenged simultaneously with both wild-type and its *cnf1* isogenic mutant; the wild-type outgrew the isogenic mutant (Rippere-Lampe, O'Brien et al. 2001). Lastly, these investigators reported that wild-type UPEC demonstrated enhanced net replication compared to the mutant when co-incubated with purified human neutrophils (Rippere-Lampe, O'Brien et al. 2001). Collectively, these results indicate that CNF1 expression by UPEC augments the acute inflammatory response during UTI and further suggest that CNF1 expression by UPEC enhanced their survival when co-incubated with PMNs.

A rat model of acute bacterial prostatitis provides another example of the role of CNF1 in UPEC pathogenesis (Rippere-Lampe, Lang et al. 2001). When male rats were transurethrally challenged in this study neither the wild-type nor the *cnf1* mutant UPEC strains had a growth advantage; however, the prostates of the rats infected with the wild-type UPEC were grossly enlarged and showed histological signs of extensive neutrophil influx and tissue damage compared to the prostates of rats infected with the *cnf1* mutant (Rippere-Lampe, Lang et al. 2001). Collectively, the evidence from epidemiological and

animal model studies supports a role for CNF1 as a virulence factor in UPEC mediated infections.

CNF1 and Rho family GTPases

Both CNF1 and CNF2 are members of a group of toxins that exert their effects through the modification of small GTPases. The small GTPases serve as signal transduction molecules in eukaryotic cells and control the spatial and temporal coordination of a large array of cellular processes. CNF1, CNF2 and the dermonecrotic toxin (DNT) from *Bordetella spp.* are unique in the family of small GTPase modifying toxins because they activate rather than inactivate the small GTPases through direct covalent modification of the GTPase. This novel mode of toxin activity is specific for these three toxins, the remaining members of the small GTPase-modifying toxin family act through ADP-ribosylation or glycosylation. Other toxins that activate the small GTPases do so in an indirect fashion rather than through direct modification of the GTPase. Although CNF1 and CNF2 have similar enzymatic activity and targets, CNF2 has limited demonstrated involvement in human disease and will not be discussed further.

The small GTPase targets of CNF1 belong to the Ras superfamily of low molecular mass GTPases (Lerm, Schmidt et al. 2000) and are members of the Rho sub-family (Boquet 2000). There are over 10 identified members of the Rho sub-family, although only three, RhoA, Rac1, Cdc 42, have been confirmed as substrates for CNF1 activity. The Rho family proteins function as molecular switches within eukaryotic cells and

initiate various intracellular signals (Boquet 2000). All members of the Ras superfamily share certain structural features essential for their proper functioning. Among the shared features are two loops known as the switch I and the switch II domains (Lerm, Schmidt et al. 2000). The switch I region undergoes extensive conformational change when the GTPases are bound to GTP or GDP; when the GTPases are bound to GTP they are in an active state and, when bound to GDP they are inactive (Figure 3). The conformational changes associated with the switch I region enable the GTPase to interact with signaling partners, and this region of the molecule is also known as the effector region. The GTPases cycle between active and inactive forms, a phenomenon that allows the cell to control the duration and location of various intracellular signals. The switch between active and inactive forms involves the GTPase, accessory molecules known as guanine nucleotide exchange factors (GEFs), guanine nucleotide activating proteins (GAPs) and guanine nucleotide disassociation inhibitors (GDIs). There are many different GEFs, GAPs and GDIs and each of them respond to different environmental stimuli; nevertheless, each type of accessory molecule exerts control over the activation status of the Rho family in a similar fashion. In response to diverse stimuli, the GTPase is released from the GDI and the GEFs facilitate the exchange of GDP for GTP (Figure 4). The release of the GTPase from the GDI exposes the GTPase fatty acid tail, an event that allows the GTPase to insert into cell membranes. The conformational changes induced in the GTPase through the binding of GTP permits the GTPase to interact with downstream

Figure 3. Structural changes in Rho family proteins when bound to GTP.

The Rho family GTPases share two important regions, the switch I and switch II domains which have specific functions in the Rho GTPases. The switch I domain changes conformation when the GTPase is bound to GTP; the structural changes allow the GTPase to interact with downstream effectors such as kinases. The switch II domain contains the nucleotide-binding pocket of the GTPases and possesses the enzymatically active Gln residue responsible for the hydrolysis of GTP to GDP. Adapted from (Boquet 2000).

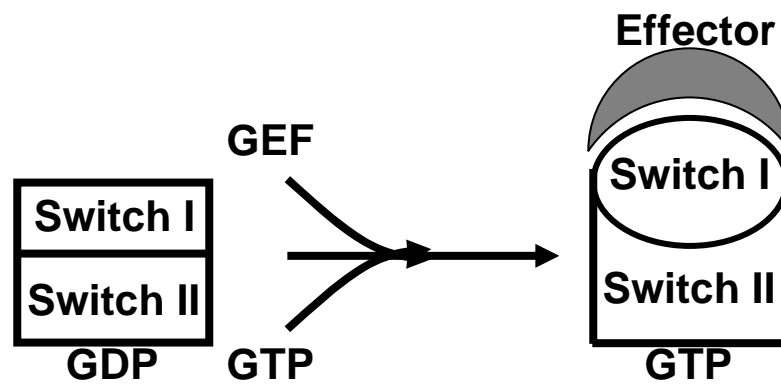
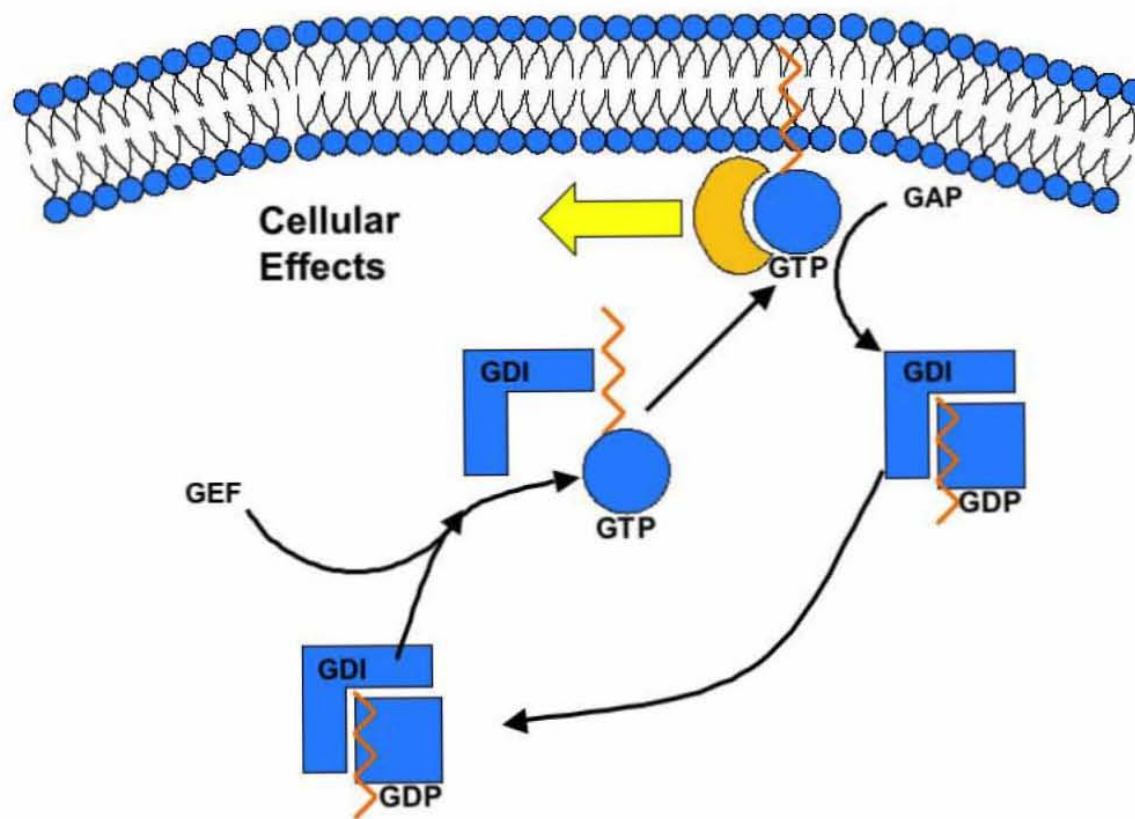


Figure 4. Rho GTPase cycles control cellular function.

Rho GTPases bound to GDP are sequestered in the cytosol by guanine nucleotide disassociation inhibitors (GDI) that block the fatty acid tail on the Rho protein. Cell stimulation releases the Rho GTPase from the GDI and activates guanine nucleotide exchange factors (GEF) that facilitate the exchange of GTP for GDP. Once bound to GTP, the switch I or effector region undergoes extensive conformational change that allows it to interact with other proteins. The fatty acid tail that is exposed when the GTPase is released from the GDI allows the GTPase to insert into cellular membranes. The active- and membrane- bound GTPase can now activate a variety of downstream signaling partners via protein-protein interaction with the switch I region. Each GTPase possesses an intrinsic rate of GTP hydrolysis that is enhanced in the presence of guanine nucleotide activating proteins (GAP). The hydrolysis of GTP to GDP deactivates the GTPase and terminates signaling; the GDI extracts the GTPase from the membrane and returns it to the cytosol and the activation/deactivation cycle begins again.



partners such as protein kinases, lipid kinases, phospholipases and a variety of adaptor proteins (Aktories and Barbieri 2005). The interaction of the GTPase with downstream partners allows the activated GTPase to activate various cellular processes. Each GTPase has an intrinsic rate of GTP hydrolysis that is greatly enhanced in the presence of GAPs; after GTP hydrolysis the GTPases are extracted from the membrane by the GDI and, now bound to GDP and with the fatty acid tail blocked the GTPase is returned to the cytosol in an inactive conformation which terminates the signal. The GTPase cycle between active and inactive forms allows the GTPase to provide temporal control over cellular events. Rho family activation occurs in discrete regions of cells through a mechanism that is not completely understood. Current studies support the hypothesis that the spatially-restricted activation of Rho proteins occurs because each GEF must interact with cell membranes before it can facilitate the exchange of GDP for GTP. This theory predicts that the GEFs limit the activation of the Rho family to specific regions of the cell in response to stimuli. Whatever the mechanism behind the discrete activation of Rho GTPases, the interaction of the activated Rho family members with various downstream effectors results in cellular changes such as actin polymerization, gene transcription, extension of membrane protrusions and other such processes.

The capacity of the Rho family to hydrolyze GTP is dependent on the proper placement of a water molecule in the nucleotide-binding pocket located in the switch II region. Once the water molecule is positioned properly, the GAPs help stabilize that water molecule which, in turn, allows the GTP hydrolysis to proceed at an increased rate. In the Rho-family switch II domain, Gln 63 in Rho and Gln 61 in Rac and Cdc42 are

responsible for the placement of the water molecule; these amino acids are also the specific residues deamidated by CNF1. The CNF1-mediated deamidation therefore prevents the proper placement of a water molecule and thus blocks the hydrolysis of GTP to GDP. This blockage then results in the constitutive activation of the Rho family GTPases. The cellular effects observed in CNF1-intoxicated cells such as cellular enlargement, multi-nucleation and extensive actin polymerization are some of the phenotypic changes in cells that result from the constitutive activation of Rho family GTPases.

To date, only members of the Rho family have been identified as targets of CNF1 activity. The reason for this specificity is not completely clear although some data suggest that a sequence unique to the Rho family is required for CNF1 recognition (Lerm, Schmidt et al. 1999; Flatau, Landraud et al. 2000). This sequence, D⁵⁹ TAGQ⁶³ EDYDRL⁶⁹, is located in the switch II domain and is present in all members of the Rho family (Lerm, Schmidt et al. 1999; Flatau, Landraud et al. 2000). The conservation of this sequence suggests that all members of the Rho family may be substrates of CNF1 (Lerm, Schmidt et al. 1999). Mutations outside of this region do not affect CNF1 deamidation, although substitutions at Arg⁶⁸ abolish CNF1 activity (Flatau, Landraud et al. 2000). The results from these amino acid change studies suggest that CNF1 recognizes a narrow section of the GTPase rather than an extended structure and that the GTPase Arg⁶⁸ in the GTPase is an important residue for CNF1 activity (Flatau, Landraud et al. 2000).

Each of the modified small GTPases is associated with certain cellular changes that can be partially reproduced by microinjection of modified RhoA, Rac1 or Cdc42 individually. For example, modified RhoA evokes membrane ruffles and actin stress fibers, modified Rac1 causes the formation of lamellipodia and modified Cdc42 results in the formation of filopodia. The multinucleation phenotype is a unique feature of CNF1 intoxication and is most likely the result of the combined effects of modified Rho family members that prevent cytokinesis but allow DNA synthesis to continue. These CNF1-mediated phenotypic changes are the most readily observable alterations in CNF1 intoxicated cells; however, intoxicated cells also respond to modified Rho family members by degradation of these modified Rho proteins through a proteasome dependent pathway. Proteasome degradation of modified Rac1 was demonstrated by Lerm and colleagues when they intoxicated HeLa cells with CNF1 and observed a decrease in the amount of Rac1 while mRNA levels for Rac1 were not diminished in these intoxicated cells (Lerm, Pop et al. 2002). When the HeLa cells were treated with the proteasome inhibitor lactocystin no loss of Rac1 was detected, a finding that suggests that the loss of Rac1 was due to a proteasome-dependent pathway (Lerm, Pop et al. 2002). Additional studies showed that the proteasomal degradation of Rac1 occurred in the nucleus (Lanning, Daddona et al. 2004). The degradation of Rac1 could be inhibited by replacing the Rac1 polybasic region that contains a nuclear localization signal (NLS), with the polybasic region of RhoA that does not contain an NLS (Lanning, Daddona et al. 2004). The proteasomal degradation was later shown to depend on the interaction of Rac1 with an unidentified effector protein; the degradation is also isotype specific because only

Rac1 was degraded while Rac2 and Rac3 were not (Pop, Aktories et al. 2004). The proteasomal destruction was also dependent on the presence of a specific sequence in the polybasic region that resembled a recently defined mitotic destruction box found on cyclins. The putative mitotic destruction box identified on Rac1 was not complete, although mutations in this region blocked the proteasomal degradation of deamidated Rac1 (Pop, Aktories et al. 2004). The putative mitotic destruction box was also identified on RhoA but not on Cdc42; Rho A is degraded by the proteasome although not nearly to the same extent as Rac1 while Cdc42 is not degraded at all (Pop, Aktories et al. 2004).

The cellular consequences of constitutive activation followed by degradation of Rac1 may modulate the inflammatory response in the host. Rac1 and Cdc42 were found to have a role in regulating the expression of MIP3 α , IL-6 and IL-8 in addition to other inflammatory mediators when endothelial cells were intoxicated with CNF1 (Munro, Flatau et al. 2004). The expression of MIP3 α was initially elevated, then, concurrent with the loss of Rac1 via proteasomal degradation, the expression of this inflammatory mediator was diminished; cells treated with proteasomal inhibitors demonstrated continued expression of MIP3 α (Munro, Flatau et al. 2004). The increased expression of inflammatory mediators, especially IL-8, has important consequences for the host because this particular chemokine acts on polymorphonuclear neutrophils and stimulates their migration into inflammatory foci.

Polymorphonuclear neutrophils and Rho GTPases

Polymorphonuclear neutrophils (PMN) are the most potent antimicrobial cells in the body and alterations in their antimicrobial capacity can place the host at increased risk of infection (Witko-Sarsat, Rieu et al. 2000). These phagocytic cells are derived from granulocytic precursors in the bone marrow where they progress through various maturation stages. As the PMNs mature in the bone marrow, they develop their full complement of lytic enzymes contained in different type of granules (Borregaard 1997). Each stage of maturation is marked by the development of different types of granules followed by the eventual segmentation of the nucleus that is a characteristic feature of PMNs (Figure 5). The mature neutrophils leave the bone marrow and enter the large blood vessels where they become part of the circulating pool of PMNs ready to respond to inflammatory stimuli (Witko-Sarsat, Rieu et al. 2000). The life span of an unstimulated, mature PMN is usually less than 48 hours. In the absence of inflammatory stimuli that will extend its life span, the PMN will undergo apoptosis and will be removed from the body (Wang, Scheel-Toellner et al. 2003). When the host cells encounter a pathogen such as UPEC, they release inflammatory mediators that stimulate endothelial cells. Endothelial cells in the vicinity of the inflammatory event express P-selectin within minutes of stimulation, then later the endothelium expresses E-selectin (Witko-Sarsat, Rieu et al. 2000). The induced P- and E-selectin expression on endothelial surfaces interacts with constitutively-expressed L-selectin present on the PMN surface. Interaction between endothelial and PMN selectins results in the PMN

Figure 5. Photomicrograph of a polymorphonuclear neutrophil.

The photomicrograph depicts a polymorphonuclear neutrophil (PMN) interacting with uropathogenic *Escherichia coli* (UPEC). The PMN was elicited from a C3H/HeOuJ mouse following an intraperitoneal injection of thioglycolate. The multilobed nucleus is visible and appears in a circular shape because the PMN was flattened by centrifugation prior to staining.



first rolling along, then tethering to the endothelial surface. The host simultaneously releases IL-8, a CXC chemokine that specifically recruits PMNs to the inflamed site. Signals transmitted through IL-8 receptors on the PMN surface initiate an anti-apoptotic program in the PMN (Kettritz, Gaido et al. 1998; Dunican, Grutkoski et al. 2000) as well as firm adhesion and spreading of PMNs on the endothelial surface (Witko-Sarsat, Rieu et al. 2000). Migration through the endothelial barrier occurs at junctions between endothelial cells and requires interactions between cell adhesion molecules present on the endothelial cells and PMNs. Once PMNs have passed through the endothelial barrier they migrate along a gradient of immobilized chemoattractants through the process of chemotaxis.

Neutrophils that respond to inflammatory signals generated during a UTI must cross the polarized epithelial surface of the urinary tract. Basolateral to apical migration of the PMN involves the disruption of epithelial tight junctions and the interaction of PMN β -2 integrins such as LFA-1 with host epithelial cell counter receptors like ICAM-1 (Vicente-Manzanares and Sanchez-Madrid 2004). Once at the inflammatory foci, PMNs perform their antimicrobial function by phagocytosing and inactivating the pathogen. The recruitment of PMNs to inflammatory sites and the PMN antimicrobial response are complex events that require the coordinated engagement of cellular receptors and localized actin polymerization through processes that are not completely understood. However, the PMN functions of chemotaxis, phagocytosis, and pathogen inactivation share a common link because the Rho family GTPases control each of these key PMN responses.

Rho GTPases and neutrophil response – *chemotaxis*

Neutrophil chemotaxis involves at least three distinct cellular processes in the neutrophil. First, the neutrophil modulates its adhesive properties through integrin affinity and avidity maturation that allows the neutrophil to adhere firmly to the endothelium (Witko-Sarsat, Rieu et al. 2000). Second, the neutrophil becomes polarized and develops a distinct front and back (Srinivasan, Wang et al. 2003). Finally, the neutrophil goes through repeated adhesive and de-adhesive events that allow it to crawl along a surface in the direction of increasing chemoattractant concentration while it maintains a polarized front (Witko-Sarsat, Rieu et al. 2000).

The engagement of integrins initiates a multitude of signals in neutrophils. Some of these signals activate Rac and Cdc42 through the recruitment of the GEFs DOCK180 and α -PIX (Schwartz and Shattil 2000). The activation of Rac and Cdc42 leads to the polymerization of actin at regions of integrin engagement (Vicente-Manzanares and Sanchez-Madrid 2004). Localized depolymerization of actin leads to transient release of integrins from the cytoskeleton, an event that allows integrins to migrate within the plane of the plasma membrane and form clusters (Kucik, Dustin et al. 1996). The clusters of integrins result in increased integrin avidity (Kucik, Dustin et al. 1996); subsequent re-attachment of integrins to the actin cytoskeleton enhances the affinity of individual integrins in the cluster and results in stronger neutrophil adhesion to the endothelium

(Schwartz and Shattil 2000; Vicente-Manzanares and Sanchez-Madrid 2004). Exposure of the neutrophil to chemokines and other chemoattractants on the surface of endothelial cells induces the development of a polarized front in the neutrophil. The development of the polarized front is dependent on a positive feedback loop that involves activated Rac1, F-actin and phosphatidylinositol 3,4,5-triphosphate (PIP₃) (Srinivasan, Wang et al. 2003). Sun and colleagues extended Srinivasan's results by the use of *Rac1*^{-/-} and *Rac2*^{-/-} mice to demonstrate that the development of the polarized front is also dependent on Rac2, an isoform of Rac found only in myeloid cells such as neutrophils (Sun, Downey et al. 2004). They further demonstrated that Rac1 is involved in the detection of chemoattractants and the increase in PIP₃ concentration at the front of the neutrophil, while Rac2 was required for the polymerization of actin and the generation of contractile forces involved in neutrophil propulsion (Sun, Downey et al. 2004). Cdc42 appears to have a specialized role in the localization of actin polymerization to the newly developed polarized front through its interaction with PAK1, a Rho family GTPase effector protein (Li, Hannigan et al. 2003). RhoA is excluded from the development of the polarized front and segregates to the rear of the neutrophil where it is hypothesized to participate in the generation of contractile forces that propel the neutrophil forward (Xu, Wang et al. 2003).

Rho GTPases and neutrophil response – *phagocytosis*

Neutrophil phagocytosis involves two different classes of cell surface receptors (Witko-Sarsat, Rieu et al. 2000) and, based on the surface receptor utilized, phagocytosis can be classified as either type 1 or type 2 (Vicente-Manzanares and Sanchez-Madrid 2004). Both type 1 and type 2 phagocytosis require pathogen opsonization; IgG opsonization and ligation of FcγR is required for type 1 phagocytosis while opsonization by C3b and interaction with CR3 is necessary for type 2 phagocytosis (Caron and Hall 1998; Vicente-Manzanares and Sanchez-Madrid 2004). Both types of phagocytosis require actin cytoskeleton rearrangements that result from the recruitment of signal transduction molecules to the site of pathogen contact. The essential role of actin polymerization in both type 1 and type 2 phagocytosis has been demonstrated by the inhibition of phagocytosis when cytochalasin is present. Cytochalasins are fungal toxins that specifically bind to actin filaments to prevent their elongation and thereby block actin polymerization. In addition to actin polymerization, type 2 phagocytosis requires supplementary inflammatory signals for efficient phagocytosis (Underhill and Ozinsky 2002). The additional signals required for CR3-mediated phagocytosis include bacterial products such as formyl methionyl peptides, LPS, and adherence to surfaces (Witko-Sarsat, Rieu et al. 2000; Underhill and Ozinsky 2002). The stimuli likely initiate protein kinase C (PKC)-dependent signaling because phorbol esters, which directly stimulate PKC, can stimulate CR3-dependent phagocytosis *in vitro* (Underhill and Ozinsky 2002).

Investigations into the role of Rho GTPases in phagocytosis have demonstrated that specific Rho family members are involved in each type of phagocytosis (Caron and Hall 1998; Massol, Montcourrier et al. 1998). The involvement of different Rho GTPases has been hypothesized to be partly responsible for the different manner in which type 1 and type 2 phagocytosis proceeds (Caron and Hall 1998). Caron and Hall used transfected COS cells that expressed either Fc γ R or CR3 and mutant Rho GTPases to demonstrate the requirement for different Rho family members in each type of phagocytosis (Caron and Hall 1998). When RhoA activity was abolished using either dominant negative RhoA or C3 transferase, the transfected COS cells were unable to phagocytose particles in a CR3-dependent fashion; however, the same cells could phagocytose particles via Fc γ R (Caron and Hall 1998). When dominant negative Rac1 and Cdc42 were present in the transfected COS cells, Fc γ R-mediated phagocytosis was abolished (Caron and Hall 1998). The results from Caron and Hall demonstrate that type 1 phagocytosis that involves Fc γ Rs requires Rac1 and Cdc42 activation (Caron and Hall 1998). These findings also provide an explanation for the zipper-like fashion in which the neutrophil lamella extend around the opsonized particle eventually enveloping it on the opposite side (Kaplan 1977). In contrast, type 2 phagocytosis requires the CR3 receptor and RhoA activation but does not need Rac1 or Cdc42 to be activated. Unlike type 1 phagocytosis, complement-opsonized particles appear to sink into the neutrophil (Kaplan 1977). The activation of RhoA at the site of pathogen contact may partly explain this morphologically distinct form of phagocytosis. RhoA activation generates contractile forces through actin/myosin contraction; thus particles attached to the neutrophil surface

via CR3 are pulled into the cell and appear to sink into the neutrophil. Phagocytosis is completed when the opsonized particle is completely surrounded and the neutrophil membrane has fused. This fusion event produces the intra-neutrophilic phagosome in which the opsonized particle is now confined. Phosphoinositide 3-kinase (PI3K) appears essential to phagosome closure based on experiments in which PI3K was inhibited by pharmacologic inhibition or microinjection of inhibitory antibodies and in mouse knock-out studies (Underhill and Ozinsky 2002). The role if any, of Rho GTPases in the final step of membrane fusion is less clear. Massol and colleagues suggested that Rac1 and/or Cdc42 may recruit protein tyrosine phosphatases to the phagocytic cup based on their observation that tyrosine phosphorylated proteins were increased and phagosome closure inhibited compared to controls when dominant negative Rac1 and Cdc42 were transfected into phagocytosing mast cells (Massol, Montcourrier et al. 1998). This concept is strengthened by the observation that the Cdc42 effector protein Wiskott-Aldrich syndrome protein (WASp) interacts with a cytoskeletal protein that associates with protein tyrosine phosphatases (Massol, Montcourrier et al. 1998).

Rho GTPases and neutrophil response - *NADPH oxidase activation*

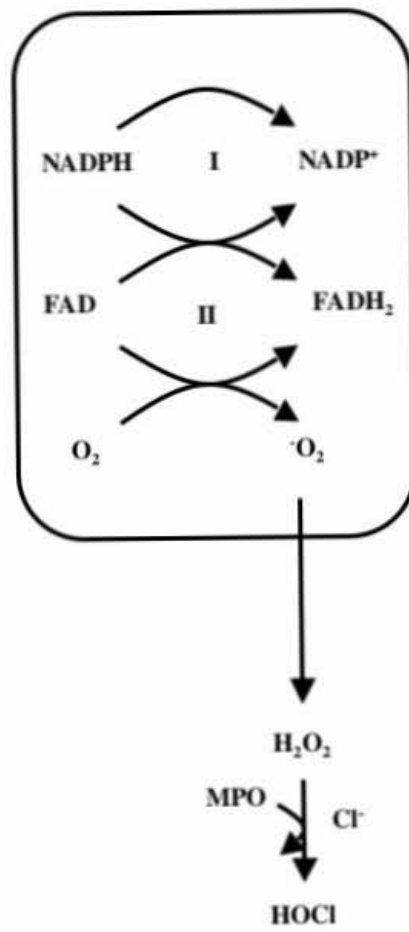
The neutrophil antimicrobial response culminates in the inactivation of phagocytosed pathogens. Multiple phagocyte components are involved in the inactivation of pathogens but they can be broadly characterized as oxygen-independent and oxygen-dependent processes. The oxygen-independent responses include the

mobilization of various types of neutrophil granules that contain lytic enzymes and cationic antimicrobial peptides to the newly formed phagosome. These compounds weaken the bacterial membrane and degrade proteins essential to bacterial viability. Oxygen-dependent pathogen inactivation requires the generation of reactive oxygen species (ROS) within the phagosome, and ROS can react with granule contents to generate additional toxic molecules. Because the phagocytosed pathogen occupies almost the entire phagosome, the remaining small volume ensures that the toxic end products generated from the chemical reactions between granule contents and ROS can reach lethal concentrations. The importance of ROS generation in host defense is exemplified by patients whose neutrophils are unable to generate ROS; these patients frequently suffer from multiple recurrent infections (Witko-Sarsat, Rieu et al. 2000). Central to the generation of ROS is the assembly of the nicotinamide adenine dinucleotide phosphate (NADPH) oxidase, also known as the phagocyte oxidase (phox), a cellular event that requires Rho GTPase participation (Nisimoto, Freeman et al. 1997; Diebold and Bokoch 2001; Bokoch and Diebold 2002).

The NADPH oxidase is an enzyme complex that consists of a membrane-bound flavocytochrome (cytochrome b₅₅₈) and cytosolic components (Rac2, p67^{phox}, p47^{phox}) (Bokoch and Diebold 2002). Activation of the neutrophil by inflammatory stimuli results in the phosphorylation of p47^{phox}; the multiple phosphorylation events are believed to disrupt inhibitory intramolecular interactions and allow p47^{phox} to interact with other components of the NADPH oxidase (Bokoch and Diebold 2002). The fully assembled oxidase generates superoxide through two electron transfer reactions (Figure 6).

Figure 6. Electron transfer reactions and generation of oxygen radical.

The phagocyte oxidase catalyzes two separate electron transfer reactions prior to generating toxic oxygen products that inactivate pathogens. Reaction I transfers electrons from NADPH to FAD to generate FADH_2 and reaction II transfers electrons from FADH_2 to molecular oxygen to generate the superoxide radical. The superoxide radical dismutates into hydrogen peroxide (H_2O_2), a substance that reacts with myeloperoxidase and chloride to produce hypochlorous acid (HOCl). Compared to superoxide and H_2O_2 , HOCl is the most potent antimicrobial compound generated through the oxygen dependent antimicrobial system in PMNs. Adapted from (Witko-Sarsat, Rieu et al. 2000)



Electrons are transferred from NADPH to FAD to create FADH₂; the second reaction transfers electrons from FADH₂ to molecular oxygen which, in turn, generates superoxide (Diebold and Bokoch 2001). Current models of NADPH oxidase activation indicate that p47^{phox} functions as an adaptor molecule that bridges the membrane bound cytochrome b₅₅₈ and p67^{phox} (Bokoch and Diebold 2002). The essential role of p47^{phox} in neutrophil antimicrobial function is best demonstrated in patients with chronic granulomatous disease (CGD) (Witko-Sarsat, Rieu et al. 2000). Neutrophils from approximately 30% of these patients do not have p47^{phox} and cannot generate ROS; accordingly, patients with CGD frequently experience recurrent bacterial infections (Witko-Sarsat, Rieu et al. 2000). The essential role of Rac2 in the generation of ROS has been demonstrated in neutrophils derived from *Rac2*^{-/-} mice (Li, Yamauchi et al. 2002) and from a patient with a point mutation in Rac2 rendering the protein non-functional (Gu, Jia et al. 2001); in each instance the neutrophils produced no or very little ROS in response to chemical stimuli. While the essential role of Rac2 has been clearly demonstrated, the specific function of Rac2 in the generation of ROS is ambiguous and three different molecular models have been proposed in an attempt to define the specific role of Rac2 in the NADPH oxidase (Nisimoto, Freeman et al. 1997; Gorzalczany, Sigal et al. 2000; Bokoch and Diebold 2002). The first two models view the role of Rac2 as an adaptor and differ only in whether or not Rac2 physically interacts with cytochrome b₅₅₈, while the third model views Rac2 as an active participant in both electron transfer reactions that generate superoxide. The first model, proposed by Lambeth and colleagues, views Rac2 as an adaptor that helps position the cytochrome activation

domain of $p67^{phox}$ in the proper orientation to allow the electron transfer reaction to proceed (Nisimoto, Freeman et al. 1997). This model is based on the results of a study by Lambeth and colleagues in which they utilized wild-type and mutant Rac1 in cell free studies of NADPH oxidase activation (Nisimoto, Freeman et al. 1997). The results of their study demonstrated that the Rac1 effector domain interacted with $p67^{phox}$ and not with other components of the oxidase system; loss of function mutations in the effector domain abolished or greatly reduced the interaction of Rac1 with $p67^{phox}$ and led to diminished NADPH oxidase activation (Nisimoto, Freeman et al. 1997). Mutations in the insert region of Rac1 had no effect on the binding of Rac1 to $p67^{phox}$ while these mutations greatly reduced the NADPH oxidase activity (Nisimoto, Freeman et al. 1997). Neither wild-type nor mutant Rac1 bound $p47^{phox}$, findings that suggested that Rac1 interacts with $p67^{phox}$ and possibly another component of the oxidase system such as cytochrome b_{558} (Nisimoto, Freeman et al. 1997). Based on these data, Lambeth and colleagues proposed their model in which Rac inserts into the neutrophil membrane and interacts with $p67^{phox}$, as well as cytochrome b_{558} to activate the NADPH oxidase (Nisimoto, Freeman et al. 1997). When a construct of Rac2 that lacked the insert domain was used in similar studies, no loss of oxidase activation was observed. This result suggested to the authors that an interaction via the Rac2 insert domain may not be essential NADPH oxidase activation (Bokoch and Diebold 2002). In support of this idea Pick and colleagues observed that Rac1 can bind with equal affinity to membranes devoid of cytochrome b_{558} as well as to membranes containing cytochrome b_{558} (Gorzalczany, Sigal et al. 2000). Further, they also demonstrated that a Rac1- $p67^{phox}$

chimera lacking the Rac1 insert domain did not affect the capacity of this chimera to supported oxidase activity (Gorzalczany, Sigal et al. 2000). Pick and colleagues then proposed a second model of Rac regulation of the NADPH oxidase in which Rac still functions as an adaptor molecule that positions p67^{phox}, but Rac does not physically associate with the cytochrome in this model (Gorzalczany, Sigal et al. 2000). Each of these groups used non-prenylated Rac1 in their experiments because non-prenylated Rac1 produced in bacteria can still interact with membranes via the polybasic region in cell-free experiments (Nisimoto, Freeman et al. 1997). However, the more physiologically relevant Rac2 isoform cannot activate the oxidase efficiently in cell-free systems unless it is prenylated (Nisimoto, Freeman et al. 1997). When Bokoch and colleagues employed prenylated Rac2 in their studies, a slightly different model emerged. In the Bokoch model, Rac2-GTP is required for both electron transfer reactions catalyzed by the NADPH oxidase (Diebold and Bokoch 2001). When Rac2-GDP was used, neither the first nor the second electron transfer reaction occurred (Diebold and Bokoch 2001). Only the first electron transfer reaction occurred when Rac2 and p67^{phox} mutants that could not interact with each other but could interact with cytochrome b₅₅₈ were used separately or together (Diebold and Bokoch 2001). This result demonstrated that Rac2 and p67^{phox} separately regulate the initial electron transfer reaction but the final electron transfer to molecular oxygen requires an interaction between Rac2 and p67^{phox} (Diebold and Bokoch 2001). A direct physical association between Rac2 and the cytochrome that was dependent on the Rac2 insert domain was also demonstrated (Diebold and Bokoch 2001). These observations led to the Bokoch model in which Rac2-GTP regulates the NADPH

oxidase at two levels. The first tier is through direct association between Rac2-GTP and cytochrome b_{558} that allows the first electron transfer reaction between NADPH and FAD. The second stage is through association with $p67^{phox}$, an interaction which aids the second electron transfer between $FADH_2$ and molecular oxygen which produces superoxide (Diebold and Bokoch 2001). The third model is attractive because it is based on data developed with the physiologically relevant prenylated Rac2 isoform and also because the regulation of the oxidase by Rac2 exclusively through its interaction with $p67^{phox}$ has been viewed as problematic in light of the weak interaction observed between purified Rac2 and $p67^{phox}$ (Bokoch and Diebold 2002). The conformational changes that might occur in cytochrome b_{558} after binding to Rac2-GTP may increase the affinity of Rac2 for $p67^{phox}$ and allow the second electron transfer to occur (Bokoch and Diebold 2002). While each model proposes different specific roles for Rac in NADPH oxidase activation, they all demonstrate that Rac-GTP is required for the activation of the phagocyte oxidase.

Chemical reactions between superoxide, myeloperoxidase delivered to the phagosome by granules, and chloride generate molecules with demonstrated lethal properties. Superoxide generated in the neutrophil can dismutate to form hydrogen peroxide (H_2O_2) although neither superoxide nor H_2O_2 are very lethal to bacteria (Rosen, Crowley et al. 2002). As shown in Figure 5, myeloperoxidase delivered to the phagosome by granules reacts with H_2O_2 , and plasma level concentrations of chloride to produce hypochlorous acid (HOCl), the most potent antimicrobial compound produced by neutrophils (Rosen, Crowley et al. 2002). The HOCl can then chlorinate bacterial

proteins, the extent of which has been demonstrated to parallel bacterial killing (Rosen, Crowley et al. 2002).

Hypothesis and specific aims

The hypothesis of this work is that CNF1 expression by UPEC modulates PMN antimicrobial function which, in turn, leads to enhanced net replication of toxigenic UPEC. This theory is based on the mechanism of action of CNF1, observations from a mouse ascending UTI model, and studies in which Rho GTPases were demonstrated to have an essential role in the antimicrobial response of PMNs. The specific aims of this study are to:

1. determine whether expression of CNF1 by UPEC results in enhanced *in vitro* survival when UPEC are co-incubated with mouse PMNs.
2. describe specific changes in the PMN antimicrobial response altered by CNF1-expressing UPEC.
3. evaluate whether biologically active CNF1 is present in outer membrane preparations from UPEC and if CNF1 from the membrane fraction can alter PMN antimicrobial responses.

Chapter 2

Cytotoxic Necrotizing Factor Type 1 Production by Uropathogenic *Escherichia coli*

Modulates Polymorphonuclear Leukocyte Function

Published as: Jon M Davis, Susan B Rasmussen, Alison D O'Brien. 2005. Cytotoxic Necrotizing Factor Type 1 Production by Uropathogenic *Escherichia coli* Modulates Polymorphonuclear Leukocyte Function. Infect. Immun. 73(9):5301-10

Abstract.

Many strains of Uropathogenic *Escherichia coli* (UPEC) produce Cytotoxic Necrotizing Factor Type 1 (CNF1), a toxin that constitutively activates the Rho GTPases RhoA, Rac1, and Cdc42. We previously showed that CNF1 contributes to the virulence of UPEC in a mouse model of ascending urinary tract infection and a rat model of acute prostatitis and that a striking feature of the histopathology of the mouse bladders and rat prostates infected with CNF1-positive strains is an elevation in levels of polymorphonuclear leukocytes (PMNs). We also found that CNF1 synthesis leads to prolonged survival of UPEC in association with human neutrophils. Here, we tested the hypothesis that CNF1 production by UPEC diminishes the antimicrobial capacity of mouse PMNs by affecting phagocyte function through targeting Rho family GTPases that are critical to phagocytosis and the generation of reactive oxygen species. We found that, as with human neutrophils, CNF1 synthesis provided a survival advantage to UPEC incubated with mouse PMNs. We also observed that CNF1-positive UPEC down regulated phagocytosis, altered the distribution of the complement receptor CR3 (CD11b/CD18), enhanced the intracellular respiratory burst, and increased levels of Rac2 activation in PMNs. From these results, we conclude that modulation of PMN function by CNF1 facilitates UPEC survival during the acute inflammatory response.

Introduction.

Urinary tract infections (UTIs) rank high among the most common types of symptomatic infections in humans (Foxman 2002; Russo and Johnson 2003). Indeed, more than 6 million cases of cystitis, *i.e.*, UTIs that are restricted to the bladder, occur annually in the United States with an estimated health-care cost of over 1 billion dollars (Russo and Johnson 2003). Uropathogenic *Escherichia coli* (UPEC) are responsible for the majority of UTIs and account for 85% - 95% of all cystitis isolates (Russo and Johnson 2003). Nearly twice as many women as men are seen by physicians for symptomatic UTI, and 40-50% of women experience at least one UTI in their lifetime (Foxman 2002). Long-term complications of UTI are rare; however, an ascending UTI can result in pyelonephritis and septicemia (Laestadius, Richter-Dahlfors et al. 2002; Kaper, Nataro et al. 2004).

The pathogenesis of *E. coli*-mediated UTI is not completely understood but likely involves the expression by the uropathogen of an array of virulence factors that facilitate colonization and evasion of the immune response. Type 1 fimbriae are established as UPEC virulence factors (Connell, Agace et al. 1996), while expression of other adhesins, such as P-pili and S-fimbriae, is strongly linked to UPEC pathogenicity (Foxman, Zhang et al. 1995). The precise role that α -hemolysin, a secreted toxin made by many UPEC isolates, plays in urovirulence is not understood. However, one possible explanation is that α -hemolysin changes host responses, a theory based on the finding that α -hemolysin modulates Ca^{2+} signaling in cultured primary renal epithelial cells (Laestadius, Richter-Dahlfors et al. 2002). Cytotoxic Necrotizing Factor Type – 1 (CNF1) is often co-produced with α -hemolysin by UPEC strains (Falbo, Famiglietti et al. 1992) and, at least

in vitro, it too mediates cellular effects (Caprioli, Falbo et al. 1983) that result from alteration of host signaling molecules (Schmidt, Sehr et al. 1997; Lerm, Selzer et al. 1999).

Three sets of observations support a role for CNF1 in the pathogenesis of UPEC-mediated UTI or acute prostatitis. First, epidemiological data from Foxman (Foxman, Zhang et al. 1995), Blanco (Blanco, Blanco et al. 1992) and Goulet (Goulet, Picard et al. 1994) suggest CNF1 is associated with increased virulence and the development of UTIs. In support of these observations, Yamamoto and colleagues determined that 61% of UPEC isolates they tested carried the *cnf1* gene compared to fewer than 10% of the commensal isolates they assessed (Yamamoto, Tsukamoto et al. 1995). Second, in a mouse model of ascending UTI, a CNF1-expressing UPEC, when compared to its isogenic *cnf1* mutant, caused a greater acute inflammatory response in the bladder, colonized the bladder more extensively in a co-infection experiment, and survived better when co-incubated with human neutrophils (Rippere-Lampe, O'Brien et al. 2001). Third, a rat model of acute prostatitis revealed that CNF1-expressing UPEC evoked more widespread gross inflammation of rat prostates in addition to more pronounced cellular infiltration by PMNs than did the corresponding *cnf1* isogenic mutant (Rippere-Lampe, Lang et al. 2001).

CNF1, which was first described by Caprioli and colleagues (Caprioli, Falbo et al. 1983), is an approximately 115 kDa single chain AB toxin that catalyzes the deamidation of the catalytically active glutamine residue of the Rho family of GTPases. The Rho GTPases include at least 10 members of which RhoA, Rac1, and Cdc42 are proven targets for CNF1 deamidation (Lerm, Schmidt et al. 2000). These GTPases function as

molecular switches that fluctuate between an active GTP bound form and an inactive GDP bound form. When the GTPases are bound to GTP they activate downstream targets such as kinases, and, when bound to GDP, the GTPases are inactive and sequestered in the cytosol. In this way, the Rho GTPases exert control over various cellular processes such as remodeling of the actin cytoskeleton (Lerm, Schmidt et al. 2000), chemotaxis (Gardiner, Pestonjamas et al. 2002), and formation of membrane extensions (Lerm, Schmidt et al. 2000). The deamidation of glutamine 63 in Rho and glutamine 61 in Rac and Cdc42 by CNF1 prevents the hydrolysis of GTP to GDP. This event results in the constitutive activation of Rho GTPases in CNF1 intoxicated cells

Rho GTPases also play a central role in both phagocytosis and the generation of reactive oxygen species (ROS) by PMNs (Witko-Sarsat, Rieu et al. 2000). Specifically, phagocytosis of complement-opsonized bacteria requires activated Rho and the β_2 -integrin CR3 (CD11b/CD18), while IgG-mediated phagocytosis is dependent on FC γ -receptors and both Cdc42 and Rac1 (Caron and Hall 1998; Underhill and Ozinsky 2002). Moreover, generation of ROS involves assembly of the nicotinamide adenine dinucleotide phosphate (NADPH) oxidase complex in the phagocyte membrane. This enzyme complex consists of a membrane bound flavocytochrome, cytosolic proteins, and Rac2 (Bokoch 1995; Witko-Sarsat, Rieu et al. 2000). The precise role of Rac2 in NADPH oxidase assembly is not completely understood. However, the integral nature of Rac2 in efficient generation of ROS was demonstrated in Rac2^{-/-} mice (Li, Yamauchi et al. 2002) and supported by the multiple rapidly progressing soft-tissue infections of a patient with a Rac2 point mutation that rendered the protein non-functional (Ambruso, Knall et al. 2000; Gu, Jia et al. 2001; Kurkchubasche, Panepinto et al. 2001). In both

cases, neutrophils from the host exhibited no or greatly reduced levels of ROS generation following stimulation.

In this study, we tested the hypothesis that CNF1 expression by UPEC partially protects the organism against the antimicrobial properties of PMNs. We found that the CNF1 expressed by UPEC downregulated phagocytosis, altered CD11b distribution on the PMN surface, and augmented the intracellular respiratory burst. These CNF1-induced phenotypic changes in PMNs culminated in enhanced net replication of CNF1-expressing UPEC and supports the hypothesis that CNF1 has a role in UTI pathogenesis by altering the innate immune response.

Materials and Methods.

Bacterial Strains and Growth Conditions. UPEC isolate CP9 (pSX34LacZ α), its isogenic derivative CP9*cnf1* (pSX34LacZ α), and the complemented clone CP9*cnf1* (pHLK140) all previously described (Rippere-Lampe, O'Brien et al. 2001) were re-created for this study because the original clones were no longer available. (see section below) Expression of CNF1 by both wild-type and complemented mutant and the absence of CNF1 expression by the isogenic mutant was confirmed by Western blot analysis. Bacterial strains were grown overnight in Luria-Bertani (LB) broth supplemented with 50 μ g/mL chloramphenicol at 37°C with shaking. An aliquot of the overnight growth was transferred to LB agar plates supplemented with 50 μ g/mL chloramphenicol and grown overnight at 37°C. The bacteria were re-suspended from the plates with 2 mL of Hanks Balanced Salt Solution (HBSS, BioWhittaker) without Ca²⁺, Mg²⁺, or phenol red. The resulting suspension was diluted to an OD A₆₀₀ of 0.7, corresponding to 6 x 10⁷ CFU/mL of a log phase culture. The suspension was further

diluted 1:10 in HBSS supplemented with 100 μM Ca^{2+} , 100 μM Mg^{2+} , 0.1% gelatin, 100 μM glucose, 50 $\mu\text{g/mL}$ chloramphenicol (HBSS-A) prior to use.

Complementation of CP9*cnf1*. Plasmids pHLK140 and pSX34LacZ α have been previously described (Rippere-Lampe, O'Brien et al. 2001). Electroporation of pSX34LacZ α into CP9 or CP9*cnf1* yielded CP9 (pSX34LacZ α), the wild-type with empty vector, and CP9*cnf1* (pSX34LacZ α), the isogenic mutant with empty vector, respectively. The electroporation of pHLK140 into CP9*cnf1* yielded CP9*cnf1* (pHLK140), the complemented mutant. Transformants were selected on LB agar that contained 50 $\mu\text{g/mL}$ chloramphenicol. A single chloramphenicol resistant colony was selected from each plate for further analysis. Growth curves of the individual strains were constructed to ensure that all strains grew equally well and that expression of CNF1 was evident by Western blotting.

Serum sensitivity. Bacteria were tested for sensitivity to mouse serum by incubating the individual bacterial strains in Hank's Balanced Salt Solution (HBSS) with various serum concentrations (2%, 5%, 10%). The mixtures were rotated end-over-end at 37°C and aliquots taken at 0, 90 and 150 minutes to determine bacterial viability by plating serial dilutions in triplicate onto LB agar supplemented with 50 $\mu\text{g/mL}$ chloramphenicol. Following overnight growth, the number of colonies on each plate was counted and the concentration in CFU/mL calculated. Controls run in parallel contained bacteria with all mixture components except serum.

PMN elicitation. Five-week-old female C3H/HeOuJ mice (Jackson Laboratory, Bar Harbor ME) were injected intraperitoneally with 2.5 mL 3% thioglycolate broth (Difco) and returned to their cages. The mice were euthanized by isoflurane overdose and

cervical dislocation five hours post injection. Seven milliliters of HBSS without Ca^{2+} or Mg^{2+} supplemented with 0.1% gelatin (HBSS-W) was instilled for peritoneal lavage of euthanized mice using a syringe and 18-gauge needle. The cells were centrifuged then pooled prior to determining the concentration of viable cells in a hemocytometer using trypan blue dye exclusion. An aliquot of the cell suspension was placed on a glass slide by a cytospin centrifuge (Cytospin II, Shandon), fixed with methanol and stained with SureStain Wright (Fisher). The percentage of PMNs in the peritoneal exudate cells was then determined visually using a 100X oil immersion objective on an Olympus microscope (BX60). The peritoneal exudate cells consisted of 92% granulocytes, 4% mononuclear cells, and 4% lymphocytes. The Uniformed Services University of the Health Sciences Institutional Animal Care and Use Committee approved all animal use protocols.

Bacterial Survival. All reactions were conducted in 1 mL volumes using HBSS-A at 37°C with end-over-end rotation. Bacterial strains were added to individual polypropylene tubes at a concentration of 5×10^5 CFU/mL. The bacteria were pre-opsonized in 10% normal mouse serum at 37°C prior to the addition of 2×10^6 PMNs. Control tubes included: i) bacteria with an equal volume of HBSS-A in place of PMNs; ii) the use of heat-inactivated serum (56°C for 45 minutes) in place of normal mouse serum; or, iii) cytochalasin D treated PMNs. Cytochalasin D treatment was done according to the method of Rest and Speert (Rest and Speert 1994). The number of viable bacteria at 0, 90, and 150 minutes was determined by plate count as above. PMN viability was checked by trypan blue dye exclusion at the end of the assay.

Bacterial association with PMNs. PMNs and bacteria were prepared as described above and co-incubated for 90 and 150 minutes at 37°C with end-over-end rotation. An aliquot was taken and affixed to a glass slide using a cytospin centrifuge. Each slide was stained using SureStain Wright (Fisher), and the number of bacteria associated with 100 total PMNs was determined microscopically. Due to the method of staining, it was not possible to discriminate intracellular from extracellular bacteria, and, therefore, the results are reported as the total number of PMN-associated bacteria.

Immunofluorescence.

PMN phagocytic capacity. PMNs (1×10^6) were allowed to adhere to glass coverslips coated with 3 mg/mL poly-D-lysine (Sigma P-0899) in 24 well cell culture dishes. Non-adherent cells were washed away, and pre-opsonized bacteria were then added at an MOI of 1:1. The PMNs and bacteria were co-incubated for 90 or 150 minutes and washed to remove non-adherent bacteria. The PMN:bacterial mixtures were fixed with fresh 3.5% paraformaldehyde (Electron Microscopy Services 15710) for 30 minutes at 37°C. The fixed infected PMNs were then washed in PBS and incubated overnight at 4°C in blocking buffer that contained 3% BSA (Sigma A-4503) and 10% heat inactivated normal goat serum (Sigma G-9023). Extracellular bacteria were labeled by incubation for 1 hour at room with rabbit anti-O4 polyclonal serum (Centers for Disease Control) diluted 1:200 in blocking buffer. The fixed infected PMNs were then washed in PBS to remove unbound primary antibody, and the secondary antibody, goat anti-rabbit Alexa 594 (Molecular Probes) 5µg/mL in blocking buffer, was applied for 1 hour at room temperature. The infected PMNs with labeled extracellular bacteria were again fixed in fresh 3.5% paraformaldehyde for 30 minutes at room temperature. Following an

additional washing, the cells were permeabilized by treatment with 0.3% Triton X-100 for 3 minutes and then washed in PBS. The cells were incubated overnight in blocking buffer at 4°C. Intracellular bacteria were then labeled following the same labeling protocol used for extracellular bacteria except that the secondary antibody was changed to goat anti-rabbit Alexa 488 (Molecular Probes). The cells were observed on an Olympus microscope (model BX60) equipped for epifluorescence with filters for FITC (Chroma Technologies, set 41001) and TRITC (Chroma Technologies, set U-M41002). The phagocytic capacity of the PMNs was determined by counting the total number of intracellular bacteria contained within 100 PMNs. The percent of PMNs engaged in phagocytosis was determined by counting the number of PMNs that contained at least one intracellular bacterium per 100 total PMNs; the results were then multiplied by 100. For both sets of counts, at least 4 separate fields were analyzed by phase contrast imaging of PMNs visualized with a 100X oil immersion lens.

CD11b staining. PMNs and bacteria were co-incubated under the same conditions used to determine phagocytic capacity. Following co-incubation, non-adherent bacteria were removed by washing and the cells blocked overnight at 4°C in blocking buffer. Goat anti-mouse Alexa 488 CD11b (Pharmingen) 5µg/mL and rabbit polyclonal α -O4 diluted 1:200 were applied in blocking buffer for 1 hour at room temperature to label CD11b and adherent bacteria respectively. After washing, goat anti-rabbit Alexa 594 (Molecular Probes) was applied at 5µg/mL for 1 hour at room temperature and subsequently washed. The cells were fixed for 30 minutes at room temperature in 3% freshly prepared paraformaldehyde (EMS) and washed in PBS before mounting the cover slips on glass slides using Fluoromount G (Southern Biotech). Images were acquired on a Zeiss LSM 5

PASCAL confocal microscope using a 100X oil lens (NA 1.4) and analyzed using the LSM 5 PASCAL software.

Nitroblue tetrazolium reduction. PMNs (1×10^6) were pre-incubated for 5 minutes with a 50 $\mu\text{g/mL}$ solution of nitroblue tetrazolium in DMSO at 37°C in polypropylene tubes. Pre-opsonized bacteria (1×10^6) were added to the PMNs and rotated end over end at 37°C. Samples were taken at 0, 15, and 30 minutes; the shorter time points were selected for this assay because of artifactual reduction of NBT at time points beyond 30 minutes. PMNs incubated without bacteria served as background controls. Samples were affixed to glass slides using a cytospin centrifuge and fixed with methanol. The cells were counter stained with Safranin O following fixation and air-dried. The percent of PMNs that contained purple formazan crystals from reduced nitroblue tetrazolium was determined on a light microscope (Olympus BX60) using a 100X oil immersion objective.

Luminol/Isoluminol-enhanced chemiluminescence. Luminol-enhanced chemiluminescence was used to measure the presence of intracellular reactive oxygen products and isoluminol enhanced chemiluminescence was used to detect the presence of extracellular reactive oxygen products. Both reactions were conducted in duplicate in 96 well microtiter plates at 37°C with periodic gentle shaking in a luminometer (Fluoroskan Ascent FL, Thermo Labsystems) according to the method of Bylund (Bylund, Samuelsson et al. 2003). We verified that we could detect intracellular and extracellular ROS under our assay conditions by stimulating PMNs with PMA (Sigma) or fMLF (Sigma). Pre-opsonized bacteria were added to duplicate wells of the microtiter plate and the light emission recorded every minute for 150 minutes with Ascent software

(Labsystems version 2.4.2). The raw data collected by the Ascent software was exported into Excel (Microsoft Corp.), and peak and time to peak values were determined.

Rac activation assay. PMNs (2×10^6) and pre-opsonized bacteria (2×10^7) were co-incubated in HBSS-A with 10% mouse serum for 150 minutes in a total volume of 1mL. The extent of Rac2 activation was determined by the Rac activation assay from Upstate Biological according to the manufacturers' protocol. The sample portion not used for affinity precipitation was retained for use as an internal control to verify equivalent loading of lanes.

Western blotting. CNF1 in mixtures of individual strains of bacteria co-incubated with PMNs for 150 minutes was detected by immunoblot as follows. Sonic lysates of the bacterial:PMN mixtures were prepared by pulsing samples on wet ice with a Sonic Dismembrator 550 (Fisher Scientific) for 3 minutes (30 seconds on, 30 seconds off). Proteins were resolved on 6.5% sodium dodecyl sulfate-polyacrylamide gel electrophoresis gels (SDS-PAGE) and transferred to nitrocellulose membranes in a semi-dry apparatus (BioRad). Protein-containing membranes were blocked overnight in a blocking buffer that consisted of 5% (w/v) skim milk in Tris-buffered saline with 0.1% Tween-20 (TBS-T), and the membranes were then probed with goat anti-CNF1 serum, diluted 1:10,000 and prepared as described previously (Mills, Meysick et al. 2000). These blots were then incubated with a horseradish peroxidase (HRP) -conjugated secondary pig anti-goat (1:10,000) (BioRad) in blocking buffer. Affinity-precipitated or total Rac2 was resolved on 12% SDS-PAGE. Following transfer to nitrocellulose membranes and overnight blocking, the membranes were probed with rabbit polyclonal anti-Rac-2 (1:400) (Santa Cruz Biotechnology) in blocking buffer. Blots were then

incubated with HRP-conjugated secondary goat anti-rabbit (1:4,000) (BioRad) in blocking buffer. Visualization of both CNF1 and Rac2 was accomplished by enhanced chemiluminescence (ECL PLUS, Amersham).

Flow cytometry. PMNs were evaluated for CD11b expression by washing cells with FACS buffer (DPBS + 0.2% FBS + 0.1% sodium azide) after co-incubation with bacteria. PMNs were washed and re-suspended in 100 μ l of FACS buffer and blocked with 1 μ g rat anti-mouse CD16/CD32 MAb 2.4G2 (Pharmingen) for 20 minutes at room temperature. PMNs were then washed twice in FACS buffer and re-suspended in 100 μ l FACS buffer. Cells were stained on ice for 30 minutes with 0.5 μ g/mL PerCP-Cy5.5 labeled rat anti-mouse CD11b MAb clone M1/70 (Pharmingen) and 0.8 μ g/mL PE labeled rat anti-mouse Gr-1 MAb clone 1A8 (Pharmingen). Cells were washed and re-suspended in FACS buffer with 0.4% paraformaldehyde (EMS). Isotype matched controls were run in parallel. Gating was set on Gr-1 positive cells and 30,000 events were collected on an LSR II flow cytometer (Becton-Dickenson), and analyzed using WinList software v 5.0.

Statistical Analysis. All calculations were performed using Statistical Package for the Social Sciences 11.0 (SPSS 11.0) in consultation with our in-house statistician, Cara Olsen. Non-parametric data were evaluated for statistical significance using the Mann-Whitney U-test. Parametric data were evaluated by ANOVA after the residuals were plotted to determine that the data were normally distributed.

Results.

CNF1 enhances UPEC replication in the presence of murine PMNs

We previously showed that wild-type UPEC strain CP9 survived better than the corresponding isogenic mutant CP9*cnf1* after 45 minutes of contact with human neutrophils (Rippere-Lampe, O'Brien et al. 2001). To extend and further characterize the impact of CNF1 expression on the interaction between these phagocytes and UPEC, we compared the growth of the wild-type strain, the CNF1-negative mutant and the complemented clone in the presence of elicited peritoneal exudate cells (92% granulocytes and hereafter called PMNs) from C3H/HeOuJ mice. This mouse strain was selected because of its use in our previously published studies on the role of CNF1 in the ascending UTI model (Rippere-Lampe, O'Brien et al. 2001).

The CP9-derived derivatives used in this investigation included the wild-type strain transformed with the cloning vector alone [CP9(pSX34LacZ α)], the isogenic CNF1-negative mutant also transformed with the cloning vector alone [CP9*cnf1*(pSX34LacZ α)], and the complemented mutant of CP9*cnf1* [CP9*cnf1*(pHLK140)], that was previously described (Rippere-Lampe, O'Brien et al. 2001) but freshly transformed for this study. Western blot analysis confirmed the presence of CNF1 in the wild type and complemented clone, but no CNF1 was detected in the mutant (data not shown). The growth curves of these three strains in media without PMNs were superimposable (data not shown). By contrast, when we compared the net replication of CP9(pSX34LacZ α) (hereafter called the wild type or the wild-type strain), CP9*cnf1*(pSX34LacZ α) (hereafter called the mutant or the isogenic mutant) and

CP9*cnf1*(pHLK140) (hereafter called the complemented mutant) after co-incubation with C3H/HeOuJ PMNs, both the wild-type and the complemented mutant grew to a significantly greater extent ($p < 0.01$) than did the mutant after 90 minutes (Figure 7). Moreover, the wild-type strain and the complemented mutant in the presence of the murine PMNs continued to demonstrate significantly ($p < 0.01$) greater net replication throughout the 150 minutes of the assay, while the isogenic mutant failed to undergo any significant net growth (Figure 7). A western blot of the assay mixtures demonstrated that CNF1 was produced under the conditions of our experiment (Figure 8). Control experiments using PMNs treated with cytochalasin D, a known inhibitor of actin polymerization and phagocytosis, resulted in all three bacterial strains growing equally well (Figure 9).

The results of this cytochalasin D experiment suggested that the growth differences observed among the three UPEC strains tested in the presence of PMNs (Figure 9) were due to an impairment of the phagocytic process, rather than the release of antimicrobial products from the PMNs into the extracellular environment. Additional control experiments using heat-inactivated serum as a source of opsonins also resulted in all three strains growing equally well; these results demonstrated that heat-labile factors are required for the observed growth differences (data not shown). Finally, to demonstrate that the three strains used were not sensitive to the concentration of normal mouse serum incorporated into the media in our experiments, all three strains were grown in the presence of 10% normal mouse serum without PMNs. Strains so cultivated demonstrated growth equivalent to strains cultured in the absence of serum (data not shown). Collectively, these results show that CNF1-expressing UPEC have a growth

Figure 7. Influence of untreated- and cytochalasin D-treated PMNs on net replication of CNF1-positive and negative UPEC.

Bacterial strains were co-incubated with PMNs and viable bacteria enumerated by plating serial dilutions at the indicated time points. Each bar represents the mean Log_{10} CFU/mL of three independent experiments done in triplicate. Counts are presented for strains depicted as follows: wild-type CP9(pSX34LacZ α), black; isogenic mutant CP9*cnfI*(pSX34LacZ α), gray; complemented mutant CP9(pHLK140), white. The error brackets indicate the 95% confidence interval for each determination. The data were analyzed by ANOVA and differences are significant ($p < 0.01$).

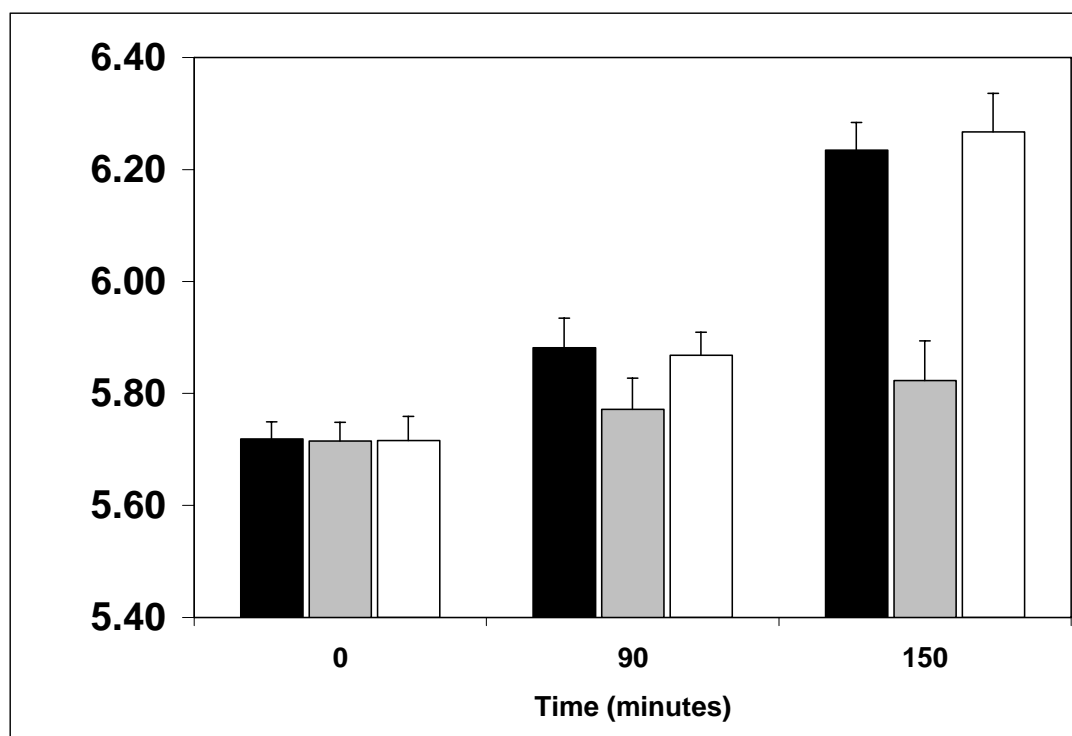


Figure 8. Western blot analysis of CNF1 in sonically-disrupted lysates of bacteria and PMNs after co-incubation.

Lane 1 purified CNF1; Lane 2 lysate of wild-type CP9(pSX34LacZ); Lane 3 lysate of isogenic mutant CP9*cnfI*(pSX34LacZ); Lane 4 lysate of complemented mutant CP9*cnfI*(pHLK140).

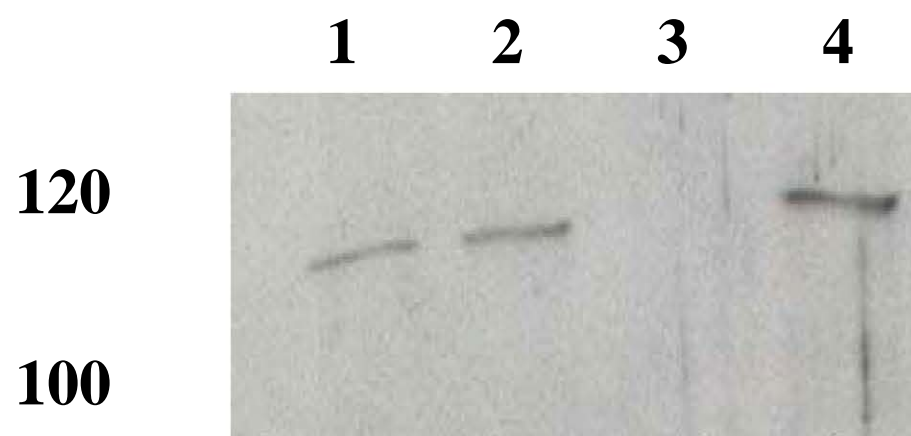
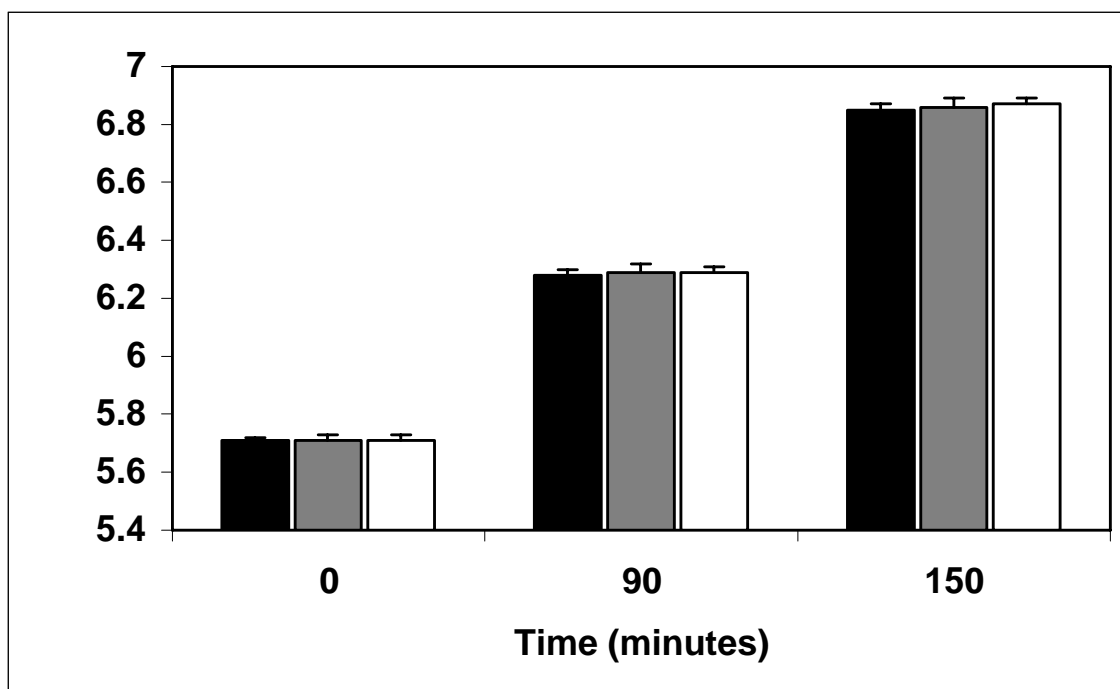


Figure 9. Influence of cytochalasin D on PMN antimicrobial capacity.

PMNs were pre-incubated with cytochalasin D prior to adding UPEC and viable bacteria were enumerated by plating serial dilutions. Each bar represents the mean Log₁₀ CFU/mL of three independent experiments done in triplicate. Counts are presented for strains depicted as follows: CP9(pSX34LacZ α), black; CP9*cnfI*(pSX34LacZ α), gray; CP9(pHLK140), white. The error brackets indicate the 95% confidence interval for each determination. The data were analyzed by ANOVA and differences are significant ($p < 0.01$).



advantage when co-incubated with PMNs from peritoneal exudates of C3H/HeOuJ mice and support our previous findings that the CNF1-positive CP9 strain grew better in the presence of human neutrophils than did its CNF1-negative isogenic mutant. In addition, the findings with murine PMNs indicate that this CNF1-dependent differential growth is due to alteration in a phagocytic process that requires heat-labile serum factors.

PMN phagocytic capacity and CD11b clustering is altered in the presence of CNF1-expressing UPEC.

Based on the results obtained in the bacterial survival experiments described above, we undertook a series of experiments to assess the extent of PMN association with the wild-type and the isogenic mutant. The number of wild-type bacteria associated with 100 PMNs was significantly increased compared to the isogenic mutant at 90 minutes (268 vs. 173, $p < 0.05$, $n = 4$). The number of wild-type bacteria associated with PMNs reached a plateau after 150 minutes of co-incubation while the mutant continued to associate in significantly greater numbers (259 vs. 400, $p < 0.05$, $n = 4$). These data further support the suggestion from the cytochalasin D experiments above that CNF1-expression by CP9 modulates phagocytosis by PMNs.

Next, we conducted a set of studies that were designed to use differential immunolabeling as a tool to evaluate the phagocytic capacity of the infected C3H/HeOuJ PMNs and the percent of PMNs engaged in phagocytosis. The results of those experiments are shown in Table 1. When co-incubated with CNF1-expressing UPEC, the phagocytic capacity of the murine PMNs was significantly diminished at both 90 and 150

Table 3. Phagocytic capacity and activity of PMNs exposed to UPEC^a.

Strain	90 Minutes		150 Minutes	
	Bacteria/100	% Phagocytosing	Bacteria/100	% Phagocytosing
	PMN	PMN	PMN	PMN
CP9 (pSX34LacZ α)	141 (135-147)	15 (11-18)	123 (120-125)	8 (7-9)
CP9 <i>cnfI</i> (pSX34LacZ α)	230 (225-235) ^b	77 (71-80) ^b	262 (256-267) ^b	77 (71-81) ^b
CP9 <i>cnfI</i> (pHLK140)	143 (138-150)	13 (11-15)	128 (124-133)	6 (4-7)

^a Data are the median and range of four independent experiments and strains are designated as follows: wild-type

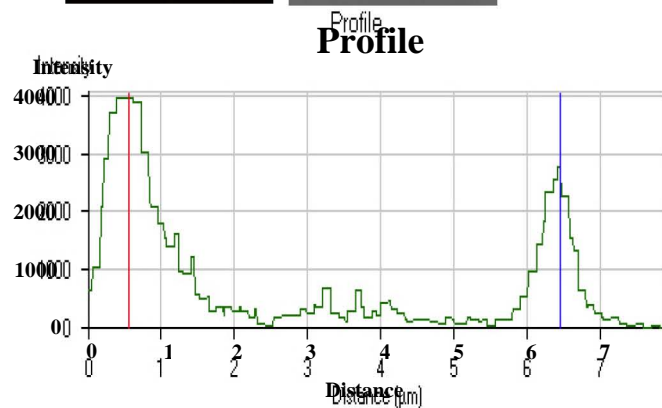
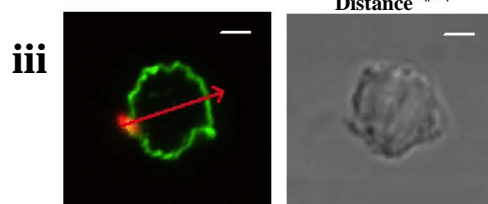
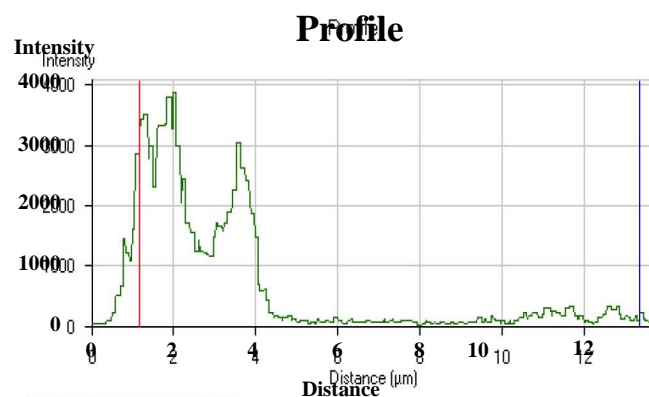
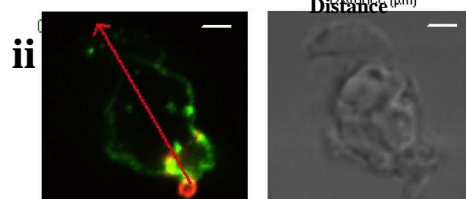
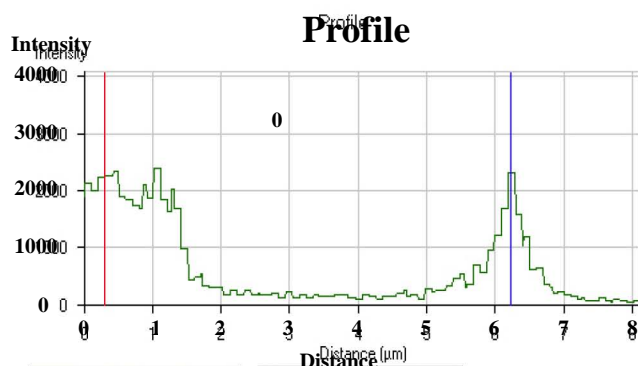
[CP9(pSX34LacZ α)], mutant [CP9*cnfI*(pSX34LacZ α)], complemented mutant [CP9*cnfI*(pHLK140)]. ^b Significantly greater compared to wild-type and complemented mutant $p < 0.01$ as determined by ANOVA.

minutes. The percent of PMNs that exhibited phagocytic activity when in contact with CNF1-expressing UPEC compared to the mutant was also significantly lower, and the phagocytic activity of these PMNs decreased over time.

The anti-phagocytic effect of CNF1 expressed by UPEC suggested that the PMNs were not interacting productively with serum-opsonized bacteria, perhaps due to failure to express or cluster complement receptor 3 (CR3, CD11b/CD18) on the PMN surface. To test this theory, we co-incubated PMNs with each of the three strains (wild-type, mutant, and complemented mutant) and analyzed the expression of CD11b on the PMN surface. FACS analysis revealed that the level of CD11b expression on the surface of elicited mouse PMNs was unchanged regardless of the bacterial strain used in these co-incubation experiments (data not shown). We then asked whether CNF1-expressing UPEC could influence the clustering of CD11b in response to serum-opsonized bacteria. To address that question, PMNs that were co-incubated with each of the bacterial strains were immunostained for both bacteria and CD11b and then examined by confocal microscopy. The results of this experiment are shown in Figure 10. PMNs co-incubated with the wild-type strain (Figure 10, panel Ai.) demonstrated a homogenous distribution of CD11b along the periphery of the leukocyte. Conversely, PMNs incubated with the CNF1-negative mutant exhibited dense regions of clustered CD11b localized mainly under bacteria (Figure 10, panel Aii.). The distribution of CD11b on the PMNs in association with the complemented mutant (Figure 10, panel Aiii.) was like that of PMNs incubated with the wild-type strain. The change in fluorescence intensity of CD11b along a line segment extending from the point of UPEC attachment to the opposite side of the PMN provided a measure of the capacity of PMNs to cluster CD11b in response to

Figure 10. Clustering of CD11b in mouse PMNs in contact with UPEC.

(A) PMNs were co-incubated with (i) wild-type CP9 (pSX34LacZ α), (ii) isogenic mutant CP9*cnf1* (pSX34LacZ α) or (iii) complemented mutant CP9*cnf1* (pHLK140) and confocal images were obtained following immunostaining for CD11b (green) and bacteria (red). PMNs co-incubated with CNF1-expressing UPEC (i and iii) show a diffuse and approximately equal distribution of CD11b around the periphery of the cell compared to PMNs in contact with the *cnf1* mutant (ii) that demonstrate a clustering of CD11b beneath the bacteria. The CD11b pixel intensity along the red arrow extending from the point of UPEC attachment to a point on the opposite side of the PMN is shown in the profile plot under each image set. The red line in each profile plot indicates the intensity at the point of UPEC attachment and the blue line indicates the intensity at the opposite side of the phagocyte. Bar represents 2 μ m.



serum- opsonized bacteria (Figure 10 A, profiles next to immunostained PMNs). PMNs exposed to CNF1-expressing UPEC exhibited a significantly ($p<0.01$) impaired capacity to cluster CD11b in response to serum-opsonized UPEC compared to PMNs exposed to the *cnf1* mutant (Figure 11). We also observed that PMNs co-incubated with CNF1-expressing UPEC appeared more compact than did PMNs exposed to the *cnf1* isogenic mutant. Indeed, when the area of PMNs exposed to each of the three strains was measured, we found that PMNs co-incubated with CNF1-expressing UPEC showed a significantly ($p<0.01$) reduced degree of spread compared to PMNs exposed to the isogenic mutant (Figure 12). The results of these experiments taken collectively demonstrate that CNF1-expressing UPEC have an anti-phagocytic effect on mouse PMNs and suggest that the anti-phagocytic effect may result from the diminished capacity of PMNs to remodel their membranes and cluster CD11b in response to the presence of serum-opsonized bacteria.

CNF1-expressing UPEC modify the PMN respiratory burst.

To examine whether or not PMNs co-incubated with the different UPEC bacterial strains also exhibited an altered competence to generate reactive oxygen species (ROS), we first measured the PMN respiratory burst using nitroblue tetrazolium (NBT) dye reduction. The percent of PMNs that contained formazan deposits was significantly greater when co-incubated with CNF1-expressing UPEC than when mixed with the *cnf1* mutant (Table 4). To verify the NBT reduction results, we used a procedure that exploits luminal- or isoluminol-enhanced chemiluminescence to specifically measure the

Figure 11. Fold change of CD11b fluorescence intensity.

The fluorescence intensity of CD11b directly under the UPEC was compared to the fluorescence intensity of CD11b on the opposite side of the PMN with the profile analysis tool in the LSM 5 PASCAL software. Each bar represents the mean fold increase in fluorescence intensity (n=30); the brackets indicate the 95% confidence intervals. The bacterial strains used in the co-incubation experiments are depicted as follows: wild-type CP9(pSX34LacZ α), black; isogenic mutant CP9*cnf1*(pSX34LacZ α), gray; complemented mutant CP9(pHLK140), white. The data were analyzed by ANOVA and differences are significant (p<0.01).

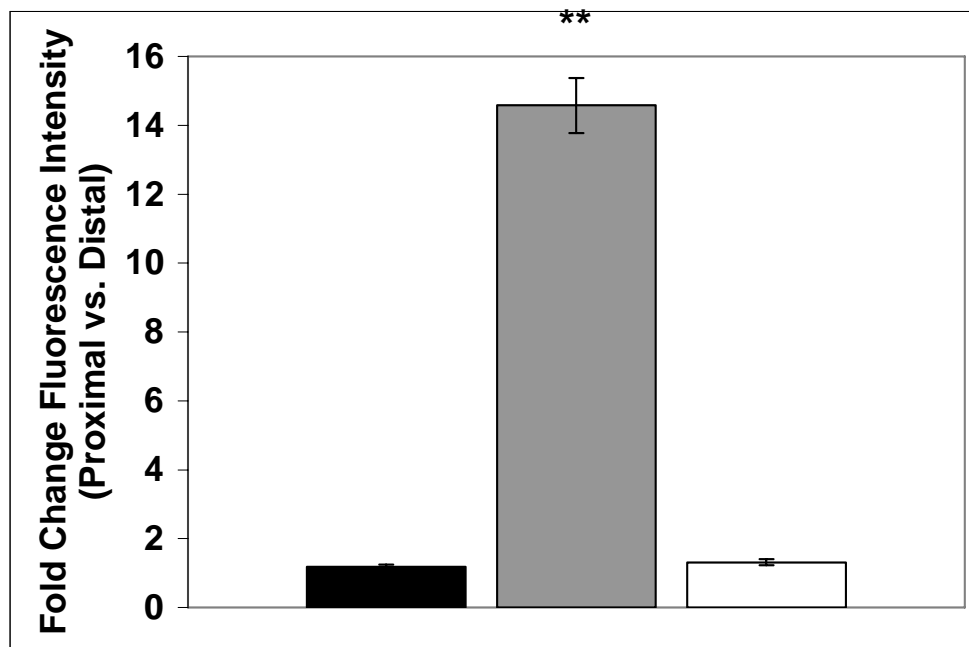


Figure 12. PMN spreading in response to UPEC.

PMNs were co-incubated with each of the bacterial strains on glass coverslips coated with poly-D-lysine for 150 minutes. Following immunostaining for CD11b, confocal images were obtained. The area occupied by a PMN was calculated by tracing the PMN perimeter (as defined by the fluorescently labeled CD11b) with the measuring tool in the LSM 5 PASCAL software. The data are shown as the mean and 95% confidence intervals (n=30). The bacterial strains used in the co-incubation experiments are represented as follows: CP9(pSX34LacZ α), black; CP9*cnfI*(pSX34LacZ α), gray; CP9*cnfI*(pHLK140), white. The data were analyzed by ANOVA and differences are significant (p<0.01).

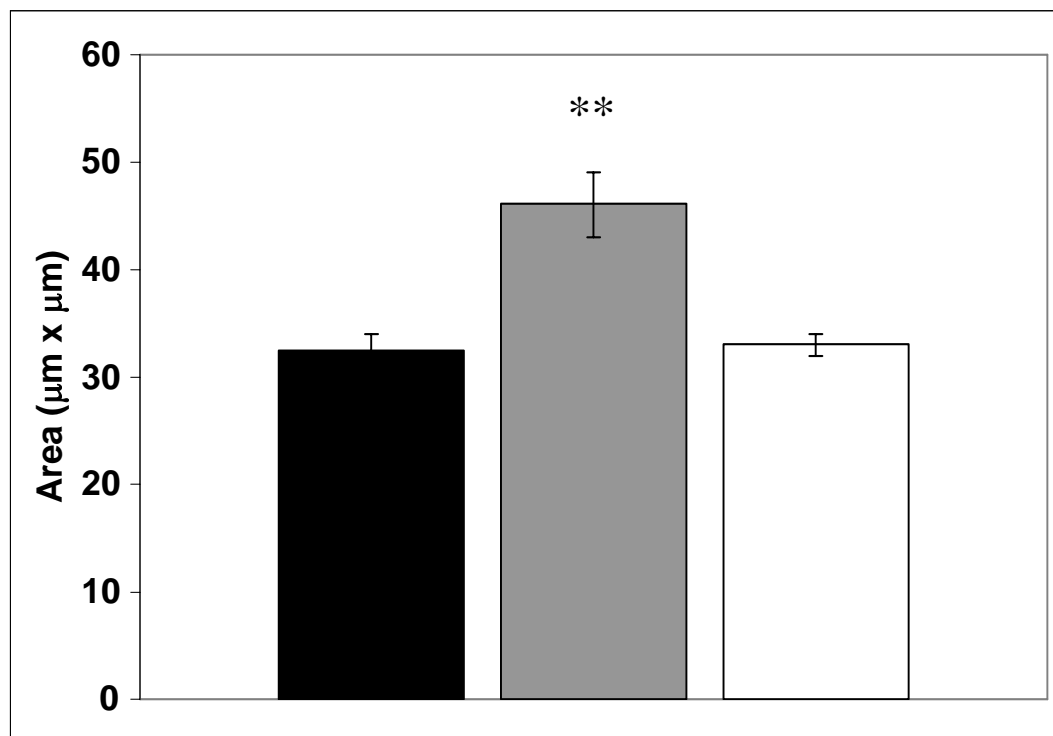


Table 4. Respiratory burst of PMNs exposed to UPEC.

Strain	NBT Reduction		Luminol Enhanced Chemiluminescence ^b	
	(% Positive) ^a		Peak Relative Light Units	Time to Peak (minutes)
	15 minutes	30 minutes		
CP9(pSX34LacZ α)	80 (79-83)	90 (87-97)	970 (654 - 1287)	47.5 (37.1 - 57.9)
CP9 <i>cnfI</i> (pSX34LacZ α)	62 (60-63) ^c	77 (67-77) ^d	452 (389 - 514) ^e	57.5 (33.5 - 81.5)
CP9 <i>cnfI</i> (pHLK140)	87 (81-89)	94 (85-96)	920 (672 - 1168)	41.2 (36.7 - 45.6)

^aData are the median and range of three independent experiments and strains are designated as follows: wild-type

[CP9(pSX34LacZ α)], mutant [CP9*cnfI*(pSX34LacZ α)], complemented mutant [CP9*cnfI*(pHLK140)]. ^b Values are shown as the

mean and 95% confidence interval of three experiments in duplicate. ^{c,d} Significantly less than wild-type or complemented mutant

p=0.05 as tested by Mann-Whitney. ^e Significantly less than wild-type and complemented mutant p < 0.01 as determined by ANOVA.

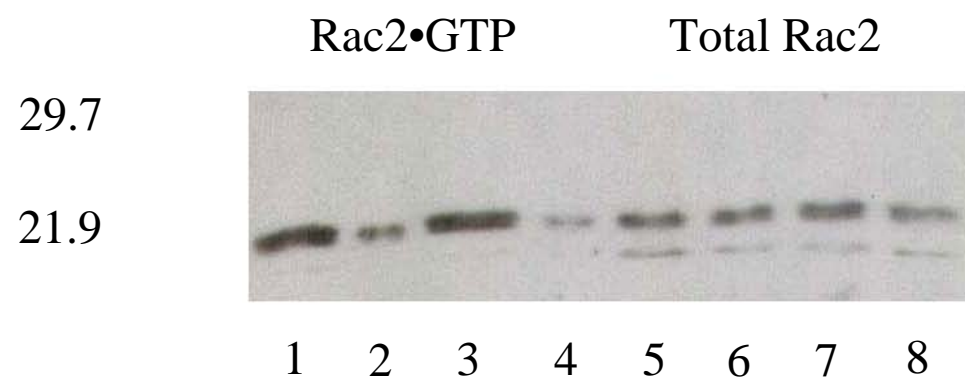
intracellular and extracellular accumulation of (ROS), respectively. When the peak and time to peak values of the isoluminol reactions were compared, no significant difference was detected in the extracellular accumulation of ROS. However, when murine PMNs were co-incubated with CNF1-expressing bacteria, the PMNs generated a significantly greater intracellular peak response in the luminol assay when compared to the *cnf1* mutant (Table 4); no difference in the time to peak was detected.

CNF1-expressing UPEC stimulate expression of enhanced levels of activated Rac2 in PMNs.

The role of the small GTPase Rac2 in the assembly of a functional NADPH oxidase in neutrophils was previously demonstrated by Kim and Dinauer (Kim and Dinauer 2001). Since CNF1 targets small GTPases, one explanation for the increased intracellular levels of ROS after exposure of PMNs to CNF1-expressing UPEC was that the toxin had activated Rac2 in those phagocytes. To evaluate this idea, we used an affinity precipitation assay and antibodies specific for Rac2 to determine the extent of Rac2 activation in PMNs exposed to our UPEC strains. As illustrated in Figure 13, PMNs exposed to CNF1-expressing UPEC contained nearly twice as much activated Rac2 as did PMNs exposed to the *cnf1* mutant; the results from each group were normalized to unstimulated PMNs. Together, these results provide evidence that exposure to CNF1-expressing UPEC results in an increased level of activated Rac2 in mouse PMNs.

Figure 13. Rac2 activation in PMNs co-incubated with UPEC.

(A) PMNs were incubated with each of the bacterial strains, and the activated form of Rac2 was affinity precipitated from whole cell lysates prior to detection by Western blotting. The unstimulated control contained PMNs only. The total Rac2 in whole cell lysates prior to affinity precipitation was used as a control to ensure that similar amounts of Rac2 were present. PMNs were exposed to CP9(pSX34LacZ α) (lane 1 and 5), CP9*cnfI*(pSX34LacZ α) (lane 2 and 6), CP9*cnfI*(pHLK140) (lane 3 and 7), or no bacteria (lane 4 and 8) for 150 minutes prior to affinity precipitation. (B) The change in the amount of activated Rac2 in PMNs exposed to CP9(pSX34LacZ α) (black bar), CP9*cnfI*(pSX34LacZ α) (white bar), CP9*cnfI*(pHLK140) (gray bar), compared to the unstimulated control (spotted bar) was determined with Image J to quantify the pixel density of each lane. The data presented are representative of 3 separate experiments with similar results.



2.5

2

1.5

1

0.5

0

Relative Pixel Density

Chapter 3

Cytotoxic Necrotizing Factor Type 1 (CNF1) Delivered by Outer Membrane Vesicles of Uropathogenic *Escherichia coli* Attenuates Polymorphonuclear Neutrophil Antimicrobial Activity and Chemotaxis

Abstract

Cytotoxic necrotizing factor type 1 (CNF1), a toxin produced by many strains of uropathogenic *Escherichia coli* (UPEC), constitutively activates small GTPases of the Rho family by deamidating a single amino acid within these target proteins. Such activated GTPases not only stimulate actin polymerization within affected cells but also, as we previously reported, decrease membrane fluidity on mouse polymorphonuclear neutrophils (PMNs). This diminished membrane movement impedes the clustering of the complement receptor CD11b/CD18 on PMNs which, in turn, leads to decreased PMN phagocytic capacity and microbicidal activity. This impaired clustering occurs on PMNs in proximity to wild-type UPEC as well as those in direct contact with CNF1-expressing UPEC. This latter observation suggests that CNF1 is released from neighboring bacteria, although an export mechanism for CNF1 has not been described. Here we present evidence that CNF1 is released from CNF1-expressing UPEC in a complex with outer membrane vesicles (OMVs) and that these CNF1-bearing vesicles transfer biologically active CNF1 to PMNs and attenuate phagocyte function. Finally, we show that CNF1-bearing vesicles act in a dose-dependent fashion on PMNs to inhibit their chemotactic response to formyl-Met-Leu-Phe (fMLP) while purified CNF1 does not. We conclude that OMVs provide a means for delivery of CNF1 from a UPEC strain to PMNs and as such, negatively impact the efficacy of the acute inflammatory response to these organisms.

Introduction

Uropathogenic *Escherichia coli* (UPEC) are responsible for the majority of community-acquired urinary tract infections (UTIs) (Russo and Johnson 2003). These infections are more frequent among women than men (Foxman 2002), and treatment costs in the United States exceed 1 billion dollars annually (Russo and Johnson 2003). The mechanisms by which UPEC cause such infections are complex but appear to reflect the impact of multiple bacterial factors linked to UPEC virulence (Johnson 1991). Such microbial components can be grouped by function and include, but are not limited to, adhesins and toxins. Of the adhesins, the best studied are the type 1 fimbriae (Connell, Agace et al. 1996) that mediate binding of the organisms to bladder epithelia (Mulvey, Schilling et al. 2000). The specific functions of toxins, such as α -hemolysin and Cytotoxic Necrotizing Factor type 1 (CNF1), in the pathogenesis of UPEC-mediated UTI are less well understood. However, these two toxins are co-expressed by many UPEC strains (Falbo, Famiglietti et al. 1992), and recent animal studies from our laboratory in collaboration with others demonstrated a role for CNF1 in both UTI and acute bacterial prostatitis (Rippere-Lampe, Lang et al. 2001; Rippere-Lampe, O'Brien et al. 2001). Moreover, CNF1 is frequently produced by UPEC that cause symptomatic UTI in humans (Foxman, Zhang et al. 1995; Yamamoto, Tsukamoto et al. 1995; Johnson, Scheutz et al. 2005), although the toxin was first detected in *E. coli* isolates from children with diarrhea (Caprioli, Falbo et al. 1983)

CNF1, a single chain AB toxin, functions as a deamidase and converts the catalytically active glutamine residue of Rho family GTPases to glutamic acid. The CNF1-catalyzed deamidation of Gln 63 in RhoA, and Gln 61 in Rac and Cdc42 results in

the loss of GTPase activity and these molecules are rendered constitutively active. The Rho family GTPases function as molecular switches within cells. When bound to GTP, the Rho family molecules are active and stimulate downstream enzymes such as kinases; after GTP is hydrolyzed to GDP, the Rho GTPases are rendered inactive and their signaling is terminated.

The cycling of Rho family members between the active and inactive forms is essential for the proper functioning of eukaryotic cells such as polymorphonuclear neutrophils (PMN). In fact, many important antimicrobial features of these phagocytic effector cells of the innate immune system reflect the cycling of Rho family members. For example, Rac1 and Cdc42 are critical for IgG-mediated phagocytosis (Caron and Hall 1998), while Rho is important in phagocytosis via CR3 (Caron and Hall 1998). Furthermore, Rac2, an isoform of Rac1, is an essential component of the neutrophil NADPH oxidase used by neutrophils to generate reactive oxygen species (ROS) and inactivate phagocytosed pathogens (Kim and Dinanuer 2001). Neutrophil chemotaxis is also controlled by Rho GTPases through processes that are now under evaluation through the use of dominant-active and dominant-negative mutants of the Rho GTPases (Allen, Zicha et al. 1998; Srinivasan, Wang et al. 2003; Xu, Wang et al. 2003). In essence, these studies propose a model of chemotaxis in which a key event is the development of a polarized front on the side of the PMN that faces the chemotactic gradient. This polarization event appears to occur through a positive feedback loop that involves activation of Rac1, actin polymerization, and an increase in the concentration of phosphatidylinositol 3,4,5-triphosphate (PIP₃) (Srinivasan, Wang et al. 2003; Xu, Wang et al. 2003). Cdc42 is also considered to play a significant role in this scenario of PMN

chemotaxis through its interactions with p21-activated kinase (PAK1). Such a Cdc42-PAK1 association is thought to lead to localized actin polymerization at the neutrophil leading edge and thus, directional sensing and persistent directional migration of these phagocytes (Li, Hannigan et al. 2003).

We recently described specific alterations in PMN antimicrobial activity coincident with exposure to CNF1-expressing UPEC strain CP9 (Davis, Rasmussen et al. 2005). In that study we noted that PMNs that were not in direct contact with wild-type CP9 exhibited a phenotype similar to PMNs that had direct contact with CP9 when examined microscopically (Davis, Rasmussen et al. 2005). This finding suggested that CNF1 may be released from wild-type UPEC and mediate toxicity in PMNs without direct cell-to-cell contact with UPEC. These observations, combined with the absence of a recognized route for CNF1 release and the recently described role of outer membrane vesicles (OMVs) in the delivery of heat labile toxin (LT) from Enterotoxigenic *Escherichia coli* and the VacA cytotoxin of *Helicobacter pylori* (Horstman and Kuehn 2000; Keenan, Day et al. 2000; Kesty, Mason et al. 2004), led us to hypothesize that CNF1-expressing UPEC release outer membrane vesicles that contain the toxin. In this investigation, we tested that theory.

Materials and Methods

Bacterial strains and growth conditions. Serogroup O4 uropathogenic *E. coli* strain CP9 and its CNF1-negative isogenic derivative, CP9*cnf1*, were previously described (Rippere-Lampe, O'Brien et al. 2001). These strains were transformed with the vector pSX34LacZ α , a low copy number plasmid with a chloramphenicol resistance

marker, to provide experimental consistency between the PMN studies detailed here and those described previously that were done in the presence of chloramphenicol (Davis, Rasmussen et al. 2005). Transformation of CP9 with this vector yielded CP9(pSX34LacZ α) and transformation of CP9*cnf1* generated CP9*cnf1*(pSX34LacZ α); these strains are hereafter referred to as CP9 or wild type, and CP9*cnf1* or isogenic mutant, respectively. Bacterial strains were grown overnight in Luria-Bertani (LB) broth at 37°C with shaking. An aliquot of the overnight growth of each bacterial strain was transferred to LB agar plates supplemented with 50 μ g/mL chloramphenicol, and the plates were grown overnight at 37°C. The bacteria were scraped from the plates and the pellet resuspended in 2 mL of Hanks Balanced Salt Solution (HBSS, BioWhittaker) without Ca²⁺, Mg²⁺, or phenol red. The suspension was diluted to an OD A₆₀₀ of 0.7 that corresponded to 6 x 10⁷ CFU/mL of a log phase culture. The suspension was further diluted 1:10 in HBSS supplemented with 100 μ M Ca²⁺, 100 μ M Mg²⁺, 0.1% gelatin, 100 μ M glucose, and 50 μ g/mL chloramphenicol (HBSS-A) prior to use.

Multinucleation assay: The HEp-2 cell multinucleation assay for CNF1 was done as previously described (Mills, Meysick et al. 2000). Purified CNF1 or membrane vesicles derived from CP9 or CP9*cnf1* were applied to HEp-2 cells and incubated at 37°C in 5% CO₂ for 4 days. The cells were then fixed, stained with Leukostat (Fisher Scientific), and examined microscopically for the presence of multinucleated HEp-2 cells.

Isolation of outer membrane vesicles. Bacterial outer membrane vesicles of bacteria were harvested from overnight cultures essentially according to the method of Beveridge (Kadurugamuwa and Beveridge 1995) with minor modifications. Briefly, bacterial cultures were grown overnight and centrifuged at 8,000 X g to pellet bacterial cells, and

supernatants were filtered through a 0.2 μm filter to eliminate residual bacterial cells.

The resulting filtrate was centrifuged at 150,000 X g in a Beckman Type 70Ti ultracentrifuge rotor for 1.5 hours at 4°C and the pellet washed and resuspended in phosphate buffered saline (PBS). The vesicle preparation was centrifuged again at 120,000 X g, and the resulting pellet was re-suspended in PBS and stored at -20°C until used.

Enzyme assays. The β -galactosidase activity in the outer membrane vesicle preparation was determined with the Beta-gal assay kit from Invitrogen according to the manufacturer's protocol. Alkaline phosphatase activity was detected as described by Maloy (Maloy, Stewart et al. 1996) with the following modification. The absorbance at 405 nm of each sample was measured in a spectrophotometer, and the concentration of para-nitrophenol calculated based on a molar extinction coefficient of $1.78 \times 10^4 \text{ cm}^{-1} \text{ M}^{-1}$. Protein concentrations of the samples were determined by the bicinchoninic acid method (BCA) from Pierce according to the manufacturer's instructions.

Determination of 2-Keto-3-deoxyoctonate (KDO) content of outer membranes. The KDO content of the outer membrane vesicle preparation was assessed by the thiobarbituric acid method as detailed by Heine (Heine 1993). The absorbance at 549 nm of each sample was measured spectrophotometrically, and the KDO concentration calculated based on a molar extinction coefficient of $6.41 \text{ cm}^{-1} \mu\text{mol}^{-1}$.

PMN elicitation. Five-week-old female C3H/HeOuJ mice (Jackson Laboratory, Bar Harbor ME) were injected intraperitoneally with 2.5 mL 3% thioglycolate broth (Difco) and returned to their cages. The mice were euthanized by isoflurane overdose and cervical dislocation five hours after injection of the thioglycolate. Peritoneal lavage of

euthanized mice was accomplished as follows. Seven milliliters of HBSS without Ca^{2+} or Mg^{2+} but supplemented with 0.1% gelatin (HBSS-W) was instilled intraperitoneally through a syringe with an 18-gauge needle followed by massage and aspiration of peritoneal fluid. The cells in the aspirate were harvested by centrifugation then pooled prior to determining the concentration of viable (as assessed through exclusion of trypan blue dye) cells in a hemocytometer. An aliquot of the cell suspension was deposited on a glass slide with a Cytospin centrifuge (Cytospin II, Shandon, Pittsburgh, PA), and the cells were then fixed with methanol and stained with Sure Stain Wright (Fisher Scientific). The percentage of PMNs in the peritoneal exudate was then determined visually with a 100X oil immersion objective on an Olympus microscope (BX60). The peritoneal exudate cells consisted of 92% granulocytes, 4% mononuclear cells, and 4% lymphocytes. The Uniformed Services University of the Health Sciences Institutional Animal Care and Use Committee approved all animal use protocols.

Bacterial survival in the presence of PMNs. Bacteria were pre-opsonized in 10% normal mouse serum in HBSS-A at 37°C prior to the addition of 2×10^6 PMNs. Bacterial strains were added to individual polypropylene tubes at a concentration of 5×10^5 CFU/mL. Tubes with mixtures of bacteria and PMNs were incubated at 37°C and rotated end over end. In some cases, bacterial culture supernatants were added to these mixtures. These supernatants were prepared as follows. One mL of an overnight growth of the specific bacterial culture was centrifuged at 8,000 X g for 5 minutes at 4°C in a bench top centrifuge (Eppendorf). The supernatant was removed and filtered through a 0.2 μm low-protein binding syringe filter. Filtrate sterility was assessed by culturing an aliquot overnight in LB broth supplemented with 50 $\mu\text{g/mL}$ chloramphenicol. A 2 μL aliquot of

this of the sterile filtrate was added to the bacterial: PMN mixture described above. This filtrate volume was selected after calculating the volume of overnight culture that would yield a bacterial concentration equivalent to the concentration of wild-type bacteria present at the end of the bacterial survival experiment. When outer membrane vesicle preparations were added to the mixtures, 2 μ l of the vesicle preparation was used in place of a sterile culture filtrate.

PMN chemotaxis. The chemotactic response of PMNs to formyl-Met-Leu-Phe (fMLP, Sigma) was measured with the QCM Chemotaxis 3 μ m 96-well cell migration assay (ECM515) from Chemicon, International according to the manufacturer's protocol. Briefly, PMNs were pre-incubated for 20 minutes with membrane vesicles from CP9 or CP9*cnf1* or with purified CNF1 or HBSS. The amount of CNF1 in the OMVs derived from CP9 was quantified by Western blot based on a standard curve of purified CNF1 run in parallel. Duplicate samples of each mixture were applied to the upper migration chamber; a chemical gradient between the upper and lower chambers was established by placing 1×10^{-4} M fMLP in the lower chamber. The cells were incubated for 1 hour at 37°C in an incubator that contained 5% CO₂, then the cells were fluorescently labeled according to the manufacturer's instructions. The fluorescence intensity of each sample was measured on a SpectaMax M2 fluorescent microplate reader using SoftMax Pro software (Molecular Devices). The number of migrated PMNs was calculated based on a standard curve run in parallel. The response of PMNs treated with membrane vesicles or purified CNF1 was normalized to untreated PMNs prior to data analysis.

Western blotting. Culture supernatants were concentrated by chloroform and methanol precipitation to enhance the detection of CNF1. This concentration method was

previously described (Wessel and Flugge 1984) and is detailed below with several modifications. A total unconcentrated sample volume of 600 μ l was split equally into three 2.0 mL Eppendorf tubes. For each 200 μ l sample, 800 μ l of methanol was added, and the sample was then mixed on a vortex and centrifuged at 9,000 X g for 10 sec. Next, 200 μ l chloroform was added and the sample briefly mixed on a vortex. Then 600 μ l of dH₂O was added, and the sample was mixed on a vortex again, and subsequently centrifuged at 9,000 X g for 10 sec. The upper phase was removed by aspiration and the split samples pooled prior to incorporating 900 μ l of methanol. The pooled sample was mixed on a vortex for a final time and centrifuged for 2 min at 9,000 X g. The supernatant was aspirated and the pellet dried under an air stream and then resuspended in SDS-PAGE loading buffer. Concentrated culture supernatant and membrane vesicle preparations were resolved on 6.5% SDS-PAGE gels and transferred to nitrocellulose membranes in a semi-dry apparatus (BioRad). After transfer, membranes were blocked overnight in blocking buffer that consisted of 5% (w/v) skim milk in Tris-buffered saline with 0.1% Tween-20 (TBS-T) then probed with goat anti-CNF1 (1:10,000) as previously described (Mills, Meysick et al. 2000). Blots were then incubated with horseradish peroxidase (HRP) -conjugated porcine anti-goat secondary antibody (BioRad) diluted 1:10,000 in blocking buffer. The O-antigen in membrane vesicle preparations was detected after OMV preparations were resolved on a 15% SDS-PAGE gel and transferred to a nitrocellulose membrane. Following transfer to the nitrocellulose membrane and overnight blocking, the membranes were probed with rabbit polyclonal anti-O-4 (CDC) serum diluted 1:400 in blocking buffer. Blots were then incubated with HRP-conjugated

goat anti-rabbit secondary antibody (BioRad) diluted 1:10,000 in blocking buffer.

Visualization of both CNF1 and O-4 antigen was accomplished by enhanced chemiluminescence (ECL PLUS, Amersham).

Electron microscopy. OMVs were prepared for electron microscopy according to previously published methods (Goping, Yedgar et al. 1992; Goping, Pollard et al. 1995).

In essence, outer membrane vesicles were fixed in a mixture of 2% paraformaldehyde and 2% glutaraldehyde in 0.1M cacodylate buffer with 2% sucrose. The samples were then washed in 0.1M cacodylate buffer then post fixed in 1% OsO₄ in 0.1M cacodylate buffer with 1% K₃Fe(CN)₆ and 1% sucrose (pH 7.4) to improve membrane contrast.

After fixation, the samples were washed again and processed in Araldite plastic embedding medium (Goping, Yedgar et al. 1992; Goping, Pollard et al. 1995). Ultra-thin sections (70-80 nm) were obtained from the Araldite blocks with a Diatome diamond knife and collected on copper hexagonal grids. Sections were stained with uranyl acetate (30 minutes) and lead citrate (5 minutes), examined in a CM 100 Philips/FEI electron microscope at a beam voltage of 80 kV, and photomicrographs of the sections were taken.

Immunofluorescence. PMNs (1×10^6) and outer membrane vesicles (2 µg total protein) were co-incubated for 150 minutes with end-over-end tumbling. All steps of the incubation were conducted at 4°C to prevent internalization by PMNs of any bound membrane vesicles. During the final 45 minutes of the co-incubation of these PMN: OMV mixtures, samples were transferred to poly-D-lysine (3 mg/mL, Sigma)- coated coverslips that had been placed on the bottom of 24- well tissue culture plates. The coverslips that contained the samples were then washed to remove unbound membrane

vesicles, fixed in 3% freshly prepared paraformaldehyde (EMS) for 30 minutes at 37°C and blocked overnight at 4°C in blocking buffer that consisted of 3% BSA and 10% heat-inactivated normal goat serum (Sigma). Rabbit polyclonal α -O4 (CDC) serum was diluted 1:200 in blocking buffer and applied to the cells for 1 hour at room temperature. The cells were then washed in PBS and goat anti-rabbit Alexa 488 (Molecular Probes) was applied at 5 μ g/mL in blocking buffer for 1 hour at room temperature. The cells were washed again in PBS and the coverslips mounted with Fluormount G (Southern Biotech) onto glass slides. The stained cells were viewed on an Olympus microscope (Model BX60) equipped for epifluorescence with a filter for fluorescein iso-thiocyanate (FITC) (Chroma Technologies, set 41001) detection. Images were obtained with a CCD camera and Spot software. The final images were prepared with ImageJ 1.34g (Rasband, W.S., ImageJ, U. S. National Institutes of Health, Bethesda, Maryland, USA, <http://rsb.info.nih.gov/ij/>, 1997-2005)

Statistical analysis. Data were evaluated for statistical significance by ANOVA after plotting the residuals to determine that the data were normally distributed. All calculations were done with the SPSS 11.0 program in consultation with our in-house statistician, Cara Olsen.

Results

CNF1 in culture supernatants alters PMN antimicrobial response.

Cytotoxic Necrotizing Factor type 1 was previously described as a cytoplasmic protein based on cell fractionation experiments (Caprioli, Donelli et al. 1984). Our earlier findings supported that conclusion since CNF1 was not detectable in overnight culture supernatants of CP9 but was readily demonstrable in sonic lysates of that organism (Davis, Rasmussen et al. 2005). However, in this study, discernable amounts of CNF1 were evident by Western blot (Figure 14) when the supernatant was concentrated by chloroform and methanol precipitation. As expected, no CNF1 was found in the concentrated supernatant of the isogenic mutant (Figure 14). We initially attributed the small amount of CNF1 in the concentrated culture supernatant of the wild-type organism to bacterial lysis in the course of overnight growth that led to the release of cytoplasmic contents that included CNF1. To test this theory, we assessed the amount of cytoplasmic protein present in the clarified culture supernatants prior to precipitation by assaying for activity of the cytoplasmic enzyme β - galactosidase. As shown in Table 5, β - galactosidase activity in the clarified supernatants was not detectable in contrast to the level of activity seen in permeabilized cell culture controls. The lack of measurable β - galactosidase activity in the clarified supernatants indicated that very little bacterial cytoplasmic protein was present in the cell- free supernatants. We reasoned that the

CNF1 detected by Western blot in concentrated supernatants was in fact not attributable strictly to bacterial lysis and cytoplasmic release.

Next, experiments were designed to assess the level of CNF1 activity in neat but not concentrated supernatants. These experiments were based on the observation that CP9 survives better than the corresponding *cnf1* isogenic mutant when co-incubated with human neutrophils (Rippere-Lampe, O'Brien et al. 2001) or mouse peritoneal exudate cells (Davis, Rasmussen et al. 2005), hereafter called PMNs. In agreement with our previous work (Davis, Rasmussen et al. 2005), when CP9 was co-incubated with elicited

Figure 14. Analysis of supernatants from CNF1-positive and negative-CP9 isogenic strains.

(A) Assessment by Western blot of the presence of CNF1 in concentrated bacterial culture supernatants. Bacteria were removed from cultures by centrifugation and filtration through 0.2µm filters prior to concentrating the supernatants with chloroform and methanol precipitation. Lane 1, purified CNF1; Lane 2, concentrated supernatant of CP9; Lane 3, concentrated supernatant of isogenic mutant CP9*cnf1*.

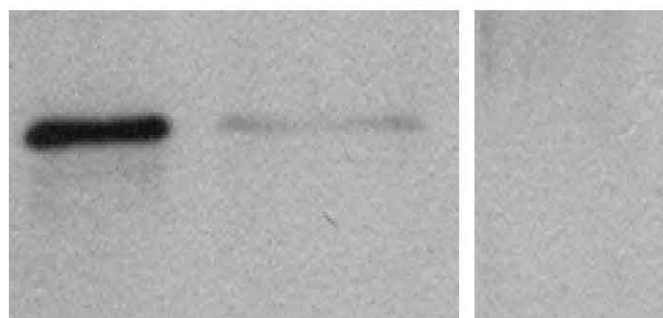
120**1****2****3**

Table 5. Biochemical characterization of OMVs derived from UPEC strain CP9 and its isogenic CNF1-negative mutant^a

Bacterial Source	Type of Preparation	Assay		
		KDO ^c (μg/mL)	β-galactosidase	Alkaline phosphatase
			[nmol/min/μg (x 10 ⁻³)]	[nmol/min/μg (10 ⁻³)]
CP9	Supernatant ^b		<5.00 ^d	ND
	OMV	30.03	<5.00 ^d	1.99±0.17
	Permeabilized cells		70.19±0.89	5.71±0.60
CP9 ^{cnf1}	Supernatant ^b		<5.00 ^d	ND
	OMV	25.53	<5.00 ^d	2.04±0.21

^a Data are shown as the mean ± standard deviation of three independent determinations calculated from the molar extinction coefficient as described in Material and Methods.

^b Clarified, filtered culture supernatant prior to ultracentrifugation

^c 2-Keto-3-deoxyoctonate

mouse PMNs, the number of viable wild-type bacteria increased over time compared to the *cnf1* mutant (Figure 15, $p < 0.01$). Moreover, when the isogenic mutant and PMNs were co-incubated and wild-type supernatant added, the isogenic mutant demonstrated net-replication equivalent to that of the wild-type (Figure 15). In contrast, when sterile LB broth or supernatant from CP9*cnf1* was used in place of wild-type culture supernatant the protective effect of the wild-type supernatant was lost (Figure 15). Taken together, these results suggest that the presence of active CNF1 in the undiluted wild-type supernatant protects the isogenic mutant from the antimicrobial properties of PMNs.

Outer membrane vesicles from CP9 are complexed with CNF1.

The presence of active CNF1 in the bacterial culture supernatant and the absence of detectable β - galactosidase activity as a marker of cytoplasmic proteins imply that a mechanism beyond bacterial lysis might contribute to CNF1 release in CP9. Many Gram-negative bacteria are known to shed pieces of outer membrane in the form of outer membrane vesicles (OMV). Therefore, we examined the possibility that the extracellular CNF1 could be a component of CP9-derived OMVs. We used a previously described method to isolate OMVs from CP9 and CP9*cnf1* culture supernatants and then applied Western blot analysis to detect CNF1 in various cellular fractions (Figure 16). CNF1 was detectable in the sedimented cellular fraction (Figure 16, Lane 2). The proteins in the supernatant that remained after ultracentrifugation were precipitated with chloroform-methanol and analyzed by immunoblot for the presence of CNF1. In contrast to the

Figure 15. Influence of PMNs treated with CP9 or CP9*cnfI* culture supernatant on the net replication of CNF1-positive and negative CP9.

Wild-type bacteria and PMNs were co-incubated in the presence of either: sterile LB broth (black bars), and *cnfI* mutant bacteria were co-incubated in the presence of either: sterile LB broth (white bars), wild-type culture supernatant (light grey bars) or *cnfI* mutant supernatant (black stripes). The concentration of viable bacteria in each condition was determined by plate count at the indicated times. The results are from three experiments in triplicate and are shown as the mean Log₁₀ CFU/mL viable bacteria; the error brackets indicate the 95% confidence intervals for each condition. The data were analyzed by ANOVA and the differences are significant ($p < 0.01$).

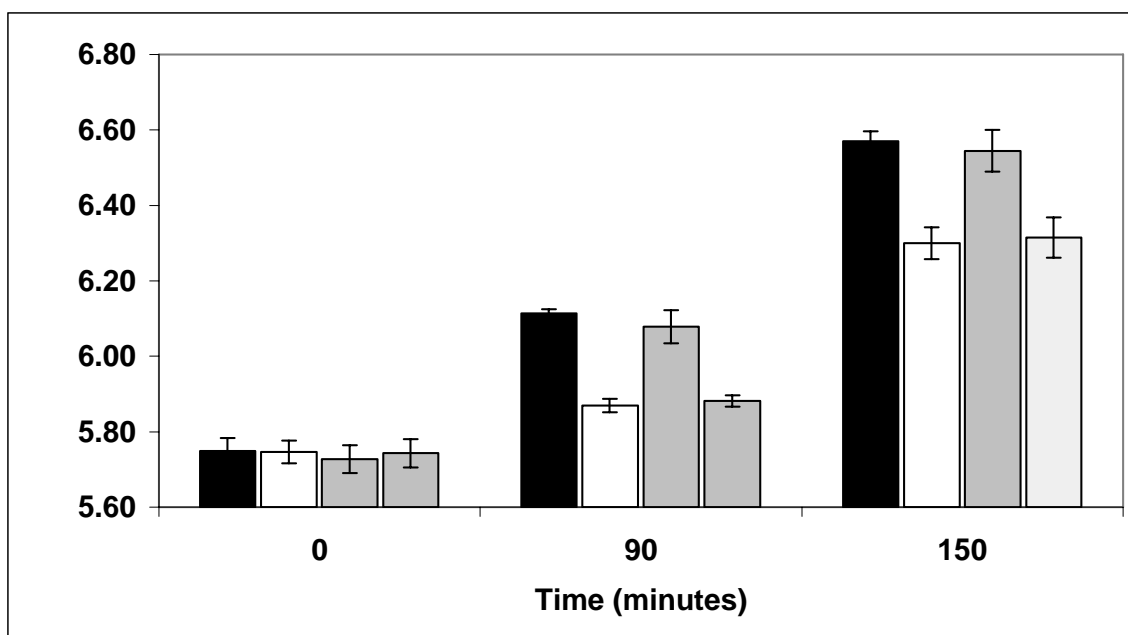


Figure 16. Immunoblot analysis of supernatant pellet.

(A) Culture supernatants were centrifuged then filtered through a 0.2 μ m filter prior to ultra-centrifugation. The supernatant fraction pelleted by ultracentrifugation was re-suspended and an aliquot analyzed by immunoblot. Lane 1, purified CNF1; Lane 2, CP9 pellet; Lane 3, CP9*cnf1* pellet.

1**2****3****120**

pelleted fraction, CNF1 was not detectable in the concentrated supernatant (data not shown). That CNF1 was sedimented out of suspension by ultracentrifugation, suggested that it existed as a complex with the outer membrane fraction rather than as a soluble protein. Further characterization of the pellet demonstrated the presence of the KDO sugar of LPS and the O4 antigen, both of which are components of the outer membrane in CP9 (Table 5 and Figure 17, respectively). We reasoned that if membrane vesicles derived from the outer membrane were present in the pelleted fraction, they would likely contain a fraction of the periplasmic contents such as alkaline phosphatase. Therefore, we measured the alkaline phosphatase activity of the sedimented fraction and found that it did indeed possess alkaline phosphatase activity (Table 5). In addition, neither the ultracentrifuged sediment nor, as noted above, the starting supernatant contained measurable quantities of β - galactosidase, findings consistent with scant cytoplasmic contamination in these fractions. In aggregate, these biochemical data indicate that the sediment formed after ultracentrifugation of the culture supernatant of UPEC strain CP9 is composed of outer membrane vesicles that contain periplasmic contents and CNF1.

Vesicles are observed by electron microscopy.

Transmission electron microscopy (TEM) was used to assess whether OMVs were indeed present in the CP9 culture supernatant pellet after ultracentrifugation. The TEM images of this sedimented material revealed the presence of many vesicles but, as predicted, no intact bacteria (Figure 18, panel i). Most of the vesicles were less than 200

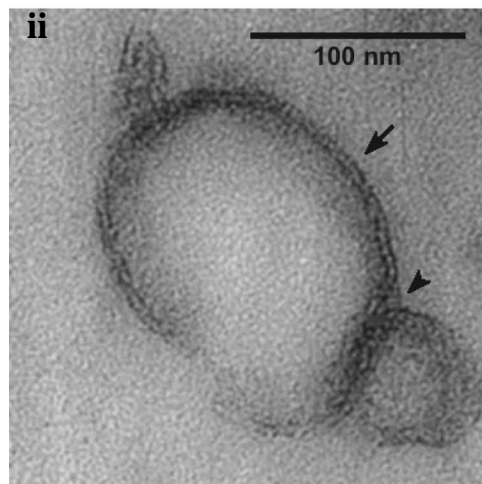
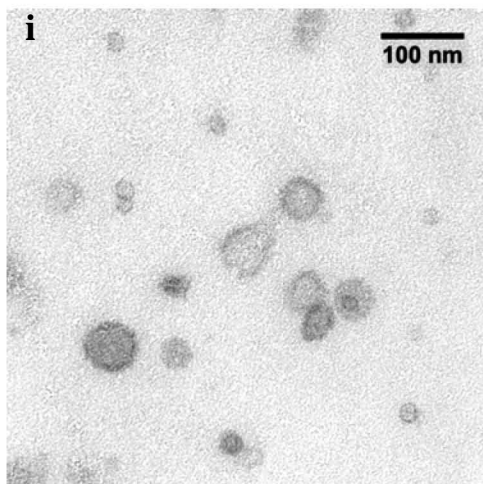
Figure 17. Detection of O4 antigen in pelleted fraction.

The pelleted fraction was analyzed by immunoblot for the presence of the O4 antigen as a marker of the bacterial outer membrane. Lane 1, CP9 pellet; Lane 2, CP9*cnf1* pellet.



Figure 18. Electron micrograph of and activity associated with membrane vesicles prepared from CP9.

Culture supernatants were prepared by centrifugation and filtration to remove bacterial cells, and insoluble material was then sedimented by ultracentrifugation. The resulting pellet was embedded and prepared for electron microscopy. (i) Wide field view of membrane vesicle preparation from CP9 showing many vesicles of various diameters. (ii) Vesicles from CP9 that illustrate the fusion of a large and small vesicle (arrowhead) and the bi-layer structure of the vesicles (arrow).



nm in size and were typically spherical in shape (Figure 18, panel i). However, some OMVs appeared to have fused with each other to generate larger irregularly shaped vesicles (Figure 18, panel ii).

Multinucleation of HEp-2 cells by OMVs.

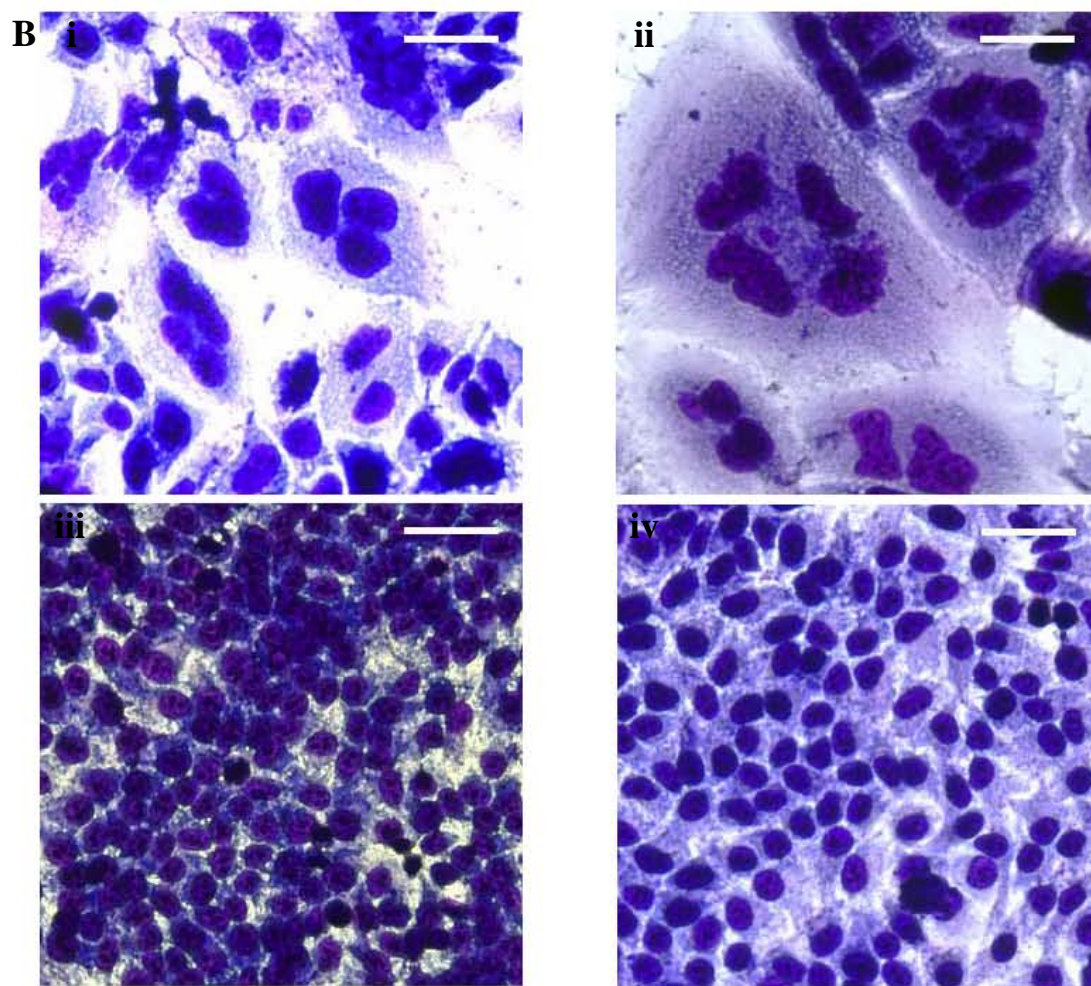
HEp-2 cells display a characteristic phenotype of multinucleation and enlargement when intoxicated with CNF1. We used this standard assay of CNF1 activity to determine whether the membrane vesicles derived from CP9 contained biologically active CNF1. We incubated HEp-2 cells with either purified CNF1 or membrane vesicles from the wild-type or isogenic mutant. We observed that HEp-2 cells displayed the characteristic features of CNF1 intoxication, such as cellular enlargement and multinucleation when incubated with membrane vesicles from CP9 (Figure 19, panel i) or purified CNF1 (Figure 19, panel ii). Cells incubated with membrane vesicles derived from the isogenic mutant exhibited cellular morphology similar to HEp-2 cells that were incubated with media only (Figure 19, compare panels iii and iv). These results demonstrate that membrane vesicles derived from wild-type UPEC CP9 contain biologically active CNF1.

OMVs interact with mouse PMNs.

The presence of outer membrane vesicles in the culture supernatants and the detrimental effect of the wild-type supernatant on PMN microbicidal activity led us to

Figure 19. Activity of outer membrane vesicles derived from CP9.

HEp-2 cells exposed to: (i) purified CNF1; (ii) OMVs from CP9; (iii) OMVs derived from CP9*cnf1*; (iv) media alone. Bars in panel B equal 50 μm .



investigate whether CP9 OMVs could interact with PMNs. To address that question, PMNs and OMVs were co-incubated and then immunostained with anti-O4 antibody to detect membrane components on the PMN surface. As depicted in Figure 20, the outer membrane vesicles derived from CP9 were associated with the mouse PMNs. We then theorized that the association of vesicles with PMNs could serve as a means to direct CNF1 to PMNs and that such OMV targeting was responsible for the altered microbicidal activity seen in PMNs treated with clarified supernatant. To test this idea, PMNs were co-cultured with bacteria and membrane vesicles derived from either CP9 or CP9*cnf1*. The concentration of viable bacteria at various time points was then determined. When CP9*cnf1* was co-incubated with PMNs in the presence of wild-type OMVs, the net replication of the mutant increased to levels comparable to that of CP9 co-incubated with PMNs (Figure 21). However, when OMVs from the isogenic mutant were added back to the PMNs cultured with CP9*cnf1*, diminished survival over time of the mutant compared to the wild type co-incubated with PMNs was observed ($p < 0.01$, Figure 21). Collectively, these results suggest that wild-type CP9 releases CNF1 complexed with OMVs and that these CNF1-bearing vesicles interact with and diminish the antimicrobial activity of PMNs.

CNF1-bearing OMVs alter PMN chemotaxis.

The effect of OMVs from wild-type CP9 on the PMN antimicrobial response led us to examine whether other features of PMN physiology were altered by wild type OMVs.

Figure 20. Fluorescently-labelled outer membrane vesicles interact with PMNs.

Outer membrane vesicles prepared from CP9 were co-incubated with PMNs at 4°C.

Fluorescent images of 2 different cells (upper panel) were obtained following immunostaining for the O-4 antigen contained in outer membrane vesicles (green); corresponding phase contrast images (lower panel) of the PMN are also shown. The co-incubation of PMNs with outer membrane vesicle preparation resulted in the presence of punctate staining of the O-4 antigen along the perimeter of the PMN indicating the presence of the O-4 antigen on the PMN membrane. The corresponding control PMNs not incubated with outer membrane vesicles did not stain (data not shown).

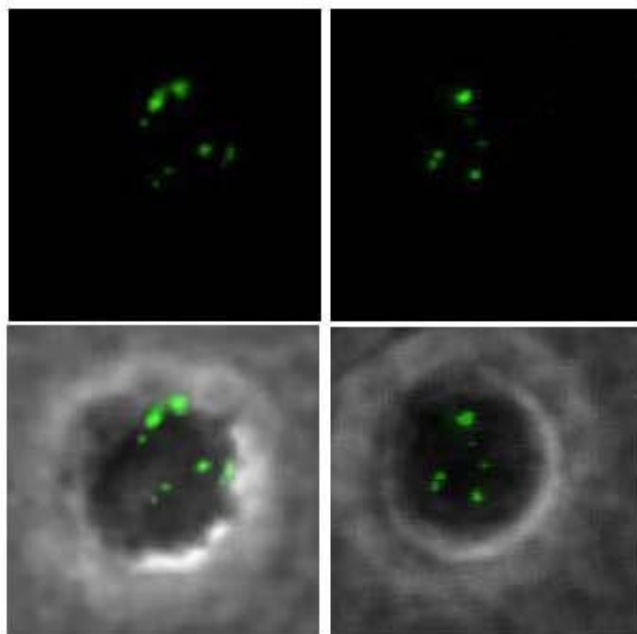
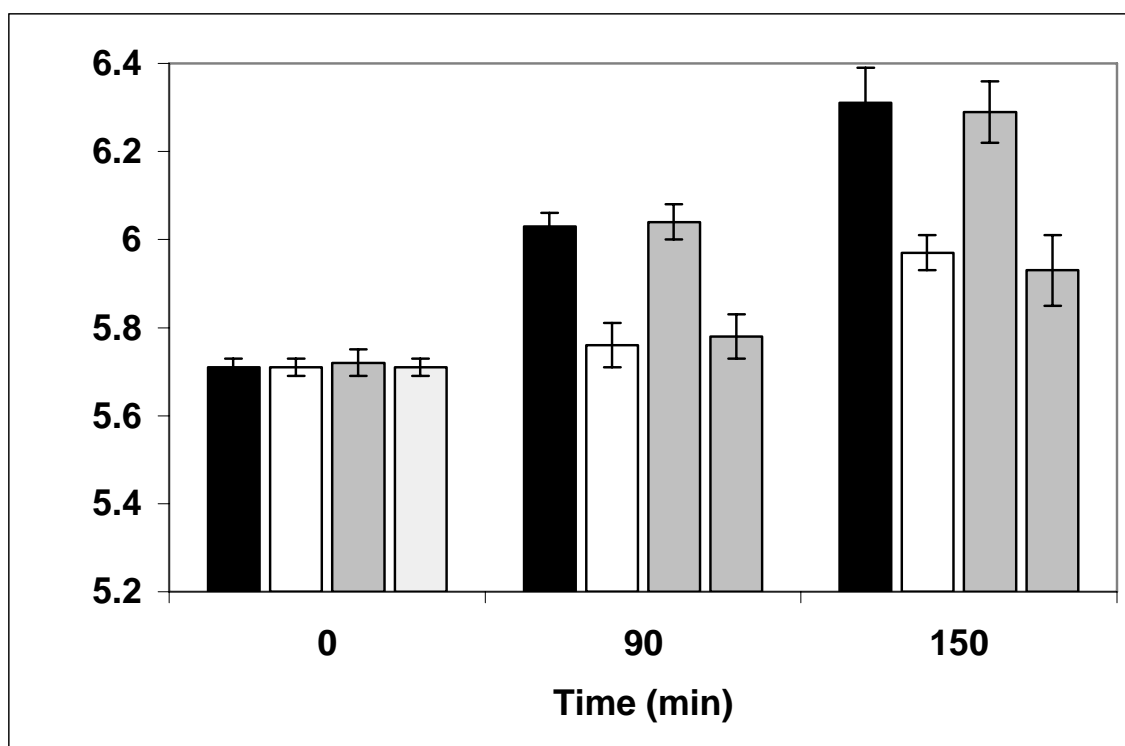


Figure 21. OMVs from CNF1-expressing CP9 reduce PMN antimicrobial capacity.

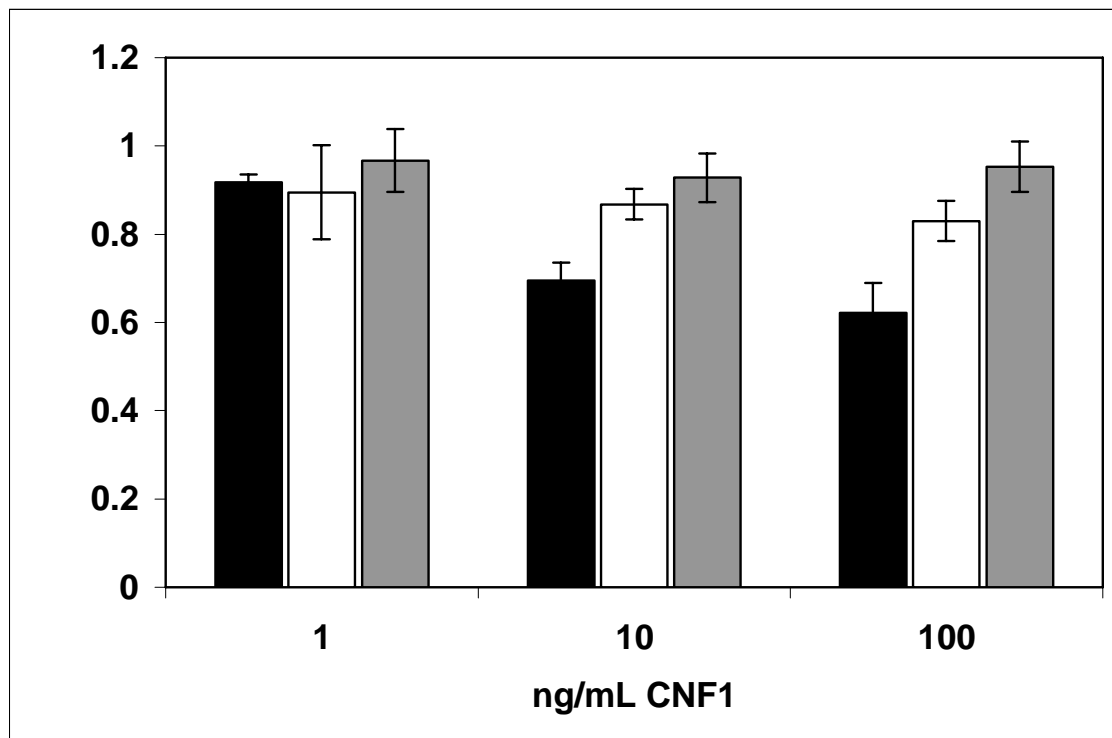
The net replication of wild-type (black) and the *cnfI* mutant of CP9 (white) co-incubated with PBS was compared to the net replication of CNF1-negative CP9 co-incubated with purified OMVs from wild-type CP9 (light gray) or OMVs from *cnfI* isogenic mutant UPEC (black stripes) in the presence of PMNs. The results are from three experiments in triplicate and are shown as the mean Log₁₀ CFU/mL viable bacteria; the error brackets indicate the 95% confidence intervals for each condition. The data were analyzed by ANOVA, and the differences are significant ($p < 0.01$).



For that purpose, we elected to examine chemotaxis of PMNs because it is controlled in part by the Rho family GTPases and, because CNF1 constitutively activates this family of GTP binding proteins. When the chemotaxis of PMNs co-incubated with OMVs from CP9 was measured relative to the untreated controls after 1 hour, the PMNs co-incubated with wild-type OMVs demonstrated significantly ($p < 0.05$) diminished chemotaxis compared to PMNs co-incubated with OMVs from the isogenic mutant in a dose dependent manner (Figure 22). Although OMVs from the isogenic mutant reduced PMN chemotaxis at the highest concentration tested, this effect was not statistically significant and was likely due to bacterial products in the OMVs competing with the fMLP gradient. Additionally, we observed that an equivalent amount of purified CNF1 to that delivered by OMVs did not affect chemotaxis (Figure 22). In total, these findings demonstrate that OMVs that contain CNF1 diminish the chemotactic response of PMNs and indicate that OMVs may intoxicate PMNs more efficiently than purified toxin.

Figure 22. PMN chemotaxis is inhibited in the presence of CNF1-containing OMVs.

The PMN chemotactic response to fMLP was evaluated in Boyden-type chambers following pre-incubation of PMNs with OMVs derived from wild-type CP9 (black), *cnf1* isogenic mutant UPEC (white) or purified CNF1 (gray). PMNs were allowed to respond to the fMLP gradient for 1 hour; the number of migrated PMNs from each condition was determined fluorescently based on a standard curve. The data were then normalized relative to the untreated control. The results of three experiments in duplicate are shown as the mean normalized chemotactic index; error brackets indicate the standard error of the mean. The normalized data were analyzed by ANOVA, and the differences are significant ($p < 0.05$).



Chapter 4

Discussion and Future Directions

Overview of results in the context of the dissertation objective and specific aims

The objective of this thesis was to evaluate the role of CNF1 expressed by UPEC in the modulation of PMN function. A model in which mouse PMNs were co-incubated with CNF1-expressing UPEC strain CP9, its isogenic CNF1-negative mutant or, in some cases, a complementing clone of this mutant was used to address each of the three specific aims. This in vitro model allowed us to measure changes in mouse PMN physiology and to make a direct comparison with previously published results obtained in an in vivo murine model of an ascending UTI. The experiments designed to evaluate the first aim of this dissertation demonstrated that CNF1 expression by UPEC led to a significant UPEC survival advantage when UPEC were exposed to mouse PMNs. A more detailed evaluation of the changes in PMN physiology in the second aim revealed that the survival advantage displayed by CNF1-expressing UPEC was the result of several CNF1-induced changes in PMN physiology that diminished the antimicrobial capacity of intoxicated PMNs. Furthermore, the results obtained from the third aim of this dissertation revealed that CNF1 is released from UPEC in a complex with outer membrane vesicles and that these vesicles deliver toxin to mouse PMNs. The PMNs intoxicated in this fashion exhibited a diminished antimicrobial response and decreased chemotaxis in response to chemical stimulation. The remainder of this section discusses the dissertation results in more detail and concludes with a model of my interpretation of

the mechanism by which CNF1- expressing UPEC subvert PMN antimicrobial responses.

CNF1 modulates the PMN antimicrobial response

Several changes in phenotype were noted in mouse PMNs exposed to UPEC that produce CNF1. First, these PMNs showed a decreased capacity to phagocytose CNF1-expressing bacteria compared to a CNF1-negative derivative. Second, exposure of PMNs to CNF1-positive UPEC resulted in redistribution of complement receptor 3 (CR3, CD11b/CD18) on the surface of the phagocyte and a diminished spreading of the PMNs. Third, CNF1 production by UPEC altered the intracellular respiratory burst as measured by luminol. Fourth, the PMNs mixed with UPEC that expressed CNF1 displayed increased levels of activated Rac2, a Rho family GTPase involved in the assembly of the NADPH oxidase complex in PMNs. The net result of these CNF1-mediated phenotypic changes in PMNs was that CNF1-producing UPEC grew better in the presence of these phagocytes than did the isogenic CNF1-negative mutant. Such variation in net replication of CNF1-positive versus CNF1-negative UPEC in the presence of PMNs supports earlier observations from a mouse UTI model of co-infection in which the CNF1-expressing UPEC out competed the isogenic, CNF1-negative mutant in the bladder (Rippere-Lampe, O'Brien et al. 2001).

CNF1-induced changes in PMN phagocytosis

To explain our finding that CNF1-expressing UPEC were not phagocytosed as effectively as the isogenic mutant, and in light of previous studies that showed that CNF1 can alter the cytoskeleton of toxin-exposed cells (Schmidt, Sehr et al. 1997; Lerm, Selzer et al. 1999; Hofman, Le Negrate et al. 2000; Mills, Meysick et al. 2000), we tested the idea that PMNs exposed to CNF1-positive UPEC are unable to re-model their plasma membranes. We reasoned that during phagocytosis, the neutrophil plasma membrane must adjust its shape in the region around the particle to be phagocytosed. Since the spreading of PMNs on surfaces requires the PMN plasma membrane to change contours, PMN spreading was used as a measure of such fluidity. PMNs that were co-incubated with CNF1-expressing UPEC failed to re-model their membrane, usually remained spherical in shape, and displayed significantly less spreading than did PMNs exposed to the *cnf1* isogenic mutant. Based on these observations, we conclude that the decreased plasticity of the plasma membrane of PMNs exposed to CNF1-expressing UPEC is in part responsible for the reduced phagocytic activity of those leukocytes.

Although the association of CNF1-expressing UPEC with PMNs was enhanced at early time points after infection, this association then reached a plateau. This latter observation suggests that available PMN receptors either were saturated or were not in the correct conformation to interact with or allow the PMN to efficiently phagocytose

serum-opsonized CNF1-expressing bacteria. We favor the first hypothesis. Indeed, if the receptors were not in the correct conformation to interact with serum-opsonized UPEC it is unlikely that we could have observed either greater numbers of associated UPEC compared to the isogenic mutant at any time point or an increase in the number of associated UPEC throughout the experiment.

The apparent inhibition of further phagocytosis by PMNs associated with CNF1-positive strains was not a consequence of insufficiently opsonized bacteria because the similarly treated *cnf1* mutant bacteria continued to associate with PMNs and were phagocytosed to a greater extent throughout the experiment. We believe a more reasonable explanation for the apparent inhibition of further phagocytosis by PMNs of CNF1-positive UPEC is that the concentration of CNF1 increased in our experimental system over time as the population of UPEC expanded. Thus, we speculate that the PMNs were continuously exposed to CNF1, which, in turn, led to decreased phagocytosis of the toxin-expressing organisms.

That CNF1-expressing UPEC exert an anti-phagocytic effect on mouse PMNs is consistent with the conclusion of Hofman et al. (Hofman, Le Negrate et al. 2000). These researchers used flow cytometric analysis to examine phagocytic uptake of a non-pathogenic, GFP- expressing strain of *E. coli* by human PMNs intoxicated 18-24 hours prior to bacterial exposure with CNF1. Hofman and colleagues showed that purified CNF1 inhibits phagocytosis by such CNF1-pretreated PMNs. Our results on the impact of CNF1 on phagocytosis of PMNs are in keeping with these data and extend the findings

to show that the anti-phagocytic effect of CNF1 can occur coincident with exposure to CNF1-expressing UPEC.

Alteration of CD11b clustering

The greater net growth of the serum-opsonized, CNF1-positive wild-type strain and complemented clone compared to serum-opsonized *cnf1* mutant bacteria when co-incubated with PMNs was negated when serum was heat-inactivated or when cytochalasin D was present. The obliteration of this differential replication effect indicates that heat-labile factors and phagocytosis are required for the control of both CNF1-positive and CNF1-negative UPEC. Complement is a heat-labile factor that can opsonize bacteria, which, in turn are then recognized by complement receptor 3 (CR3) on the surface of PMNs. The recognition of opsonized bacteria by and subsequent clustering of CR3 then results in the phagocytosis of complement-opsonized bacteria. Consistent with the requirement for CR3 clustering beneath opsonized bacteria, we observed by confocal microscopy that CR3 did not aggregate beneath bacteria when PMNs were exposed to CNF1-expressing UPEC. However, clustering of CR3 did occur in PMNs co-incubated with CP9*cnf1*. In contrast to our results, Hofman demonstrated that CNF1 intoxication of human PMNs resulted in many punctate patches of CR3 (Hofman, Le Negrate et al. 2000). The reason our results and those of Hofman and colleagues are at variance may reflect our different experimental strategies. We used a UPEC-PMN

infection model and examined early time-points while Hofman and co-workers intoxicated the PMNs with CNF1, then assessed CD11b clustering at later time points. In addition, the PMNs used in our experiments were likely at a different state of activation when exposed to UPEC then the human PMNs purified by Hofman and colleagues from venous blood. Other aspects of our results were similar to those of Hofman and co-workers; for example, we also did not detect any difference in the amount of CR3 exposed on the surface of the PMN. Precisely how CNF1 affects the distribution of CR3 is not clear, but it is known that the Rho GTPases that are targets of CNF1 can influence the avidity maturation of integrins (Schwartz and Shattil 2000), possibly by controlling the polymerization state of actin (Kucik, Dustin et al. 1996). Indeed, Kucik and colleagues (Kucik, Dustin et al. 1996) showed that increased lateral mobility of the β_2 integrin LFA-1 could be explained by the release of LFA-1 from its cytoskeletal constraints by depolymerization of actin with cytochalasin D. The release of LFA-1 was accompanied by a 10-fold increase in lateral mobility and increased adhesion to ICAM-1.

CNF1 enhanced ROS generation

We also demonstrated that CNF1-expressing UPEC developed a more robust luminol-dependent chemiluminescent signal compared to the CNF1-negative strain, a result that indicates that the intracellular generation of ROS was increased compared to

the isogenic mutant. The finding that intracellular ROS generation was increased in spite of a decrease in phagocytic capacity is at first counter intuitive. However, we believe that both the increase in intracellular ROS and diminished phagocytic capacity are the result of CNF1 activity on Rho family members in PMNs. Our detection of increased Rac2-GTP in PMNs exposed to CNF1-expressing UPEC provides an explanation for the observed ROS increase in our model. The NADPH oxidase complex was the first characterized Rho GTPase regulated system (Bokoch and Diebold 2002). That Rac2 can regulate the NADPH oxidase complex required for generation of ROS was demonstrated in a cell-free system with Rac2 purified from human PMNs (Knaus, Heyworth et al. 1992). Additional support for the role of Rac2 in the oxidase was provided by animal and human studies (Ambruso, Knall et al. 2000; Gu, Jia et al. 2001; Kurkchubasche, Panepinto et al. 2001; Li, Yamauchi et al. 2002). Thus, our results are consistent with the recognized role of Rac2 in NADPH oxidase assembly and ROS generation and support and extend the findings of Hofman et. al. who showed that purified CNF1 enhances the production of ROS in PMNs (Hofman, Le Negrate et al. 2000). In our experimental system, the observed increase in intracellular ROS generation can be viewed as a consequence of toxin activity that led to increased levels of Rac2-GTP rather than from increased PMN phagocytic capacity.

In spite of the large increase in intracellular ROS in PMNs exposed to CNF1-producing UPEC, no increased release of ROS into the extracellular environment was detected. The finding that extracellular levels of ROS were similar for PMNs exposed to

CNF1-positive and CNF1-negative UPEC was surprising and suggests that intoxicated PMNs are unable to deliver the intracellular ROS to the extracellular environment. The accumulation of extracellular ROS has been hypothesized to aid in the inactivation of bacteria that are poorly phagocytosed by PMNs (Lock, Dahlgren et al. 1990). Therefore, by blocking this aspect of phagocyte physiology, CNF1-expressing UPEC may avoid oxidative killing by PMNs.

Our findings of increased Rac2-GTP are consistent with the result of Pop et. al. who demonstrated that CNF1 may be capable of modifying Rac2 (Pop, Aktories et al. 2004). Pop et. al. made the additional finding that activated Rac2 in CNF1-intoxicated cells is not degraded by the proteosome as is Rac1 (Pop, Aktories et al. 2004). The degradation of modified Rac1 would limit the extent of signaling by Rac1-GTP in a cell intoxicated by CNF1. If activated Rac2 is not degraded, it could participate in prolonged signaling events such as enhanced assembly of the NADPH oxidase. Such an event could, in turn, result in the increased generation of ROS that was observed in this study.

Membrane vesicles target CNF1 to PMNs

The CNF1-induced changes in PMN physiology described so far, provide an explanation for the observed survival advantage of UPEC that express this toxin. In these

phagocytic capacity experiments, PMNs that were not in direct contact with CNF1 expressing UPEC displayed a phenotype similar to PMNs that were in direct contact with toxigenic UPEC. This observation indicated that direct UPEC: PMN interaction was not necessary for CNF1 intoxication and suggested that CNF1 may be released by UPEC. However, the mechanism responsible for the export of CNF1 from UPEC strains was not known at the initiation of these studies, and analysis of this process provided the basis for the third aim of this dissertation.

A series of experiments designed to address this aim produced evidence that CNF1 from UPEC strain CP9 is associated with an acellular fraction that contains membrane vesicles with characteristics of the bacterial outer membrane. These experiments also demonstrated that mouse PMNs exhibit an altered phenotype when co-incubated with membrane vesicles. Specifically, PMNs that were treated with wild-type membrane vesicles displayed an altered antimicrobial capacity and a diminished chemotactic response compared to PMNs treated with membrane vesicles from the CNF1-negative mutant. These findings suggest that biologically active CNF1 from UPEC can be delivered to PMNs via outer membrane vesicles.

CNF1 is complexed with outer membrane vesicles

Initially, we were surprised to detect CNF1 in the vesicle fraction, because CNF1

does not possess a signal sequence that would facilitate its release from the cytoplasm. However, the hypothesis that CNF1 might be present in the outer membrane is not unique to this investigation. Landraud and colleagues demonstrated that high level CNF1 expression was due to the transcription of a single long mRNA that encodes both hemolysin and CNF1 (Landraud, Gibert et al. 2003). The expression of this transcript is under the control of the hemolysin operon promoter upstream of *cnf1* and is enhanced by RfaH, a transcriptional activator known to control the expression of transcripts of many proteins destined for the outer membrane of *E. coli*. From those findings, these investigators proposed that CNF1 may also be destined for the outer membrane (Landraud, Gibert et al. 2003).

Two alternative explanations for our finding of CNF1 in the vesicle fraction are also possible. First, bacterial lysis may have released cytoplasmic contents that included CNF1 or, second, CNF1 may have formed multimers or a precipitate that sedimented during ultracentrifugation. The argument against the first possibility is the finding of negligible levels of β -galactosidase activity under our experimental conditions. Our line of reasoning against the second scenario, the possible formation of CNF1 multimers, is that the apparent molecular weight of CNF1 in our vesicle fraction was very close to the predicted molecular weight of CNF1. We believe that multimers large enough to be sedimented during ultracentrifugation would have an apparent molecular weight greater than the predicted molecular weight of CNF1, or that multiple bands of CNF1 would have been detected by immunoblot analysis.

OMVs interact with and alter antimicrobial responses of PMNs

We propose that for OMVs to convey biologically active toxin to the PMN these vesicles must first interact with these phagocytes. The membrane vesicles appeared to fulfill this requirement as evaluated by co-incubation studies with mouse PMNs. Indeed, in these co-incubation experiments, we noted by immunostaining the formation of many punctate patches of O4 antigen on the PMNs. This observation suggests that the membrane vesicles may have merged with the PMNs. Kesty and colleagues also reported similar interactions between the toxin-bearing vesicles of ETEC with eukaryotic cells (Kesty, Mason et al. 2004). That our vesicles contained biologically active toxin was demonstrated by three separate phenotypic assays. First, when HEp-2 cells were incubated with OMVs derived from CP9, these cells demonstrated a pattern of multinucleation similar to HEp-2 cells incubated with purified toxin. The multinucleation pattern is a classic phenotype of CNF1 intoxication in HEp-2 cells. Second, the net replication of the CP9*cnfI* was significantly less than the net replication of CP9 in the presence of PMNs and OMVs collected from the *cnfI* isogenic mutant. However, when wild-type vesicles were substituted for mutant vesicles in similar studies, the net replication of the *cnfI* isogenic mutant was essentially equivalent to the wild-type

CP9. Finally, the chemotactic response of PMNs to fMLP was altered in a dose dependent fashion following treatment with CNF1-bearing vesicles but not when PMNs were treated with membrane vesicles from the CNF1 mutant or purified toxin. The results of our chemotaxis experiments revealed that CNF1-bearing vesicles diminish PMN chemotaxis in response to chemical attractants and indicated that CNF1 acts directly on PMNs.

The constitutive activation of Rho family GTPases by CNF1 provides a potential explanation for our observation of diminished chemotaxis of PMNs in the presence of CNF1-containing OMVs. Chemotaxis is a complex process in which neutrophils must detect the chemotactic stimuli and become oriented in a polarized fashion (Xu, Wang et al. 2003). The precise mechanism that controls this cellular response is unclear, but Rho family GTPases do have distinct roles in this process (Allen, Zicha et al. 1998; Li, Hannigan et al. 2003; Srinivasan, Wang et al. 2003; Xu, Wang et al. 2003). For example, Srinivasan and colleagues reported that differentiated HL-60 cells transfected with a dominant active form of Rac (RacV12) demonstrated a uniform distribution of activated Rac compared to untransfected control cells that showed a more polarized distribution of Rac in response to a gradient of fMLP (Srinivasan, Wang et al. 2003). In addition, Allen and colleagues detected a decreased chemotactic response in macrophages microinjected with dominant active RhoA, Rac1 and Cdc42 (Allen, Zicha et al. 1998). These investigators hypothesized that constitutively active RhoA would be antagonistic to Rac and the development of a polarized morphology. Indeed, this theory was proven by Xu

who used differentiated HL-60 cells transfected with dominant active RhoA to show that these transfected cells failed to develop a polarized morphology or undergo chemotaxis in response to fMLP (Xu, Wang et al. 2003). Based on these earlier observations and our own studies, we speculate that the diminished chemotaxis demonstrated by neutrophils exposed to wild-type vesicles reflects the constitutive activation of Rho GTPases by CNF1. Specifically, we propose that the CNF1-catalyzed deamidation of RhoGTPases results in a reduction in the capacity of intoxicated neutrophils to establish and maintain a polarized front in response to a gradient of fMLP.

When we exposed PMNs to purified CNF1, we did not detect any effect on chemotaxis. Similar results were obtained by Hofman and colleagues, who saw negligible effects from CNF1 on migration of human neutrophils through polarized T24 cell monolayers (Hofman, Flatau et al. 1998). In contrast, as discussed above, we observed a clear chemotactic effect on PMNs in response to CNF1-containing outer membrane vesicles. The delivery of CNF1 via membrane vesicles may target toxin to the PMN membrane and possibly the cytosol more effectively than the receptor-mediated pathway previously described for CNF1 (Contamin, Galmiche et al. 2000; Chung, Hong et al. 2003). The detection of CNF1 associated with outer membrane vesicles derived from UPEC strain CP9, and the observed biological effects of such vesicles on PMNs suggest that OMVs may provide an important vehicle for delivery of CNF1 by UPEC during infection. Such delivery of CNF1 may, in turn, lead to interference with PMN antimicrobial capacity and chemotaxis.

Conclusions and model

The results of this dissertation support the hypothesis that CNF1 expression by UPEC modulates PMN antimicrobial function which, in turn, leads to enhanced net replication of toxigenic UPEC. Expression of CNF1 by UPEC prevented CD11b clustering, diminished the phagocytic capacity of PMNs, increased the extent of Rac2 activation and enhanced the generation of intracellular ROS. Furthermore, a mechanism of CNF1 release from UPEC via outer membrane vesicles was described, and these vesicles were shown to bear biologically active toxin that altered PMN antimicrobial capacity and diminished chemotaxis. The diminished chemotaxis displayed by PMNs exposed to CNF1-expressing UPEC is significant because such PMNs would not be able to migrate through tissue in pursuit of UPEC. In addition, the membranes of the intoxicated and paralyzed PMNs may eventually rupture; the loss of membrane integrity could lead to the release of enzymes that could damage surrounding tissue. The data from this dissertation collectively defines a new molecular model of UPEC interaction with host PMNs in the course of a UTI (Figure 23). This model helps to explain, in part, the often severe infections associated with CNF1-expressing UPEC. In this model, UPEC release CNF1 into the extracellular environment via outer membrane vesicles. These vesicles diffuse through the environment and deliver CNF1 to PMNs. In this

Figure 23. Proposed model for CNF1 modulation of PMN function.

(A) PMN interaction with CNF1-negative UPEC results in membrane remodeling and clustering of CD11b followed by phagocytosis of opsonized UPEC. After the PMN phagocytose the bacteria, the NADPH oxidase complex generates reactive oxygen species that inactivates the internalized UPEC strain. (B) CNF1-expressing UPEC escape the antimicrobial properties of PMNs by impairing membrane remodeling and clustering of CD11b, events that prevent the phagocytosis of opsonized UPEC. Outer membrane vesicles from UPEC convey CNF1 to PMNs in the vicinity of the CNF1-expressing UPEC. Simultaneously, CNF1 enhances the intracellular generation of reactive oxygen species independently of phagocytosis by increasing the amount of Rac2-GTP. Dashed arrows indicate the hypothesized deamidation and constitutive activation of Rac2.

A


 O_2 $\cdot O_2$

Rac2-GTP

Rac2-GDP

C3b

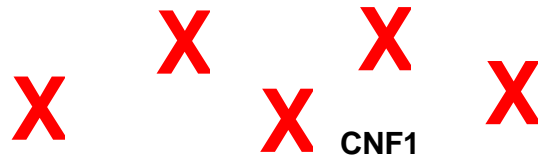
NADPH

CD11b

OMV

UPEC

B


 O_2 $\cdot O_2$
^{*}Rac2-GTP O_2 $\cdot O_2$

CNF1

^{*}Rac2-GTP

manner CNF1-expressing UPEC modulate key aspects of PMN physiology, in part, by altering Rho-GTPase activity which, in turn, leads to enhanced replication of these bacterial strains. Specifically, CNF1- expressing UPEC decrease the extent of membrane remodeling and CD11b clustering, events that result in a decreased phagocytic capacity while simultaneously increasing the extent of Rac2-GTP in PMNs. This increase in activated Rac2 then promotes an enhanced intracellular respiratory burst. Concomitantly, PMNs that are exposed to CNF1 via membrane vesicles fail to undergo chemotaxis in response to formyl methionyl peptides. In sum, we propose that the release of membrane vesicles that convey CNF1 to PMNs allows CNF1-expressing UPEC to reduce phagocytosis by PMNs and to limit the release of ROS. Simultaneously, PMNs exposed to vesicle- delivered CNF1 fail to follow a chemotactic gradient. The net effect of these CNF1- mediated alterations of PMN physiology allows the bacteria to survive the acute inflammatory response and facilitates enhanced net replication of the organisms. Such an expanding bacterial population in an otherwise sterile site may allow deeper tissue penetration by these strains.

Future directions

The results presented in this dissertation provide a novel paradigm for the role of CNF1 in UPEC pathogenesis. Concurrently, these findings also lead to new avenues of

investigation into the interaction of CNF1 with PMNs as well as toxin expression by UPEC. For example, an analysis of the changes induced by CNF1 in the transcriptome of PMNs is a logical step. Rho family proteins control not only actin cytoskeletal changes but also exert control over gene transcription. PMNs have recently been shown to undergo extensive changes in transcription in the course of pathogen contact. Activation of Rho family proteins is associated with increased NF κ B activation that could lead to enhanced production of the chemokine IL-8 (MIP2- α in mice). Intoxicated PMNs may therefore contribute to the escalation of the acute inflammatory response in the presence of CNF1-expressing UPEC. Epithelial cells may also respond in a similar fashion to Rho GTPase activation and contribute to enhanced recruitment of PMNs.

Another area of research that is a logical extension of the findings in this dissertation is an analyses of the anatomical location of and level of CNF1 expression by UPEC in the mouse UTI model. Low-level CNF1 expression appears to be constitutive, but whether enhanced CNF1 synthesis occurs in vivo remains an open question. The results of this dissertation suggest that CNF1 expression would be beneficial to UPEC soon after bladder epithelial cell penetration has occurred and when initial contact with PMNs is made. Toxin expression studies in situ would test this theory and might reveal environmental signals that stimulate increased CNF1 synthesis.

References

- Aktories, K. and J. T. Barbieri (2005). "Bacterial cytotoxins: targeting eukaryotic switches." Nat Rev Microbiol **3**(5): 397-410.
- Allen, W. E., D. Zicha, et al. (1998). "A role for Cdc42 in macrophage chemotaxis." J Cell Biol **141**(5): 1147-57.
- Ambruso, D. R., C. Knall, et al. (2000). "Human neutrophil immunodeficiency syndrome is associated with an inhibitory Rac2 mutation." Proc Natl Acad Sci U S A **97**(9): 4654-9.
- Bahrani-Mougeot, F. K., E. L. Buckles, et al. (2002). "Type 1 fimbriae and extracellular polysaccharides are preeminent uropathogenic *Escherichia coli* virulence determinants in the murine urinary tract." Mol Microbiol **45**(4): 1079-93.
- Beveridge, T. J. (1999). "Structures of gram-negative cell walls and their derived membrane vesicles." J Bacteriol **181**(16): 4725-33.
- Blanco, J., M. Blanco, et al. (1992). "Characteristics of haemolytic *Escherichia coli* with particular reference to production of cytotoxic necrotizing factor type 1 (CNF1)." Res Microbiol **143**(9): 869-78.
- Blanco, M., J. E. Blanco, et al. (1994). "Virulence factors and O groups of *Escherichia coli* strains isolated from cultures of blood specimens from urosepsis and non-urosepsis patients." Microbiologia **10**(3): 249-56.
- Bokoch, G. M. (1995). "Regulation of the phagocyte respiratory burst by small GTP-binding proteins." Trends Cell Biol **5**(3): 109-13.

- Bokoch, G. M. and B. A. Diebold (2002). "Current molecular models for NADPH oxidase regulation by Rac GTPase." Blood **100**(8): 2692-6.
- Boquet, P. (2000). "Small GTP binding proteins and bacterial virulence." Microbes Infect **2**(7): 837-43.
- Borregaard, N. (1997). "Development of neutrophil granule diversity." Ann N Y Acad Sci **832**: 62-8.
- Bylund, J., M. Samuelsson, et al. (2003). "NADPH-oxidase activation in murine neutrophils via formyl peptide receptors." Exp Cell Res **282**(2): 70-7.
- Caprioli, A., G. Donelli, et al. (1984). "A cell division-active protein from *E. coli*." Biochem Biophys Res Commun **118**(2): 587-93.
- Caprioli, A., V. Falbo, et al. (1983). "Partial purification and characterization of an *Escherichia coli* toxic factor that induces morphological cell alterations." Infect Immun **39**(3): 1300-6.
- Caron, E. and A. Hall (1998). "Identification of two distinct mechanisms of phagocytosis controlled by different Rho GTPases." Science **282**(5394): 1717-21.
- Cattell, W. R. (1996). Infections of the kidney and urinary tract. Oxford; New York, Oxford University Press.
- Chung, J. W., S. J. Hong, et al. (2003). "37-kDa laminin receptor precursor modulates cytotoxic necrotizing factor 1-mediated RhoA activation and bacterial uptake." J Biol Chem **278**(19): 16857-62.
- Connell, I., W. Agace, et al. (1996). "Type 1 fimbrial expression enhances *Escherichia*

- coli* virulence for the urinary tract." Proc Natl Acad Sci U S A **93**(18): 9827-32.
- Contamin, S., A. Galmiche, et al. (2000). "The p21 Rho-activating toxin cytotoxic necrotizing factor 1 is endocytosed by a clathrin-independent mechanism and enters the cytosol by an acidic-dependent membrane translocation step." Mol Biol Cell **11**(5): 1775-87.
- Davis, J. M., S. B. Rasmussen, et al. (2005). "Cytotoxic Necrotizing Factor Type 1 Production by Uropathogenic *Escherichia coli* Modulates Polymorphonuclear Leukocyte Function." Infect Immun **73**(9): 5301-10.
- De Rycke, J., E. A. Gonzalez, et al. (1990). "Evidence for two types of cytotoxic necrotizing factor in human and animal clinical isolates of *Escherichia coli*." J Clin Microbiol **28**(4): 694-9.
- De Rycke, J., J. F. Guillot, et al. (1987). "Cytotoxins in non-enterotoxigenic strains of *Escherichia coli* isolated from feces of diarrheic calves." Vet Microbiol **15**(1-2): 137-50.
- Diebold, B. A. and G. M. Bokoch (2001). "Molecular basis for Rac2 regulation of phagocyte NADPH oxidase." Nat Immunol **2**(3): 211-5.
- Duncan, A., P. Grutkoski, et al. (2000). "Neutrophils regulate their own apoptosis via preservation of CXCR receptors." J Surg Res **90**(1): 32-8.
- Elliott, S. J., S. Srinivas, et al. (1998). "Characterization of the roles of hemolysin and other toxins in enteropathy caused by alpha-hemolytic *Escherichia coli* linked to human diarrhea." Infect Immun **66**(5): 2040-51.

- Falbo, V., M. Famiglietti, et al. (1992). "Gene block encoding production of cytotoxic necrotizing factor 1 and hemolysin in *Escherichia coli* isolates from extraintestinal infections." Infect Immun **60**(6): 2182-7.
- Fiorentini, C., G. Arancia, et al. (1988). "Cytoskeletal changes induced in HEp-2 cells by the cytotoxic necrotizing factor of *Escherichia coli*." Toxicon **26**(11): 1047-56.
- Flatau, G., L. Landraud, et al. (2000). "Deamidation of RhoA glutamine 63 by the *Escherichia coli* CNF1 toxin requires a short sequence of the GTPase switch 2 domain." Biochem Biophys Res Commun **267**(2): 588-92.
- Foxman, B. (2002). "Epidemiology of urinary tract infections: incidence, morbidity, and economic costs." Am J Med **113 Suppl 1A**: 5S-13S.
- Foxman, B., L. Zhang, et al. (1995). "Bacterial virulence characteristics of *Escherichia coli* isolates from first-time urinary tract infection." J Infect Dis **171**(6): 1514-21.
- Gardiner, E. M., K. N. Pestonjamas, et al. (2002). "Spatial and temporal analysis of Rac activation during live neutrophil chemotaxis." Curr Biol **12**(23): 2029-34.
- Goping, G., H. B. Pollard, et al. (1995). "Effect of MPTP on dopaminergic neurons in the goldfish brain: a light and electron microscope study." Brain Res **687**(1-2): 35-52.
- Goping, G., S. Yedgar, et al. (1992). "Flat embedding and immunolabelling of SW 1116 colon carcinoma cells in LR white: an improved technique in light and electron microscopy." Microsc Res Tech **21**(1): 1-9.
- Gorzalczany, Y., N. Sigal, et al. (2000). "Targeting of Rac1 to the phagocyte membrane is sufficient for the induction of NADPH oxidase assembly." J Biol Chem

275(51): 40073-81.

Goullet, P., B. Picard, et al. (1994). "Correlation between esterase electrophoretic polymorphism and virulence-associated traits in extra-intestinal invasive strains of *Escherichia coli*." Epidemiol Infect **112**(1): 51-62.

Gu, Y., B. Jia, et al. (2001). "Biochemical and biological characterization of a human Rac2 GTPase mutant associated with phagocytic immunodeficiency." J Biol Chem **276**(19): 15929-38.

Gunther, N. W. t., V. Lockatell, et al. (2001). "In vivo dynamics of type 1 fimbria regulation in uropathogenic *Escherichia coli* during experimental urinary tract infection." Infect Immun **69**(5): 2838-46.

Haraoka, M., L. Hang, et al. (1999). "Neutrophil recruitment and resistance to urinary tract infection." J Infect Dis **180**(4): 1220-9.

Heine, H. S. (1993). Biosynthesis of Enterobacterial Common Antigen. The ECA-Trace Phenotype of *Salmonella typhimurium* and the Role of the rfe Gene in O8 Side-chain Synthesis in *Escherichia coli*. Microbiology and Immunolgy. Bethesda, Maryland, Uniformed Services University: 255.

Hofman, P., G. Flatau, et al. (1998). "*Escherichia coli* cytotoxic necrotizing factor 1 effaces microvilli and decreases transmigration of polymorphonuclear leukocytes in intestinal T84 epithelial cell monolayers." Infect Immun **66**(6): 2494-500.

Hofman, P., G. Le Negrate, et al. (2000). "*Escherichia coli* cytotoxic necrotizing factor-1 (CNF-1) increases the adherence to epithelia and the oxidative burst of human

- polymorphonuclear leukocytes but decreases bacteria phagocytosis." J Leukoc Biol **68**(4): 522-8.
- Horiguchi, Y. (2001). "*Escherichia coli* cytotoxic necrotizing factors and Bordetella dermonecrotic toxin: the dermonecrosis-inducing toxins activating Rho small GTPases." Toxicon **39**(11): 1619-27.
- Horstman, A. L. and M. J. Kuehn (2000). "Enterotoxigenic *Escherichia coli* secretes active heat-labile enterotoxin via outer membrane vesicles." J Biol Chem **275**(17): 12489-96.
- Johnson, J. R. (1991). "Virulence factors in *Escherichia coli* urinary tract infection." Clin Microbiol Rev **4**(1): 80-128.
- Johnson, J. R., F. Scheutz, et al. (2005). "Phylogenetic and pathotypic comparison of concurrent urine and rectal *Escherichia coli* isolates from men with febrile urinary tract infection." J Clin Microbiol **43**(8): 3895-900.
- Kadurugamuwa, J. L. and T. J. Beveridge (1995). "Virulence factors are released from *Pseudomonas aeruginosa* in association with membrane vesicles during normal growth and exposure to gentamicin: a novel mechanism of enzyme secretion." J Bacteriol **177**(14): 3998-4008.
- Kaper, J. B., J. P. Nataro, et al. (2004). "Pathogenic *Escherichia coli*." Nat Rev Microbiol **2**(2): 123-40.
- Kaplan, G. (1977). "Differences in the mode of phagocytosis with Fc and C3 receptors in macrophages." Scand J Immunol **6**(8): 797-807.

- Keenan, J., T. Day, et al. (2000). "A role for the bacterial outer membrane in the pathogenesis of *Helicobacter pylori* infection." FEMS Microbiol Lett **182**(2): 259-64.
- Kesty, N. C., K. M. Mason, et al. (2004). "Enterotoxigenic *Escherichia coli* vesicles target toxin delivery into mammalian cells." Embo J **23**(23): 4538-49.
- Kettritz, R., M. L. Gaido, et al. (1998). "Interleukin-8 delays spontaneous and tumor necrosis factor-alpha-mediated apoptosis of human neutrophils." Kidney Int **53**(1): 84-91.
- Kim, C. and M. C. Dinarello (2001). "Rac2 is an essential regulator of neutrophil nicotinamide adenine dinucleotide phosphate oxidase activation in response to specific signaling pathways." J Immunol **166**(2): 1223-32.
- Kim, K. J., J. W. Chung, et al. (2005). "67-kDa laminin receptor promotes internalization of cytotoxic necrotizing factor 1-expressing *Escherichia coli* K1 into human brain microvascular endothelial cells." J Biol Chem **280**(2): 1360-8.
- Knaus, U. G., P. G. Heyworth, et al. (1992). "Purification and characterization of Rac 2. A cytosolic GTP-binding protein that regulates human neutrophil NADPH oxidase." J Biol Chem **267**(33): 23575-82.
- Kucik, D. F., M. L. Dustin, et al. (1996). "Adhesion-activating phorbol ester increases the mobility of leukocyte integrin LFA-1 in cultured lymphocytes." J Clin Invest **97**(9): 2139-44.
- Kurkchubasche, A. G., J. A. Panepinto, et al. (2001). "Clinical features of a human Rac2

- mutation: a complex neutrophil dysfunction disease." J Pediatr **139**(1): 141-7.
- Laestadius, A., A. Richter-Dahlfors, et al. (2002). "Dual effects of *Escherichia coli* alpha-hemolysin on rat renal proximal tubule cells." Kidney Int **62**(6): 2035-42.
- Landraud, L., M. Gibert, et al. (2003). "Expression of *cnf1* by *Escherichia coli* J96 involves a large upstream DNA region including the *hlyCABD* operon, and is regulated by the RfaH protein." Mol Microbiol **47**(6): 1653-67.
- Lanning, C. C., J. L. Daddona, et al. (2004). "The Rac1 C-terminal polybasic region regulates the nuclear localization and protein degradation of Rac1." J Biol Chem **279**(42): 44197-210.
- Lerm, M., M. Pop, et al. (2002). "Proteasomal degradation of cytotoxic necrotizing factor 1-activated rac." Infect Immun **70**(8): 4053-8.
- Lerm, M., G. Schmidt, et al. (2000). "Bacterial protein toxins targeting rho GTPases." FEMS Microbiol Lett **188**(1): 1-6.
- Lerm, M., G. Schmidt, et al. (1999). "Identification of the region of rho involved in substrate recognition by *Escherichia coli* cytotoxic necrotizing factor 1 (CNF1)." J Biol Chem **274**(41): 28999-9004.
- Lerm, M., J. Selzer, et al. (1999). "Deamidation of Cdc42 and Rac by *Escherichia coli* cytotoxic necrotizing factor 1: activation of c-Jun N-terminal kinase in HeLa cells." Infect Immun **67**(2): 496-503.
- Li, S., A. Yamauchi, et al. (2002). "Chemoattractant-stimulated Rac activation in wild-type and Rac2-deficient murine neutrophils: preferential activation of Rac2 and

- Rac2 gene dosage effect on neutrophil functions." J Immunol **169**(9): 5043-51.
- Li, Z., M. Hannigan, et al. (2003). "Directional sensing requires G beta gamma-mediated PAK1 and PIX alpha-dependent activation of Cdc42." Cell **114**(2): 215-27.
- Lim, J. K., N. W. t. Gunther, et al. (1998). "In vivo phase variation of *Escherichia coli* type 1 fimbrial genes in women with urinary tract infection." Infect Immun **66**(7): 3303-10.
- Lock, R., C. Dahlgren, et al. (1990). "Neutrophil killing of two type 1 fimbria-bearing *Escherichia coli* strains: dependence on respiratory burst activation." Infect Immun **58**(1): 37-42.
- Maloy, S. R., V. J. Stewart, et al. (1996). Genetic analysis of pathogenic bacteria: a laboratory manual. Plainview, N.Y., Cold Spring Harbor Laboratory Press.
- Massol, P., P. Montcourrier, et al. (1998). "Fc receptor-mediated phagocytosis requires CDC42 and Rac1." Embo J **17**(21): 6219-29.
- Menard, S., E. Tagliabue, et al. (1998). "The 67 kDa laminin receptor as a prognostic factor in human cancer." Breast Cancer Res Treat **52**(1-3): 137-45.
- Mills, M., K. C. Meysick, et al. (2000). "Cytotoxic necrotizing factor type 1 of uropathogenic *Escherichia coli* kills cultured human uroepithelial 5637 cells by an apoptotic mechanism." Infect Immun **68**(10): 5869-80.
- Montuori, N. and M. E. Sobel (1996). "The 67-kDa laminin receptor and tumor progression." Curr Top Microbiol Immunol **213 (Pt 1)**: 205-14.
- Mulvey, M. A., Y. S. Lopez-Boado, et al. (1998). "Induction and evasion of host defenses

- by type 1-piliated uropathogenic *Escherichia coli*." Science **282**(5393): 1494-7.
- Mulvey, M. A., J. D. Schilling, et al. (2000). "Bad bugs and beleaguered bladders: interplay between uropathogenic *Escherichia coli* and innate host defenses." Proc Natl Acad Sci U S A **97**(16): 8829-35.
- Munro, P., G. Flatau, et al. (2004). "Activation and proteasomal degradation of rho GTPases by cytotoxic necrotizing factor-1 elicit a controlled inflammatory response." J Biol Chem **279**(34): 35849-57.
- Nisimoto, Y., J. L. Freeman, et al. (1997). "Rac binding to p67(phox). Structural basis for interactions of the Rac1 effector region and insert region with components of the respiratory burst oxidase." J Biol Chem **272**(30): 18834-41.
- Nowicki, B., M. Rhen, et al. (1984). "Immunofluorescence study of fimbrial phase variation in *Escherichia coli* KS71." J Bacteriol **160**(2): 691-5.
- Pop, M., K. Aktories, et al. (2004). "Isotype-specific degradation of Rac activated by the cytotoxic necrotizing factor 1." J Biol Chem **279**(34): 35840-8.
- Rest, R. F. and D. P. Speert (1994). "Measurement of nonopsonic phagocytic killing by human and mouse phagocytes." Methods Enzymol **236**: 91-108.
- Rippere-Lampe, K. E., M. Lang, et al. (2001). "Cytotoxic necrotizing factor type 1-positive *Escherichia coli* causes increased inflammation and tissue damage to the prostate in a rat prostatitis model." Infect Immun **69**(10): 6515-9.
- Rippere-Lampe, K. E., A. D. O'Brien, et al. (2001). "Mutation of the gene encoding cytotoxic necrotizing factor type 1 (cnf(1)) attenuates the virulence of

- uropathogenic *Escherichia coli*." Infect Immun **69**(6): 3954-64.
- Rosen, H., J. R. Crowley, et al. (2002). "Human Neutrophils Use the Myeloperoxidase-Hydrogen Peroxide-Chloride System to Chlorinate but Not Nitrate Bacterial Proteins during Phagocytosis." J. Biol. Chem. **277**(34): 30463-30468.
- Russo, T. A. and J. R. Johnson (2003). "Medical and economic impact of extraintestinal infections due to *Escherichia coli*: focus on an increasingly important endemic problem." Microbes Infect **5**(5): 449-56.
- Schilling, J. D., M. A. Mulvey, et al. (2001). "Dynamic interactions between host and pathogen during acute urinary tract infections." Urology **57**(6 Suppl 1): 56-61.
- Schmidt, G., P. Sehr, et al. (1997). "Gln 63 of Rho is deamidated by *Escherichia coli* cytotoxic necrotizing factor-1." Nature **387**(6634): 725-9.
- Schwartz, M. A. and S. J. Shattil (2000). "Signaling networks linking integrins and rho family GTPases." Trends Biochem Sci **25**(8): 388-91.
- Srinivasan, S., F. Wang, et al. (2003). "Rac and Cdc42 play distinct roles in regulating PI(3,4,5)P3 and polarity during neutrophil chemotaxis." J Cell Biol **160**(3): 375-85.
- Sun, C. X., G. P. Downey, et al. (2004). "Rac1 is the small GTPase responsible for regulating the neutrophil chemotaxis compass." Blood **104**(12): 3758-65.
- Uehling, D. T., D. B. Johnson, et al. (1999). "The urinary tract response to entry of pathogens." World J Urol **17**(6): 351-8.
- Uhlen, P., A. Laestadius, et al. (2000). "Alpha-haemolysin of uropathogenic *E. coli*

- induces Ca^{2+} oscillations in renal epithelial cells." Nature **405**(6787): 694-7.
- Underhill, D. M. and A. Ozinsky (2002). "Phagocytosis of microbes: complexity in action." Annu Rev Immunol **20**: 825-52.
- Van Bost, S., S. Roels, et al. (2001). "Necrotoxicogenic *Escherichia coli* type-2 invade and cause diarrhoea during experimental infection in colostrum-restricted newborn calves." Vet Microbiol **81**(4): 315-29.
- Vicente-Manzanares, M. and F. Sanchez-Madrid (2004). "Role of the cytoskeleton during leukocyte responses." Nat Rev Immunol **4**(2): 110-22.
- Wang, K., D. Scheel-Toellner, et al. (2003). "Inhibition of neutrophil apoptosis by type 1 IFN depends on cross-talk between phosphoinositol 3-kinase, protein kinase C-delta, and NF-kappa B signaling pathways." J Immunol **171**(2): 1035-41.
- Wessel, D. and U. I. Flugge (1984). "A method for the quantitative recovery of protein in dilute solution in the presence of detergents and lipids." Anal Biochem **138**(1): 141-3.
- Witko-Sarsat, V., P. Rieu, et al. (2000). "Neutrophils: molecules, functions and pathophysiological aspects." Lab Invest **80**(5): 617-53.
- Xia, Y., D. Gally, et al. (2000). "Regulatory cross-talk between adhesin operons in *Escherichia coli*: inhibition of type 1 fimbriae expression by the PapB protein." Embo J **19**(7): 1450-7.
- Xu, J., F. Wang, et al. (2003). "Divergent signals and cytoskeletal assemblies regulate self-organizing polarity in neutrophils." Cell **114**(2): 201-14.

Yamamoto, S., K. Nakata, et al. (1996). "Assessment of the significance of virulence factors of uropathogenic *Escherichia coli* in experimental urinary tract infection in mice." Microbiol Immunol **40**(9): 607-10.

Yamamoto, S., T. Tsukamoto, et al. (1995). "Distribution of virulence factors in *Escherichia coli* isolated from urine of cystitis patients." Microbiol Immunol **39**(6): 401-4.

